UNIVERSITY OF JYVÄSKYLÄ
DEPARTMENT OF CHEMISTRY
RESEARCH REPORT No. 126

STRUCTURAL CHARACTERISTICS AND PROPERTIES OF SUBSTITUTED CHOLANOATES AND *N*-SUBSTITUTED CHOLANAMIDES

BY

ARTO VALKONEN

Academic Dissertation
for the Degree of
Doctor of Philosophy

Jyväskylä, Finland
2008

DEPARTMENT OF CHEMISTRY, UNIVERSITY OF JYVÄSKYLÄ
RESEARCH REPORT No. 126

STRUCTURAL CHARACTERISTICS AND PROPERTIES OF SUBSTITUTED CHOLANOATES AND *N*-SUBSTITUTED CHOLANAMIDES

BY

ARTO VALKONEN

Academic dissertation for the degree of
Doctor of Philosophy

To be presented, by permission of the Faculty of Mathematics and Natural Sciences of the University of Jyväskylä, for public examination in Auditorium FYS 1, on October 18th, 2008, at 12 noon.

Jyväskylä, Finland
ISBN 978-951-39-3316-6
ISSN 0357-346X

URN:ISBN:978-951-39-9058-9
ISBN 978-951-39-9058-9 (PDF)
ISSN 0357-346X

Jyväskylän yliopisto, 2022

ABSTRACT

Valkonen, Arto
Structural characteristics and properties of substituted cholanoates and *N*-substituted cholanamides.
Jyväskylä: University of Jyväskylä, 2008, 80 p.
Department of Chemistry, University of Jyväskylä
ISBN 978-951-39-3316-6
ISSN 0357-346X

The present thesis reports the synthesis and more detailed structural characterization of some bile acid derivatives based on naturally common cholanoic acids. The structure determination is an important part of efforts to understand the properties and function of these biologically active compounds, which have been of concern to many scientists for decades. This thesis provides new structural information about some derivatives of auxiliary substances of human digestion, namely cholic acid and chenodeoxycholic acid, also called primary bile acids. These primary bile acids are cholesterol metabolites and they can be further transformed to secondary bile acids. In addition to structural data of the derivatives of primary and secondary bile acids, their thermal properties were also examined.

A total of five methyl ester (cholanoates), 15 *N*-hydroxyalkyl amide (cholanamides) and two cyclic cholaphane derivatives of cholanoic acids with their intermediates were prepared. The structures of these compounds were analyzed by powder and single crystal x-ray crystallographic, solid and liquid state NMR, IR as well as mass spectrometric methods. Exact solid state structures of four cholanoates, six cholanamides and two cholanamide solvates were determined by single crystal x-ray crystallography. Thermal analyses included differential scanning calorimetric and thermogravimetric methods.

Bile acids are very useful natural tools in organic, bioorganic and supramolecular chemistry. The bile acid nucleus is one of the largest rigid units readily available with enantiomeric purity, unique amphiphilicity and low cost. Cholanoate derivatives are important intermediates in the synthesis of various cholanoic acid derivatives and they can also have utilizable properties themselves, for example in gelation processes or sensing. Cholanamides provide also an attractive backbone for many possible applications, including pharmaceuticals, drug delivery, gelators and other supramolecular systems. Cholaphanes are well-known host molecules in supramolecular chemistry binding various ionic guests, and they can serve as possible model compounds for more complex biological systems.

Keywords: structural chemistry, solid state, cholanoic acid derivatives, NMR spectroscopy, CP-MAS, powder and single crystal x-ray crystallography, thermal analysis

Author´s address

Arto Valkonen
Department of Chemistry
P.O. Box 35
40014 University of Jyväskylä
Finland
arto.valkonen@jyu.fi

Supervisor

Professor Erkki Kolehmainen
Department of Chemistry
University of Jyväskylä
Finland

Reviewers

Professor Uday Maitra
Indian Institute of Science
Department of Organic Chemistry
Bangalore, India

Professor Olga Bortolini
University of Calabria
Department of Chemistry
Italy

Opponent

Professor Kristiina Wähälä
University of Helsinki
Department of Chemistry
Finland

PREFACE

The present work was carried out at the Department of Chemistry, University of Jyväskylä from May 2002 to November 2007.

I express my deepest gratitude to my supervisor Professor Erkki Kolehmainen for giving me the opportunity to struggle with the chemistry of bile acids and NMR spectroscopy. Without his continuous encouragement, support, and advice this thesis would have been an endless mission. I thank Professor Kari Rissanen for his help and advice in crystallography as well as for the opportunity to participate in many interesting and valuable scientific meetings. I also thank him for employing me until the end of 2010. Professors Maija Nissinen and Reijo Sillanpää are gratefully acknowledged for their help and guidance in crystallography, especially using diffractometers. I thank the former head of the department, Professor Henrik Kunttu, for providing the opportunity to work here.

Professors Olga Bortolini and Uday Maitra are acknowledged for their detailed review of the present thesis. Professor Emeritus Matti Nurmia is acknowledged for revising the language of this thesis. Professor Nikolai V. Lukashev and his research group members are acknowledged for their kind cooperation within the cholaphane project. My sincere thanks go to Docent Manu Lahtinen for his cooperation and the huge number of powder XRD and thermoanalytical experiments. His share in this research is remarkable. I like to thank Docent Elina Sievänen for MS and modeling studies and all members of the BA & NMR group for their cooperation and the pleasant working atmosphere. I wish to thank Special Laboratory Technicians Mirja Lahtiperä and Reijo Kauppinen for the MS and NMR measurements. My special thanks go to all the people at the Laboratory of Organic Chemistry for the friendly and inspiring working environment.

I wish to warmly thank my parents Pirkko and Taisto for their endless support throughout my struggle with this work and my studies. You have always been there for me. I also thank my sister Tuula, her husband Karri, and my goddaughter Ava for their encouragement and for bringing delight into my life. I wish to thank my friends and relatives for their support. I feel sorry for abandoning you over these hectic years. Finally I would like to express my gratitude and love to Elina. You are my sunshine and my inspiration – you mean everything to me.

This thesis was funded by the University of Jyväskylä, giving the author the opportunity to work as an assistant and researcher. This thesis was also funded in part by the Magnus Ehrnrooth Foundation and the Academy of Finland. The Russian cooperation was financially supported by the RFBR Grant N 04-03-32995. The author gratefully acknowledges this financial support.

Jyväskylä, August 29th 2008

Arto Valkonen

LIST OF ORIGINAL PUBLICATIONS

This thesis is based on the following original publications, which are referred to in the text by their Roman numerals.

I A. Valkonen, M. Lahtinen, E. Virtanen, S. Kaikkonen, E. Kolehmainen, Bile acid amidoalcohols: simple organogelators, *Biosens. Bioelectron.* **2004**, *20*, 1233–1241.

II A. Valkonen, E. Kolehmainen, M. Lahtinen, E. Sievänen, V. Noponen, M. Tolonen, R. Kauppinen, Structural, thermoanalytical and molecular modeling studies on *N*-(3-hydroxypropyl) 3α,12α-dihydroxy-5β-cholan-24-amide and its monohydrates, *Molecules* **2007**, *12*, 2161–2178.

III A. Valkonen, E. Sievänen, S. Ikonen, N.V. Lukashev, P.A. Donez, A.D. Averin, M. Lahtinen, E. Kolehmainen, Novel lithocholaphanes: syntheses, NMR, MS, and molecular modeling studies, *J. Mol. Struct.* **2007**, *846*, 65-73.

IV A. Valkonen, M. Lahtinen, J. Tamminen, E. Kolehmainen, Solid state structural studies of five bile acid derivatives, *J. Mol. Struct.* **2008**, *886*, 197-206.

V A. Valkonen, M. Lahtinen, E. Kolehmainen, Syntheses and Structural Study of Bile Acid Amidoalcohols, *Steroids* **2008**, *73*, 1228-1241.

ABBREVIATIONS

ACOT	acylcoenzyme A thioesterase
BACAT	bile acid-coenzyme A:amino acid *N*-acyltransferase
BnOH	benzyl alcohol
BSE	bovine spongiform encephalopathy
CA	cholic acid
CDCA	chenodeoxycholic acid
COSY	correlation spectroscopy
CP-MAS	cross polarization magic angle spinning
CS	cholylsarcosine
DBU	1,8-diazabicyclo[5.4.0]undec-7-ene
DCA	deoxycholic acid
DCC	*N,N'*-dicyclohexylcarbodiimide
DCM	dichloromethane
DEPT	distortionless enhancement by polarization transfer
DHCA	dehydrocholic acid
DIAD	diisopropyl azodicarboxylate
DMAP	4-(dimethylamino)pyridine
DPPA	diphenylphosphoryl azide
DQF	double quantum filtered
DSC	differential scanning calorimetry
DTA	differential thermal analysis
EEDQ	2-ethoxy-1-ethoxycarbonyl-1,2-dihydroquinoline
ESI-TOF	electrospray ionization time-of-flight
EtOH	ethanol (or ethyl alcohol)
Et_3N	triethylamine
GC	glycocholate
GIAO	gauge independent atomic orbital
HBTU	*O*-2-(*1H*-benzotriazol-1-yl)-1,1,3,3-tetramethyluronium hexafluorophosphate
HMBC	heteronuclear multiple bond correlation
HMQC	heteronuclear multiple quantum coherence
IR	infra-red
LAH	lithium aluminium hydride
LC	liquid chromatography
LCA	lithocholic acid
LCSC	low critical solution concentration
LCST	low critical solution temperature
MeC	methyl cholate
MeCDC	methyl chenodeoxycholate
MeDC	methyl deoxycholate
MeLC	methyl lithocholate
MeOH	methanol (or methyl alcohol)
MeUDC	methyl ursodeoxycholate
MS	mass spectrometry
NaDC	sodium deoxycholate

NMR	nuclear magnetic resonance
PAM	peptidylglycine α-amidating monooxygenase
PFG	pulsed field gradient
PFPOH	pentafluorophenol
SBS	short bowel syndrome
TC	taurocholate
TG	thermogravimetry
THF	tetrahydrofuran
TPP	triphenyl phosphine
TrCl	triphenylmethyl chloride (or tritylchloride)
UDCA	ursodeoxycholic acid
XRD	x-ray diffraction

TABLE OF CONTENTS

ABSTRACT
PREFACE
LIST OF ORIGINAL PUBLICATIONS
ABBREVIATIONS
TABLE OF CONTENTS

1 INTRODUCTION 11

2 CHOLANOIC ACIDS AND DERIVATIVES 13
2.1 General 13
2.2 Sources and uses 17
2.3 Cholanoates 18
2.4 Cholanamides 20

3 EXPERIMENTAL 22
3.1 Starting materials 22
3.2 Compounds 22
3.2.1 Cholanoates 22
3.2.2 Cholanamides 23
3.2.3 Cholaphanes 25
3.3 IR and NMR spectroscopy 25
3.4 Mass spectrometry 25
3.5 X-ray crystallography 26
3.6 Calculations 26
3.7 Gelation tests 27

4 RESULTS AND DISCUSSION 28
4.1 Cholanoates 28
4.1.1 Structures 29
4.1.2 Thermal properties 33
4.2 *N*-Hydroxyalkyl cholanamides 34
4.2.1 Preparation 35
4.2.2 Structures 36
4.2.3 Thermal properties 45
4.2.4 Gelation properties 48
4.3 Cholaphanes and their intermediates 49
4.3.1 Structures 49
4.3.2 Cation binding 50

5 CONCLUSIONS 53

REFERENCES 55

APPENDIX 65

1 INTRODUCTION

Bile acids are found in the bile of vertebrates, which is produced in the liver and stored in the gallbladder. Bile acids are metabolic products of cholesterol, which undergoes hydroxylations, oxidations and reduction in the liver followed by the loss of an isopropyl group from the side chain and oxidation of C24 resulting in primary bile acids. These primary bile acids are largely conjugated in the next step, usually with amino acids, to form more soluble bile salts under physiological conditions. The conjugated forms are then secreted into the bile and stored in the gallbladder, and upon eating a meal containing fat, emptied into the upper region of the small intestine, where the bile acids have an essential role in the digestion and absorption of lipids and lipid-soluble vitamins through the intestinal wall. More than 85 % of bile acids are then reabsorbed along with dietary lipids at the lower end of the small intestine and carried to the liver via the portal vein. This cycle is called the enterohepatic circulation. In humans it happens 6–15 times per day.[1-4]

Cholanoic acids are important bile acids, which play a significant role in the digestion of lipophilic substances in the human intestines. These biologically active steroidal carboxylic acids are also potential carriers of drugs targeted against intestinal diseases, as well as against viruses and fungal growth, for example. The metabolism of cholesterol to cholanoic acids is also the major sink of cholesterol and by controlling the amount of these acids in the small intestine it is possible to control the cholesterol levels.[3,5] As a drawback, bile acids are found to play a key etiologic role in gastrointestinal cancers. Many studies indicate that bile acids cause DNA damage, strongly suggesting their mutagenic and carcinogenic potential. Bile acids can act as promoters but likely they are themselves carcinogens.[6]

Structural organic chemistry is the elucidation of molecular structures of organic compounds, from the simple to the more advanced. Knowledge of the chemical formula of an organic compound is not sufficient information because many isomers, polymorphs and their mixtures can exist. Nowadays, many methods exist to characterize the molecular structure of organic compounds and they are used daily in countless research laboratories. Crystallography is the most precise method to obtain information about the structure in the solid state. Unfortunately, growing crystals of sufficient size for single crystal diffraction analysis is often difficult and the frequently observed low crystallinity of materials in powder diffraction analysis makes this method less appropriate. Spectroscopic methods such as NMR or MS are commonly used to characterize structures of synthetic and natural products. In addition to standard liquid state analysis, solid state NMR offers an important tool for the characterization of solid materials, especially in the case of insufficient crystallographic data. NMR methods can often give enough information for a complete structure determination. MS and elemental analysis are important tools for the determination of the molecular composition and purity of the compound. Furthermore, methods such as IR, UV/VIS and optical rotation analysis can give extra information about the presence of some functional group(s) as well as quantity or handedness of the compound, respectively. Thermal analysis gives important information about the presence and quantity of solvents or other guests in the structure, as well as about its phase transitions and thermal stability.

In the beginning of this project the aim was to develop neurotransmitter-related steroidal cyclopeptides[7-10] based on conjugates of cholanoic acids and amino acids. The lack of success in the synthetic efforts to link the desired compounds to each other led to the preparation of *N*-(aminoalkyl) amides of cholanoic acids and furthermore to the corresponding *N*-(hydroxyalkyl) amides. The latter ones immediately showed potential organogelator properties during the NMR measurements. That was the start of the main research content of this project. The teamwork within our research group also gave a possibility to characterize the structures of other cholanoic acid derivatives. The cooperation with our Russian colleagues also made a significant contribution to this project.

Our research group is working on the field of steroids and more specifically on the synthesis, structural chemistry and possible applications of them. In this project we concentrated on the structural, thermal, solid state and gelation properties of *N*-(hydroxyalkyl) cholanamides,[I-II,V] 3-substituted cholanoates,[IV] lithocholaphanes[III] and their intermediates. Furthermore, the aim was to obtain compounds for use as drugs, drug carriers, organogelators or liquid crystals. The methods utilized in this study include NMR spectroscopy, powder and single crystal x-ray crystallography, differential scanning calorimetry, thermogravimetry, mass spectrometry and IR spectroscopy.

2 CHOLANOIC ACIDS AND DERIVATIVES

2.1 General

The most abundant mammalian bile acids are derivatives of cholanoic acid (5β-cholan-24-oic acid), substituted by hydroxyl groups, usually at the steroidal ring system (Figure 1).[7] The term "cholan" denotes a particular steroid structure of 24 carbons, and the "24-oic acid" indicates that the carboxylic acid group is found at position 24, which happens to be at the end of the side chain. The "5β" part of the name denotes the *cis* orientation of the junction between rings A and B of the steroid nucleus, instead of the usual *trans* juncture of steroids. All primary C24 bile acids have a hydroxyl group at positions C3 and C7, as cholesterol 7α-hydroxylation (Figure 2) is the rate-limiting step in bile acid biosynthesis.[11]

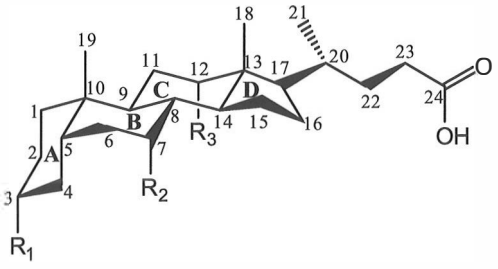

R_1,R_2,R_3 = H, Cholanoic acid
R_1,R_2,R_3 = OH, Cholic acid
R_1,R_2 = OH, R_3 = H, Chenodeoxycholic acid
R_1,R_3 = OH, R_2 = H, Deoxycholic acid
R_1 = OH, R_2,R_3 = H, Lithocholic acid

Figure 1. General structure and numbering of cholanoic acids.

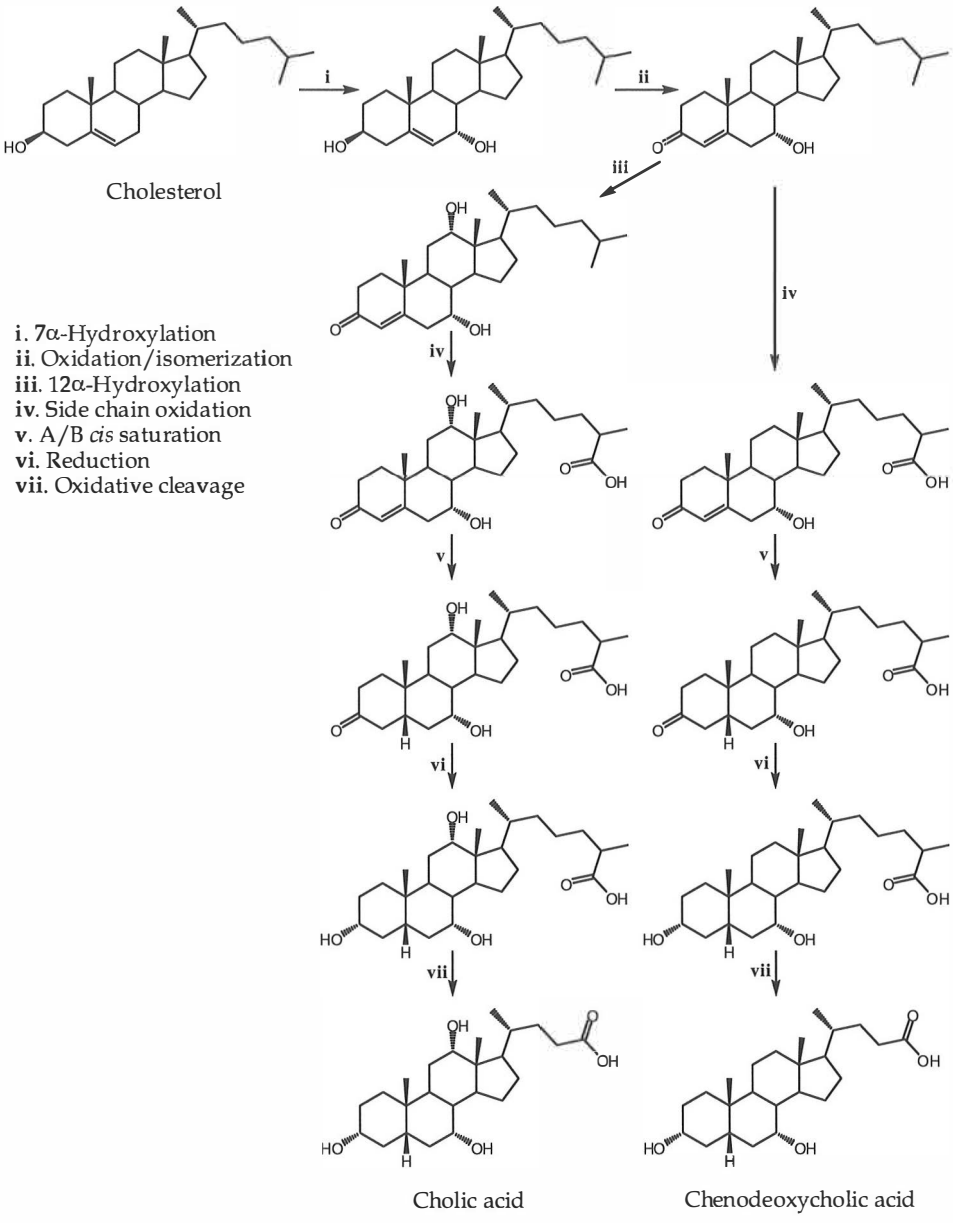

Figure 2. Biosynthesis of primary bile acids from cholesterol.[4]

In the human body liver hepatocytes metabolize cholesterol *via* many enzymatic steps (Figure 2) to cholic acid (CA) and chenodeoxycholic acid (CDCA), which are called primary bile acids. This metabolic route involves 17 different enzymes.[12] Primary bile acids are secreted into the intestines in combination with sodium salts of glycine or taurine, in which the conjugation occurs *via* an amide bond. These bile salts, glycocholate (GC) and taurocholate (TC, Figure 3), keep lipids emulsified and aid their digestion and resorption.[4] In

addition, when stored in the gallbladder they prevent cholesterol from precipitating. The primary bile acids can be further transformed in the small intestine to secondary bile acids, deoxycholic (DCA) and lithocholic acids (LCA), by a bacterial 7α-dehydroxylase enzyme, which removes the hydroxyl group from position 7α (Figure 4). Bacterial oxidases and reductases can also attack steroidal positions C3, C7 and C12, leading to a complex mixture of bile acids. The primary bile acids cover over 70 %, deoxycholic acid less than 20 % and lithocholic, ursodeoxycholic (UDCA), and other rarer bile acids the rest of the total human bile acid contents.[3]

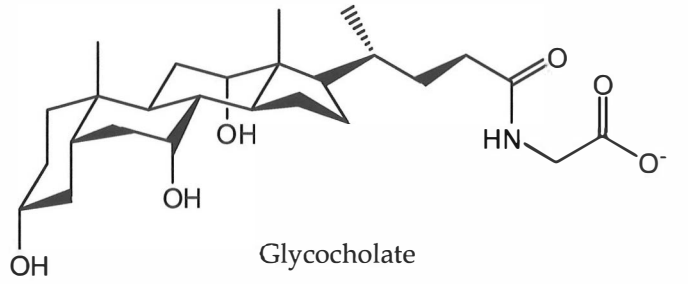

Glycocholate

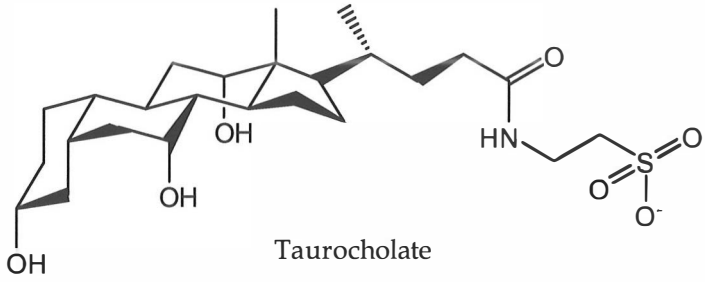

Taurocholate

Figure 3. Conjugated cholic acids: glycocholic acid and taurocholic acid.

The present thesis concentrates on the structural and thermal properties of some derivatives of LCA, DCA, CDCA, UDCA and CA. As seen from Figures 2 and 4, the secondary hydroxyl groups of bile acids are easily oxidized to oxo groups in biological systems. They can also be easily oxidized in the laboratory, for example under conditions involving Cr(VI) oxides.[13-16] One commercially available synthetic oxoacid is 3,7,12-trioxo-5β-cholan-24-oic acid or briefly dehydrocholic acid (DHCA), which is a known bile flow increasing hydrocholeretic drug.[17] Two derivatives of DHCA were also prepared and characterized within this thesis.[V]

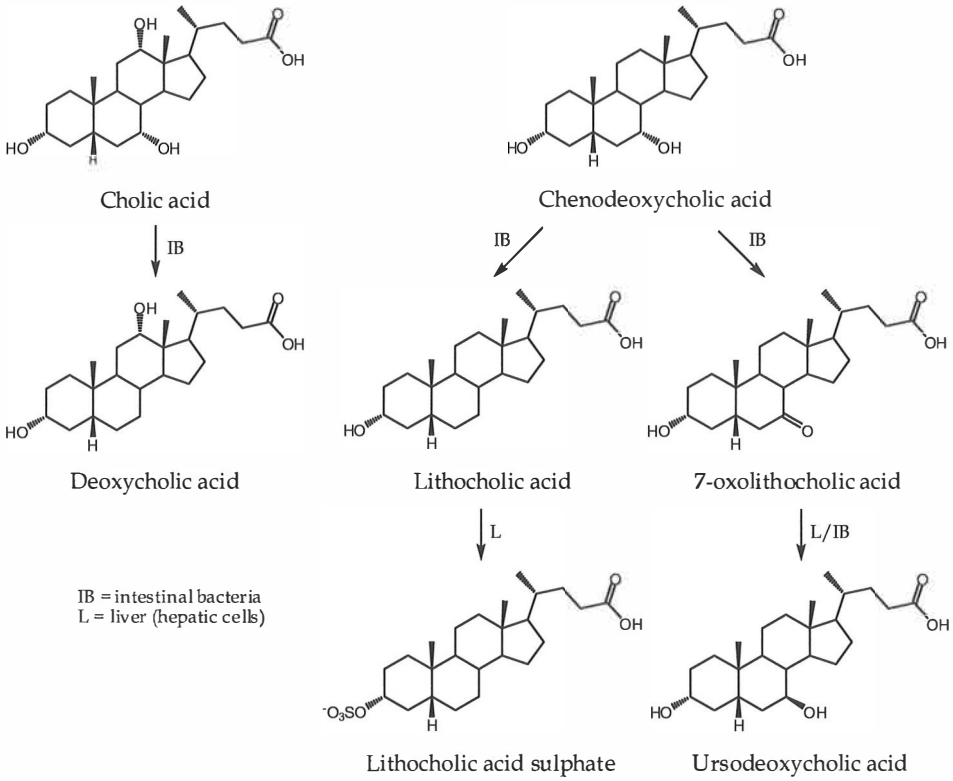

Figure 4. Biosynthesis of secondary bile acids and ursodeoxycholic acid.

Bile acids usually have a structure where the hydroxyl groups are oriented in the same spatial direction generating a hydrophilic face (α-face) of the molecule. The opposite face (β-face) with methyl groups is strongly hydrophobic and lipophilic. Bile acids have two different faces and, therefore, are amphipathic molecules.[4] Bile acids are capable of forming "pairs or dimers" (Figure 5a)[I] through hydrophobic or hydrophilic interactions or, in general, they are organized so that the α-face of the molecule interacts with the α-face(s) of the other molecule(s), while the β-face associates with hydrophobic face(s) of other molecule(s) as shown in Figure 5b. In an aqueous environment bile salts form micelles, where aggregation is mostly driven by hydrophobic interactions of β-faces, but further aggregation can occur by hydrophilic interactions of α-faces to form larger micelles. In the small intestine these micelles mixed with lecithin and glycerides (mixed-micelles) solubilize fat and cholesterol.[1,4] The α-face attracts water opening the way for hydrate formation.[II,V] Furthermore, the interactions of the α-face provide an interesting scope from a supramolecular point of view.[18] Bile acid derivatives working as host molecules have been studied recently by many research groups. Cyclic cholaphanes consisting of two to four bile acid units are among them.[III,2]

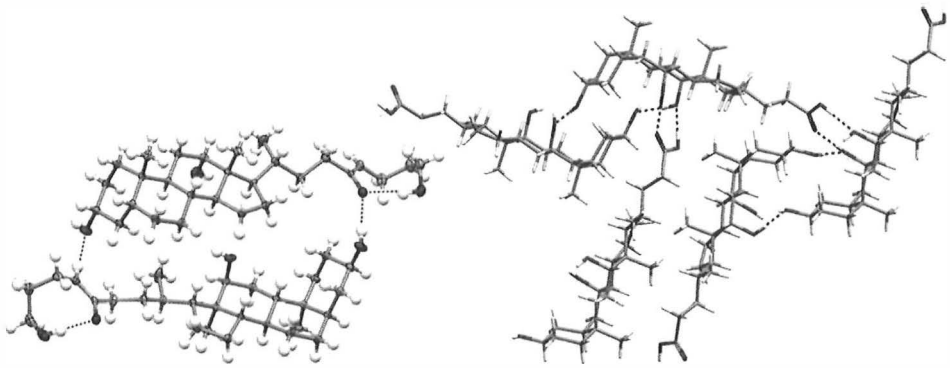

Figure 5. a) A pair of *N*-(3-hydroxypropyl) 3α,12α-dihydroxy-5β-cholan-24-amide molecules[1] and b) packing of CA[19] in crystalline forms.

2.2 Sources and uses

Bile acids can be extracted from the bile of vertebrates and/or prepared synthetically from readily available bile acids. For example, cholic acid is extracted commercially from bovine bile.[4,20] The regulative properties of bile acids in cholesterol production and extraction in humans, the high specificity and capacity of the bile acid transport system, as well as their potential use as drug carriers offer an excellent possibility to utilize them or their derivatives in pharmacological applications as cholesterol-lowering agents and for tissue- or organ-specific targeting.[2,3,21-24] Other potential medical applications of bile acids and their derivatives exists in gene therapy acting as non-opiate analgesics,[25] antiviral[26,27] and anti-fungal agents,[28-32] sensitizers of Gram-negative and Gram-positive bacteria to antibiotics,[33-37] DNA transfection agents[38,39] and radiopharmaceuticals.[40] As already mentioned, bile acids are well known compounds in supramolecular chemistry,[2,7,41] such as in molecular recognition[42-46] and gelation.[41,47-49] For the majority of these applications it is necessary to chemically modify the natural bile acid, normally by attaching electron-donor groups to it to enable binding to transition-metal ions or other electron-deficient moieties.

The primary commercial use of cholic acid (CA) is as an intermediate in the synthesis of chenodeoxycholic acid (CDCA) and ursodeoxycholic acid (UDCA), which are important pharmaceutical products.[20] CA is also used in traditional Asian medicine and it is one of the ingredients used to formulate artificial bezoar.[50] Chenodeoxycholic acid (CDCA) can be produced synthetically from cholic acid or stigmasterol,[51] and also be purified from pig bile.[52] CDCA is also used as an intermediate in the production of UDCA. Both CDCA and UDCA are active pharmaceuticals, which assist in the dissolution and prevention of cholesterol gallstones in humans,[2,52-54] and which are used in the prevention and treatment of liver diseases[20] and also utilized in traditional Asian medicine.[55,56] Deoxycholic acid (DCA) is extracted commercially from bovine bile. DCA has been used as a starting material in the preparation of

cortisone and as a virus activity reducer in the production of influenza vaccines.[20] DCA is also used as an ingredient in pharmaceutical formulations, artificial bezoar and other Asian medicine formulations. Its salt, sodium deoxycholate (NaDC), is used as a biological and laboratory detergent to lyse cells and solubilize cellular and membrane components.[57,58] DCA is found to be toxic to esophageal cells and it can have potential carcinogenic and mutagenic effects,[59] but it is still known to be (as well as CA, CDCA and UDCA) less toxic than lithocholic acid (LCA), when they accumulate in the enterohepatic circulation.[11,60] The known possible effects of LCA include segmental bile duct obstruction, destructive cholangitis, hyperplasia and choledocholithiasis, which make it unfavorable in pharmacological applications, although humans have an unique ability among vertebrates in being able to sulfate LCA and rapidly detoxify it. LCA can easily be synthesized from deoxycholic acid and it is still used as a biochemical;[60] furthermore it can substitute for vitamin D in some of its classical functions in vitamin D-deficient individuals.[61] Dehydrocholic acid (DHCA) is an unnatural bile acid, commercially manufactured by oxidation of cholic acid with sodium hypochlorite. It does not readily form micelles with lipids. DHCA can increase the water content and volume of bile and it is used as cholagogue, hydrocholeretic, diuretic, laxative and diagnostic aid.[62] All important bile acids are mostly derived from bovine bile. Due to the globally problematic BSE disease a safer source of these pharmacologically important compounds, such as stigmasterol, is now desired.[51]

2.3 Cholanoates

Cholanoates are 24-ester derivatives or salts of cholanoic acids; for example, the ester product from cholic acid and ethanol would be named ethyl 3α,7α,12α-trihydroxy-5β-cholan-24-oate (or trivially ethyl cholate). In this thesis only the ester forms are considered and in the present work the esters of bile acids, mostly methyl cholanoates (Figure 6), are successfully utilized as intermediates[I-V] and products.[IV] Cholanoates are easier to handle in syntheses owing to their better solubility in non-polar solvents than that of free acids. They are used as important synthetic intermediates on routes to produce various bile acid derivatives, such as cyclic structures.[63,64] They can also possess interesting characteristics, such as gelling,[65,66] amphiphilic, sensor[67] and possibly enantiodifferentiating properties.

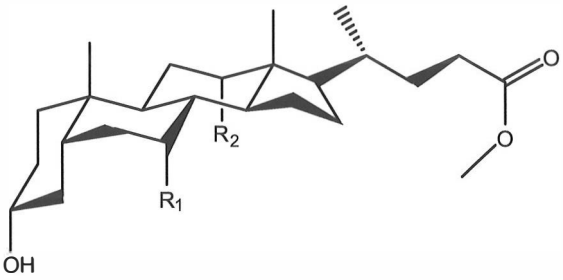

R_1, R_2 = H; **MeLC**
R_1 = H, R_2 = OH; **MeDC**
R_1 = OH, R_2 = H; **MeCDC**
R_1 = OH, R_2 = OH; **MeC**

Figure 6. Methyl cholanoates used in this study. (Missing MeUDC is like MeCDC, but with a hydroxyl group R_1 at position 7β)

Naturally cholanoates can occur at least in the blood and urine of patients with cholestasis as a form of ester-type acyl glucuronides, formed from 6-hydroxylated bile acids[68] and glucuronic acid.[69-72] The LC/MS analysis of healthy human urine has also shown the existence of 24-galactosides of DCA and CA (Figure 7).[73,74] The other potential 24-glycosidic cholanoates possibly found and separated in the future are glucosides and *N*-acetylglucosaminides due to the widespread occurrence of various hydroxyl-linked analogs in human biological materials.[75-77] Alkyl cholanoates do not occur widely in nature, but methyl cholate (MeC) has recently been extracted from the fungus *Rhizopus oryzae* and it was found to act as an inhibitor of cholesterol biosynthesis *in vitro*.[78] An oxo-acid ester, methyl 3-oxo-cholan-24-oate, was reportedly isolated from the Red Sea sponge *Raspailia* species.[79]

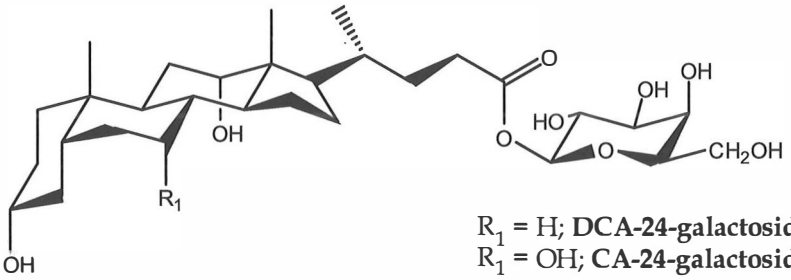

R_1 = H; **DCA-24-galactoside**
R_1 = OH; **CA-24-galactoside**

Figure 7. Cholanoates found in human urine.[73]

Cholanoates can be easily prepared in the laboratory by an acid-catalyzed reaction between cholanoic acid and some alcohol. In this study[I,II,IV,V] the methyl esters were prepared with quantitative yields by this Fischer-type esterification method.[13] Many other research groups have recently utilized this esterification method.[80-87] Benzyl lithocholate was obtained in this study[III] by a reaction of LCA with benzyl alcohol in the presence of DCC/DMAP.[88] Alkyl halides are also very good reagents for converting cholanoic acids to cholanoates in the presence of a variety of catalysts and reagents. Recently published alkyl halide esterifications have been done in the presence of DCC/DMAP,[89] Cs_2CO_3,[66,90] K_2CO_3,[91] DBU,[92,93] or NaH,[94] for example. Other known esterification methods with activated acyl groups of steroids are also

often used in the preparation of larger size cholanoates, such as acid chlorides in the preparation of cholanoate-based dendritic macromolecules,[95-99] cyclic cholanoates,[63] and dimers,[100] as well as anhydride intermediate methods to prepare phenol esters,[101] for example.

2.4 Cholanamides

Primary bile acids form conjugates *in vivo* with sodium salts of glycine or taurine via an amide linkage, as already mentioned. These bile salts occur widely in nature and they can be characterized as cholanamides, which are 24-amide derivatives of cholanoic acids. As an example, cholic acid and 2-aminoethanol (ethanolamine) can be easily combined to form a cholanamide, *N*-(2-hydroxyethyl) 3α,7α,12α-trihydroxy-5β-cholan-24-amide or simply *N*-(2-hydroxyethyl) cholamide (Figure 8).[V] These *N*-hydroxyalkyl cholanamides have been extensively studied in this thesis.[I,II,V] Cholanamides are potential compounds to be used as antimicrobials,[30,102,103] antifungals,[30-32] antiparasitics,[104] anticancer agents,[31,105,106] drug delivery moieties,[107-109] gelators[41,47,48,65,110-113] and in other supramolecular systems.[2,4,7,42,114-119]

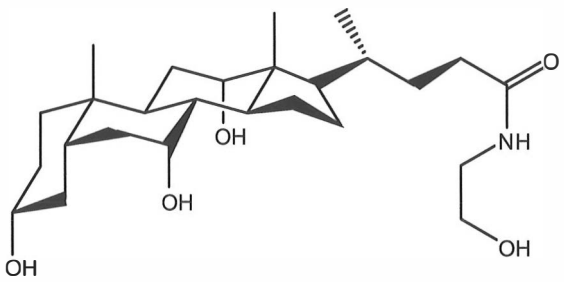

Figure 8. *N*-(2-hydroxyethyl) 3α,7α,12α-trihydroxy-5β-cholan-24-amide, cholanamide conjugate of CA and 2-aminoethanol.[V]

In addition to common bile salts, a literature search about the natural occurrence of cholanamides gave only one result. Bifunctional peptidylglycine α-amidating monooxygenase (PAM) can transform the cholanoic acid glycine conjugates to cholanamides via oxidation to carbinolamide intermediates and subsequent cleavage of glyoxylate.[120] Natural preparation of bile salts from cholanoic acids and glycine or taurine occurs with the aid of an enzyme named bile acid-coenzyme A:amino acid *N*-acyltransferase (BACAT).[121-125] This protein related to the ACOT[121,126] family has been characterized from several species. Synthetic bile salts (Figure 9), for example sarcosine (*N*-methylglycine) conjugates of cholanoic acids[127] or taurocholate,[128] and other amino acid conjugates, such as *N*-lithocholyl-L-cysteine ethyl ester,[129] *N*-cholyl glycine or N-cholyl-L-lysine methyl esters,[128] can be prepared by an activated anhydride method using alkyl chloroformate as the anhydride formation agent. EEDQ-based activated anhydrides can also be utilized in the cholanamide synthesis.[130] Anhydride intermediates[131] and acid chlorides[44,45] have also been recently used to synthesize *N*-alkyl or *N*-aryl substituted cholanamides. Simple nucleophilic

substitutions of alkyl esters[I,II,V,132-135] as well as activated pentafluorophenyl,[III] *N*-hydroxysuccinimide[114,131,136-141] and HBTU[106,142,143] esters with amine are also efficient methods to obtain cholanamides.

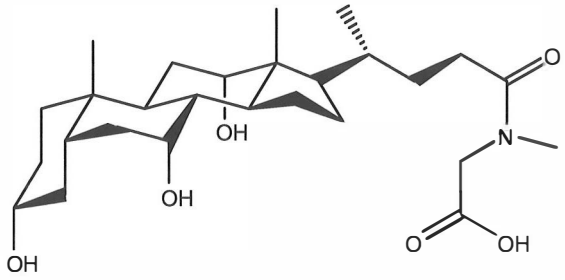

Figure 9. Cholylsarcosine (CS), a semisynthetic bile salt precursor that may be useful in the bile salt replacement therapy of short bowel syndrome (SBS).[144]

3 EXPERIMENTAL

All synthetic and analytical work of publications I, II, IV, and V was performed in Jyväskylä. The synthetic part of publication III was performed in the Department of Chemistry of Lomonosov Moscow State University and the analytical part partly in Moscow and mostly in Jyväskylä. In addition to this experimental section, more detailed information about the methods and specific conditions used can be found in publications I-V.

3.1 Starting materials

All cholanoic acids and other organic reagents used were purchased from Sigma-Aldrich Co. (trademarks Sigma, Aldrich, Riedel and Fluka), except DIAD (diisopropyl azodicarboxylate), which was purchased from Acros Organics. Other reagents and solvents were of analytical grade and were purchased from several chemical suppliers.

3.2 Compounds

3.2.1 Cholanoates

All cholanoic acid methyl esters were prepared with quantitative yields according to the Fischer-type esterification method reported by Fieser and Rajagopalan.[13] These methyl esters are well-known compounds, extensively characterized in the literature, and they are handled in this thesis as intermediate products without further discussion. The derivatives **1-3** (Scheme 1) were previously prepared from methyl esters and spectroscopically

characterized, as reported by Tamminen *et al.*[145] Compounds **1-3** were obtained as by-products in the synthesis of 2,2′-bipyridine-4,4′-dicarboxylates of corresponding cholanoic acid methyl esters by the Yamaguchi method.[146] Compounds **4** and **5** were prepared from methyl 3α-hydroxy-5β-cholan-24-oate (MeLC) by the Mitsunobu reaction[147,148] with diphenylphosphoryl azide (DPPA) for **4** or formic acid for **5** as nucleophiles, in the presence of triphenyl phosphine (TPP) and DIAD.[149] Suitable single crystals for x-ray diffraction analysis were obtained by slow evaporation of the solvent (*p*-xylene for **2-4** and CD_3CN for **5**) from tightly closed test tubes. Benzyl lithocholate and two other *bis*-cholanoates were also prepared and used as intermediates in the synthesis of lithocholaphane (see 3.2.3).

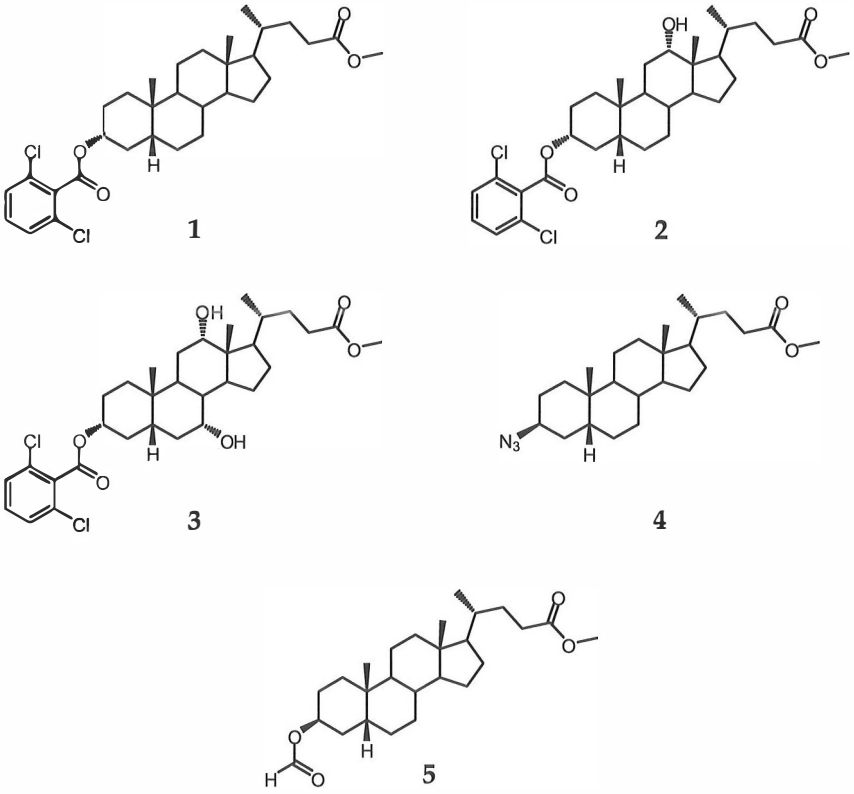

Scheme 1. The cholanoates investigated.

3.2.2 Cholanamides

N-hydroxyalkyl cholanamides **6–9**, **12–15** and **18–20** (Scheme 2) were prepared from methyl esters of cholanoic acids (3.2.1) by a nucleophilic substitution reaction with aminoalcohols in methanol. This method was adapted from the preparation of *N*-aminoalkyl amides reported by Pandey *et al.*,[134,135] and both the room, as well as refluxing, temperature methods were utilized. Compounds **10**, **11**, **16** and **17** were also obtained by a nucleophilic substitution reaction of an

ester, namely *N*-hydroxysuccinimide ester, of the cholanoic acid in question.[114] Suitable single crystals for x-ray analysis were obtained by dissolving the compounds in boiling solvent and allowing the solution to cool and crystallize. The solvents used in the crystallizations were $CHCl_3$ for chloroformate of **8** (**8** · $CHCl_3$), CH_3CN for **9** and **11**, EtOH/H_2O (1:1 v/v) for **12–15** and EtOH/H_2O (2:1 v/v) for monohydrate of **9** (**9a** · H_2O).

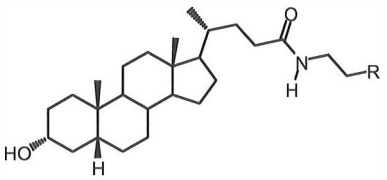

6 R = OH
7 R = CH_2OH
18 R = OCH_2CH_2OH

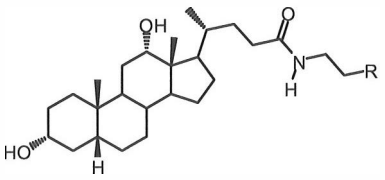

8 R = OH
9 R = CH_2OH

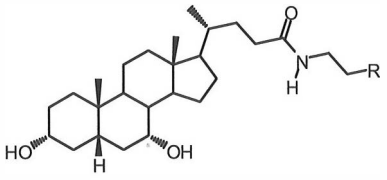

10 R = OH
11 R = CH_2OH

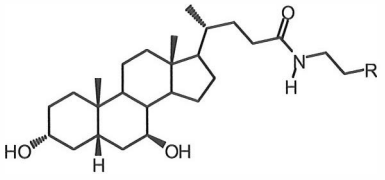

12 R = OH
13 R = CH_2OH

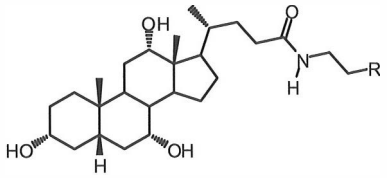

14 R = OH
15 R = CH_2OH

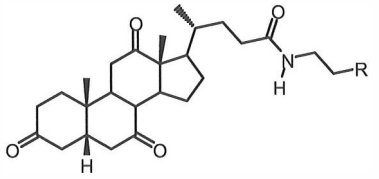

16 R = OH
17 R = CH_2OH

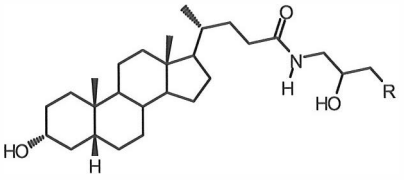

19 R = OH
20 R = NH_2

Scheme 2. The prepared and investigated *N*-hydroxyalkyl cholanamides.

3.2.3 Cholaphanes

Cholaphanes **25** and **30** were prepared from LCA according to Scheme 3. Cholanoates **26**, **27** and **29** were used as intermediate products, as previously mentioned. Lithocholaphane **30** is also a cholanamide derivative.

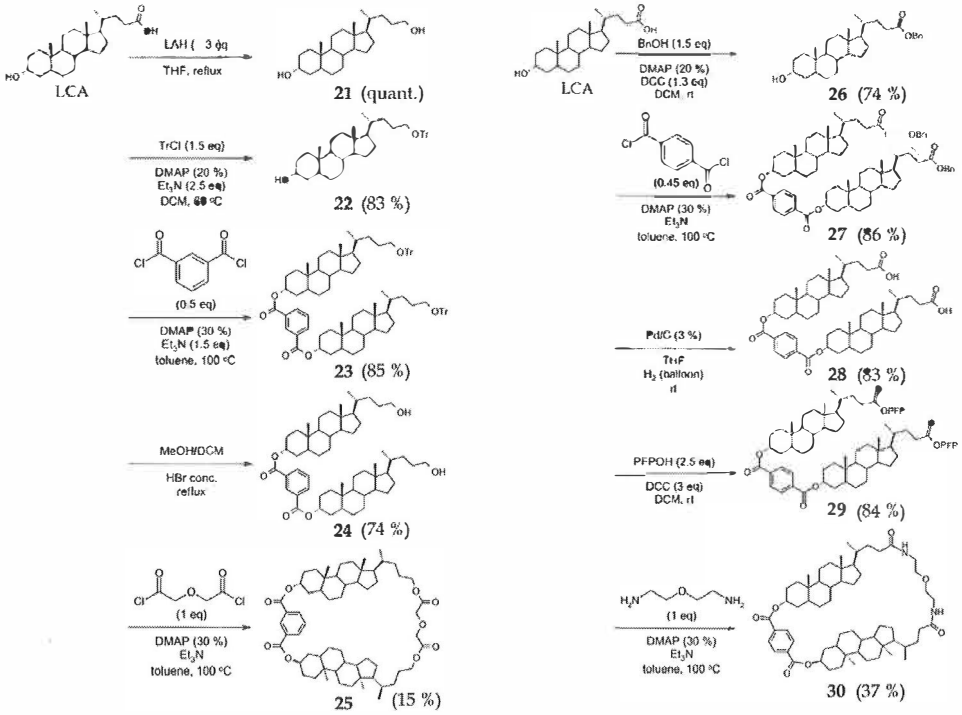

Scheme 3. Preparation of lithocholaphanes **25** and **30**.[III]

3.3 IR and NMR spectroscopy

IR absorption spectra were recorded with a Mattson Satellite FTIR spectrometer. KBr discs for the analysis were prepared from ~1 mg of the sample and 150 mg of dry anhydrous KBr. Liquid state NMR spectra were recorded with a Bruker Avance DRX 500 spectrometer working at 500.13 MHz (for ^{1}H) and 125.77 MHz (for ^{13}C), respectively. One-dimensional ^{1}H, ^{13}C and ^{13}C DEPT-135, as well as two-dimensional PFG[150] DQF ^{1}H,^{1}H COSY,[151,152] PFG ^{1}H,^{13}C HMQC[153,154] and PFG ^{1}H,^{13}C HMBC[155] experiments were utilized. Solid state ^{13}C CP-MAS measurements were performed with a Bruker Avance 400 NMR spectrometer.

3.4 Mass spectrometry

Mass spectrometric measurements were performed using an LCT time-of-flight (TOF) mass spectrometer with electrospray ionization (ESI; Micromass LCT).

Positive ion detection mode was used. The adduct formation experiments for lithocholaphanes with alkali metal chlorides were performed by preparing 0.05 mM solutions of LiCl, NaCl, KCl, and RbCl (first dissolved in H_2O and then diluted with CH_3CN or MeOH, respectively). The lithocholaphanes were first dissolved in $CHCl_3$ and then diluted to a concentration of 0.05 mM using CH_3CN (**25**) or MeOH–HCOOH (0.1%) mixture (**30**). An equal volume of each individual alkali metal chloride solution was taken, mixed thoroughly, and the same volume of the lithocholaphane solution added resulting in a molar ratio of 1:1 (cation/ligand). After 15 min the measurement for the equimolar mixture of the alkali metal chlorides and the ligand was performed. For **30** adduct formation with alkaline earth metal chlorides was tested as well. $MgCl_2$, $CaCl_2$, and $SrCl_2$ were first dissolved in H_2O and then diluted to a concentration of 0.05 mM with MeOH. The experimental procedure was analogous to that described for the adduct formation experiments with alkali metal chlorides.

3.5 X-ray crystallography

The single crystal x-ray data were collected with a Nonius Kappa CCD or Bruker-Nonius Kappa APEX-II diffractometer at a temperature of 173 ± 1 K using graphite monochromated MoK_α (λ = 71.073 pm) or CuK_α (λ = 154.184 pm) radiation. All data were processed with DENZO-SMN.[156] The structures were solved by direct methods, using SHELXS-97[157] or SIR2002,[158] and refined on F^2, using SHELXL-97.[157] All crystallographic diagrams and other figures were drawn with Ortep-3 for Windows[159] or Mercury.[160] All crystallographic data (excluding structure factors) have been deposited with the Cambridge Crystallographic Data Centre (see Appendix). Copies of the data can be obtained free of charge on application to CCDC, 12 Union Road, Cambridge CB2 1EZ UK. The x-ray powder diffraction data were obtained at room temperature by the Huber imaging-plate Guinier camera 670 using germanium monochromated $CuK_{\alpha1}$ radiation (λ = 154.06 pm). The simulated powder diffraction patterns were calculated by Mercury[160] from the CIF-files of the compounds under investigation.

3.6 Calculations

Theoretical NMR chemical shifts for crystallized forms were calculated with DFT B3LYP/6-311G* level of theory using gauge independent atomic orbital (GIAO)[161] method by Gaussian98[162] software. The single crystal structure was first optimized using molecular mechanics (MM+ force field)[163-165] and semiempirical PM3 method[166] with HyperChem molecular modeling software.[167] Finally, the structure was forwarded for geometry optimization at *ab initio* HF/6-31G* level of theory into a Gaussian98[162] package. The NMR chemical shifts were then calculated for the optimized structures. For cholaphanes the molecular frameworks were drawn in HyperChem software,[167] after which the geometries were optimized using MM+ force field[163-165] and PM3[166] methods.

3.7 Gelation tests

In the gelation experiments a mixture containing 1% (w/v) of the solid gelator in solvent was warmed to the boiling point and warming continued until the solid was dissolved (if soluble). The tube (test tube or truncated NMR tube) was sealed with a cap and allowed to cool down to room temperature. After a few minutes the tube was turned upside down. The sample was defined as a gel if no flow was observed. If the sample was still liquid or a viscous solution, it was cooled in a refrigerator overnight and analyzed with a similar method. Some other concentrations were also utilized in the determination of critical values. The most promising gelatinous samples were dried in a vacuum and investigated by JEOL JSM-T200 scanning electron, JEOL 1200EX transmission electron, and WILD M5 optical microscopes.[I] The gelation behavior was also followed during crystallization attempts, in which the concentration of the compound was not adjusted by any means.

4 RESULTS AND DISCUSSION

The molecular structure of cholanoic acids and their derivatives is usually variable only in the conformation of their alkyl side chain or in their substituents. The steroidal ring system mostly remains in the same conformation.[168] Furthermore, the properties, biological activities and mutual differences of these compounds are comprehensively related to the orientation of the side chain and other substituents of steroidal ring.[4,116] The occurrence of different solid forms of the same compound, *i.e.* polymorphs, and their influence on the properties should also be taken into account. Therefore, in order to study the activity and properties of cholanoic acid-based compounds, their structures and conformations should be characterized as precisely as possible. The modern and standard analytical methods, such as spectroscopy, crystallography and thermal analysis, are indispensable for this purpose.

4.1 Cholanoates

The ester derivatives of cholanoic acids have been widely investigated in the literature, either as a target molecule(s) of the study in question or as intermediates in the preparation of other derivatives. In addition to the utilization of cholanoates in the preparation of a large number of bile acid derivatives, the structures of these esters are also usually characterized with a variety of methods, including IR, MS and NMR spectroscopic methods[7,80,169-173] as well as x-ray diffraction.[9,15,80,172-175]

4.1.1 Structures

The preliminary structural characterization (MS and liquid state NMR) of synthetic products **1–3** was performed in an earlier study of our research group.[145] Although, the purity and the structure of these compounds were already known, it was desired to characterize the structures also in the solid state to gain information about their exact conformations and weak intermolecular interactions. Compound **1** was analyzed only with ^{13}C CP-MAS measurements and powder x-ray studies. The results show the powdery product **1** to be isostructural with product **2**, both having similar diffraction patterns and ^{13}C resonances. The induced chemical shift changes of the O-H group in **2**, compared to the shifts of **1**, correspond exceedingly well with the changes found also in the liquid state.[145] For example, the more shielded resonance of C21 in **2** is observed in both states. The crystallinity of products **1–3** was also found to be high according to the intense diffraction peaks and ^{13}C resonances.

The measured IR data of compounds **2** and **3** indicated the presence of hydrogen bond-free O-H groups, which was later verified with single crystal x-ray studies for **3**. Sharp absorption bands in both compounds in the wave number region >3500 cm^{-1} were found to arise from free O-H. In **3**, for O-H donor positioned to 7α, no acceptor was found, but in **2**, the single O-H donor at 12α has a close contact to the carbonyl oxygen of a neighboring molecule in the single crystal structure. However, the crystal structure of **2** (Appendix 1) was not obtained from the same polymorph at the IR spectrum, which was measured from the synthetic powdery product. The high wave number band at 3627 cm^{-1} most probably arises from the free O-H at 12α. The occurrence of forms with non-hydrogen bonded O-H donors in the crystalline state of steroid are also found, for example, in 4,4-dimethyl-23-phenyl-24-nor-5α-chola-8,14-dien-3β-ol[176] and methyl 7α,12α-dihydroxy-3α-methacryloyloxy-5β-cholan-24-oate.[177] Many steroidal compounds have been found to have hydrogen bond-free hydroxyl groups in solutions,[178-180] but in the solid state they are rare according to a literature search. In general, all donors should have acceptors in the solid state.

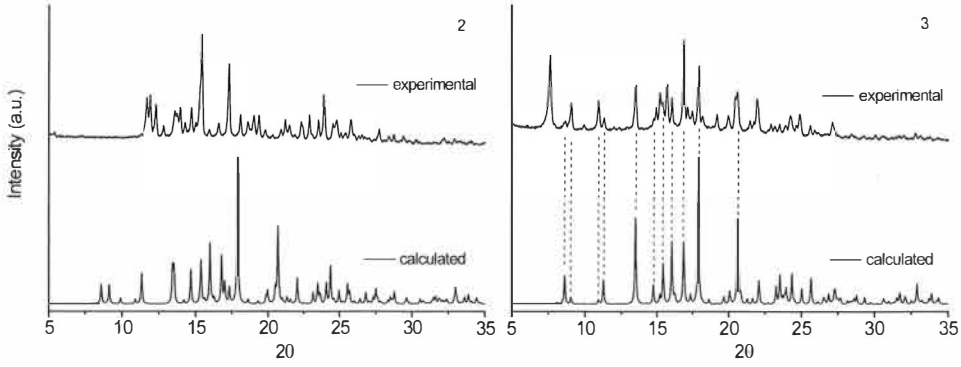

Figure 10. Comparison of experimental and simulated powder x-ray diffraction patterns of compounds **2** and **3**.

Evidence about the existence of two different forms of **2** was obtained from powder x-ray studies, which showed a different diffraction pattern from the one simulated from the single crystal structure, as shown in Figure 10. The single crystal structure of **2** was found to be isostructural with the one of **3** (Appendix 2), showing similar diffraction patterns and crystal parameters. The powder sample of compound **3** was found to consist of two polymorphs (Figure 10), the first one being consistent with the single crystal structure, while the exact structural properties of the other one remain unknown. The reason for the polymorphism is most probably a different orientation of the weak hydrophilic interactions, or the conformation of the side chain.

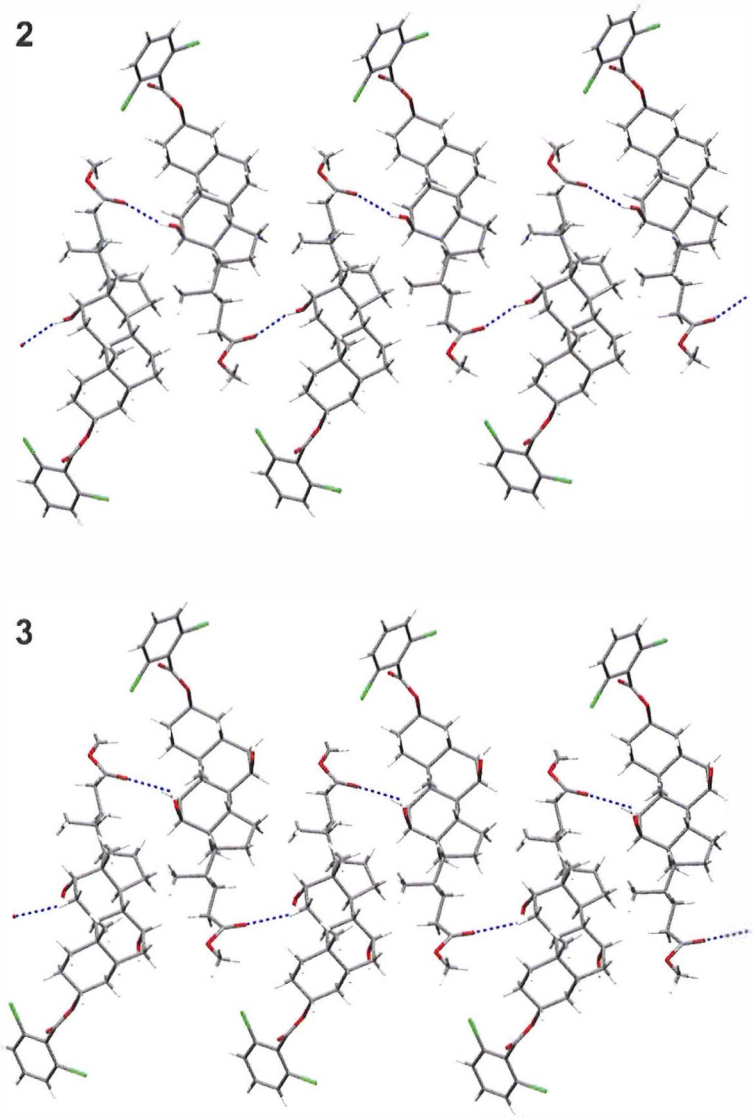

Figure 11. Hydrogen bonding network of compounds **2** and **3**.

The intermolecular hydrogen bond framework found from the single crystal structures of compounds **2** and **3** is shown in Figure 11. In addition to the O12-H12···O24 hydrogen bond in **2** discussed previously (O12 is bonded to C12), the same contact was also found in **3**. With these hydrogen bond interactions the molecules form a coplanar chain in the transversal direction, in contrast to the longitudinal axis of the molecules. This planar chain is connected to adjacent chains with weaker interactions, for example with C-H···O and C-H···Cl contacts. The free OH group of **3** is also seen in Figure 11. These compounds do not show any clear π···π interactions.

The liquid state NMR characterization for azide **4** published by Rensen *et al.*[83] was found to be entirely incomprehensible, at least for the ^{13}C resonances. At this point it must be stated that a reliable characterization of bile acid derivatives on the basis of a previously unknown NMR spectrum and chemical shifts often proves impossible without adequate correlation spectroscopy. With correlation spectra it was possible to characterize all ^{13}C resonances and the most important ^{1}H ones for **4**. The ^{13}C resonances are presented in Table 1 with the literature results. Rensen *et al.*[83] did not report the ^{1}H chemical shift for the proton at the 3α-position, which was found to be 3.95 ppm, the most deshielded resonance found in $CDCl_3$, and they reported only 24 ^{13}C resonances. The MS studies showed the typical tendency of organic azides to lose N_2 or HN_3, as reported by Xiao *et al.*[181] for cholesteryl 3'-azido-3'-deoxythymidine phosphonates.

Table 1. ^{13}C NMR chemical shifts (ppm) of **4** compared to literature results.

Carbon	δ (lit.[83]) in $CDCl_3$	Carbon	δ (lit.[83]) in $CDCl_3$
18	12.1 (11.8)	10	35.0 (40.0)
21	18.3 (18.1)	20	35.4 (35.1)
11	21.0 (20.8)[a]	8	35.7 (35.4)
19	23.8 (23.6)	5	37.3 (39.9)
15	24.2 (23.9)[a]	9	40.2 (37.1)
2	24.7 (24.5)[a]	12	40.2 (34.7)[a]
7	26.3 (26.1)[a]	13	42.8 (42.5)
6	26.6 (26.3)[a]	25	51.4 (56.4)
16	28.2 (28.0)[a]	17	56.0 (51.2)
4	30.2 (30.0)[a]	14	56.6 (55.8)
1	30.7 (30.5)[a]	3	58.8 (58.5)
22[b]	31.0 (30.8)[a]	24	174.7 (174.4)
23[b]	31.1 (-)[a]		

[a] not assigned by Rensen *et al.*[83]; [b] assignments could be interchanged.

The crystal structure of **4** (Appendix 3) appears very similar to **2** and **3**, except for the different geometry around the carbon C3 and the lack of classical intermolecular hydrogen bonds in **4**. Only weak intermolecular H25c···O24 and H25b···O25 hydrogen bonds were found (symmetry operation x+½, -y+½, -z), the latter being similar to those found in methyl esters of oxocholic acids.[15] Also additional C-H···O interaction can be found between H3b and O24 (x+½, -y+½,

-z+1). The azido group is disordered showing two possible positions for terminal nitrogen N3, as should probably be found also for N2 and N1. In the structure of **5** (Appendix 4) the side chain is disordered, indicating two possible positions for oxygens O24 and O25, as well as for the methyl C25 with hydrogens. The formyl group and especially oxygen O26 show large thermal ellipsoids, also due to disorder. Two molecules form a pair by C-H···O interactions (-x+2, y+½, -z+1) connected to each other with H2a···O24 and H4b···O24 contacts. This pair is further connected to another pair with an H21c···O25 contact (-x+2, y+½, -z+2). These weak interactions of **4** and **5** are illustrated in Figure 12. The crystallinity of powdery products of **4** and **5** was also found to be high.

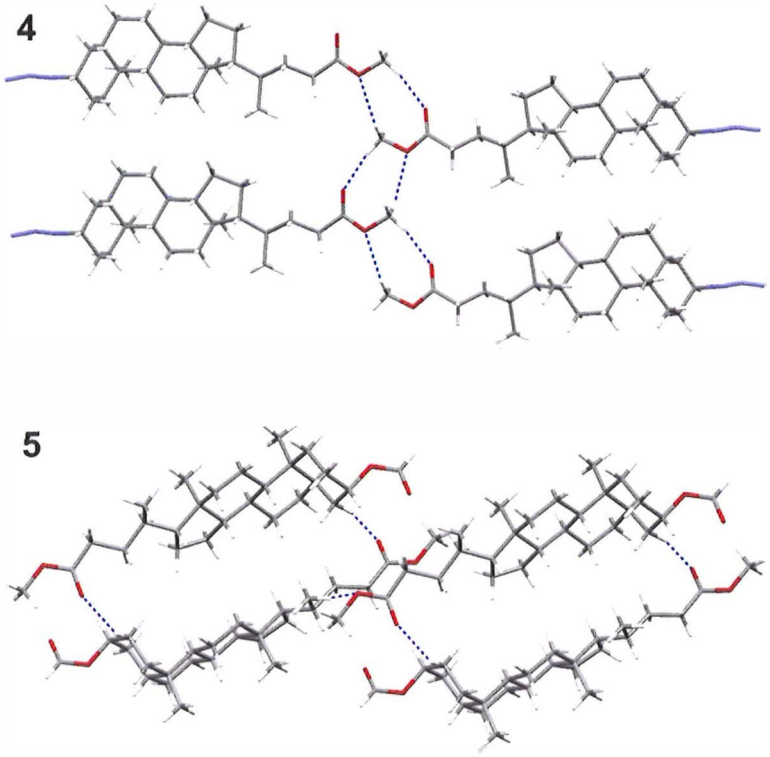

Figure 12. Hydrogen bonding network of compounds **4** and **5**.

In **2–5** the side chain bonded to C17 is in *trans* (or *anti*) conformation, which is observed from the C17-C20-C22-C23 dihedral angles being close to linear (180°).[182] Similar values of this dihedral angle are also found in methyl 3-oxo-5β-cholan-24-oate (**a**) and methyl 3,12-dioxo-5β-cholan-24-oate (**b**),[15] as observed in Table 2. This *trans* conformation seems to be slightly more common in the side chain of cholanoic acid derivatives, according to 1) a short review of the CSD database,[183] 2) related literature by other authors, e.g. Nakano *et al.*[182] or Bertolasi *et al.*,[184] and 3) the results of this thesis. Compounds **c**[174] and **d**[80] (Table 2) show angles closer to intermediate values, while compound **e**[175] has

gauche side-chain conformation, with an angle value close to 60°. The conformation depends on the hydrogen bond interactions of the side chain and the *trans* conformation is favored when the side chain has no hydrogen bonds,[185] being sterically more spacious. A more comprehensive concept of the side-chain conformation can be obtained by examinating all dihedral angles in the side chain. This is often presented as a combination of four angles,[184,186,187] the first four presented in Table 2, using letters *t*, *g* or i for the conformations in question. The major component of **5** has an almost perfect zigzag (all-*trans*, *tttt*) conformation, the minor one being *ttt*i similar to **2-4**. In cholanoic acid derivatives the cyclohexane rings A, B and C are considered rigid, whereas the cyclopentane ring D is more flexible and related to the conformation of the side chain.[168,185] These cholanoate structures also support this view.

Table 2. Side-chain dihedral angles[a] (°) of **2–5** and some related methyl esters.

Dihedral angle	**2**	**3**	**4**	**5**	**a**	**b**	**c**	**d**	**e**
C13-C17-C20-C22	178	179	169	177	172	173	177	178	172
C17-C20-C22-C23	175	177	172	170	168	170	157	148	55
C20-C22-C23-C24	167	166	166	173	67	66	77	72	166
C22-C23-C24-O25	147	145	144	179[c]	165	164	162	67	129
C23-C24-O25-C25	177	178	175	176[c]	180	179	176	175	178
Conformation[b]	*ttt*i	*ttt*i	*ttt*i	*tttt*[c]	*ttgt*	*ttgt*	*ttgt*	*tigg*	*tgt*i

[a] the sign of the angle value ignored; [b] *t* = *trans*, *g* = *gauche*, i = intermediate; [c] major component; **a** = methyl 3-oxo-5β-cholan-24-oate[15]; **b** = methyl 3,12-dioxo-5β-cholan-24-oate[15]; **c** = methyl 3α,7α,12α-trihydroxy-5β-cholan-24-oate ethanol solvate[174]; **d** = methyl 3α,12α-diacetoxy-7α-((3'-iodobenzoyl)oxy)-5β-cholan-24-oate[80]; **e** = methyl 3α,12α-diacetoxy-3',15β-dihydro-cyclopropa(14,15)-5β-chol-8-en-24-oate.[175]

4.1.2 Thermal properties

The thermal behavior of **1–5** was examined by TG and DSC. The results are summarized in Table 3. The compounds **1–3**, differing only in the number of hydroxyl groups in the steroid skeleton, showed melting transitions at 193, 200 and 193 °C, respectively. By changing both the 2,6-dichlorobenzoyloxy group on the 3-position either to azido or formyloxy and with epimerization, the melting points decrease significantly from ~200 °C to 126 °C and 105 °C for compounds **4** and **5**. Some differences can be observed on the second heating scan for the 3α-(2,6-dichlorobenzoyloxy) derivatives: instead of crystallization (either on cooling (**1**) or via glass transition and cold crystallization (**2**)) and remelting, only the glass transition can be observed in compound **3**. The 3β-azido derivative **4** crystallized already partially on cooling and showed both glass transition and cold crystallization on the second heating prior to melting at 126 °C. The 3β-formyloxy derivative **5** also showed glass transition and cold crystallization on the second heating prior to melting.

The thermal decomposition of the compounds **1–5**, except compound **4**, started in the vicinity of 300 °C as can be seen in Table 3. In the case of **4**, the

decomposition started at a slightly lower temperature (238 °C) and progressed more gradually than in the other compounds. The easy loss of gaseous components (e.g. N_2)[181] observed by MS is the most probable reason for this gradual decomposition. These particles are able to create a microatmosphere around the sample, causing it to decompose by charring. Furthermore, the low oxygen content of **4** may also partly favor a more gradual decomposition via charring.

Not many references were found in the literature about the thermal properties of cholanoates or cholanoic acids for a comparison with these results. Zhang *et al.*[188] reported that DSC thermograms of methyl 3α-(11-methacryloyloxy-undecanoyloxy)-7α,12α-dihydroxy-5β-cholan-24-oate and methyl 3α-(11-methacryloyloxy-undecanoyloxy)-5β-cholan-24-oate monomers did not show clear thermal transitions. A few reports contain thermal data of cholanoic acids analyzed by DSC[189-192] and TG.[192,193] The thermal stability of inclusion complexes of CA[193,194] (DSC and TG-DTA-MS) and its adsorption on the multiwalled carbon nanotubes[195] (TG-DTA) have also been investigated. One DSC study about the binding of cholate salts by one bacterial ATP synthase was found.[196] The melting transition temperatures are similar in the investigated cholanoates and corresponding cholanoic acids,[189,193] but no general conclusions about their thermal behavior could be made.

Table 3. The glass transition temperatures, melting points, enthalpy changes and decomposition of compounds **1–5**.

Comp.	Mw.	1st Heating T_x, (ΔH), [ΔC_p]	2nd heating T_x, (ΔH), [ΔC_p]	Dec. (°C)
1	563.61	T_m 193.2 (60.82) [a]	T_m 197.1 (64.49)	283
2	579.61	T_m 200.2 (62.46)	T_g 61.7 [0.36] T_c 120.3 (-41.19) T_m 199.9 (54.36)	303
3	595.61	T_m 193.5 (48.49)	T_g 80.9 [0.32]	299
4	415.62	T_m 126.4 (80.27)	T_g -17.3 [0.30] T_c 13.1 (-30.90) [b] T_m 125.8 (79.01)	238
5	418.62	T_m 104.6 (63.35)	T_g -3.1 [0.29] T_c 42.2 (-38.61) T_m 104.1 (54.79)	279

T_m = melting transition (°C), T_c = crystallization transition (°C), ΔH = enthalpy change (J g^{-1}), T_g = glass-transition (°C) and ΔC_p = heat capacity change [J g^{-1} °C^{-1}]; [a] crystallized on cooling; [b] crystallized partially on cooling.

4.2 *N*-Hydroxyalkyl cholanamides

N-Hydroxyalkyl cholanamides have proven to be biologically interesting and active compounds. Some of them are found to act as antimicrobials and

antifungals[30] and they could also possibly be used in the therapeutic treatment of inflammations and diseases such as cholelithiasis[197,198] and autoimmune diseases.[199-201] These compounds can have an effect on the ileal bile salt transport system.[202] One study claims that pathogenic strains could also biotransform human cholic acid (CA) derivatives to *N*-(2-hydroxyethyl) 3α,7α,12α-trihydroxy-5β-cholan-24-amide (**14**).[203] The ability of these compounds to gel organic solvents[204] and aqueous solutions[47,113] is also significant. *N*-(2-hydroxyethyl) cholanamide moieties have also been used in the preparation of novel biodegradable amphiphilic copolymers,[205] which could potentially be used as drug carriers, and of selective high-affinity ligands,[206] which have shown activity against non-Hodgkin's lymphoma cells. Solid state structures of these compounds are mainly unexplored and, in order to characterize the structure and function of these compounds more extensively, a total of 15 *N*-hydroxyalkyl cholanamides were structurally and thermoanalytically characterized in this thesis.

4.2.1 Preparation

The preparation of *N*-hydroxyalkyl cholanamides **6-20** succeeded rather easily and with moderate to good yields for their structural characterization and thermal analysis. Compounds **6-9**[I] and **18-20** were originally prepared by a reaction of methyl ester with aminoalcohol at room temperature,[134,135] while for compounds **12-15** (later also for **9** and **18-20**) the solvent refluxing method was utilized with improved yields. No other specific optimizations of synthetic conditions were performed. Chenodeoxycholamide derivatives **10** and **11** did not precipitate out from water solution, not even after standing for weeks at room temperature, as the other compounds did in varying quantities. For example, ursodeoxycholamides **12** and **13**, the 3α,7β-dihydroxy epimers of chenodeoxycholamides (3α,7α), as well as cholamides **14** and **15** (3α,7α,12α-trihydroxy), supposed to have a better solubility, precipitated out from water. The reason for this different precipitation behavior remained unclear and known water solubilities of cholanoic acids[207] did not give an explanation. To obtain derivatives **10** and **11** the *N*-hydroxysuccinimide method,[114] which gave desired results also with **16** and **17**, was utilized. A literature search showed that Bundy *et al.*[202] had reported the preparation of compounds **10, 14** and **16** by the EEDQ anhydride method with yields in excess of 60 %. A much simpler preparation of compound **8** with the isobutyl chloroformate anhydride method with a yield of ~90 % was reported by della Valle *et al.*[199,200]

Compound **9** was obtained in three different solid forms depending on the conditions of the synthesis and the reaction time. The first synthetic procedure, with 5 days reaction at room temperature, resulted in the mixture of two forms, which were found to be anhydrous **9** and monohydrate **9a** · H_2O. This procedure has not been successfully repeated, because all subsequent preparation endeavors under these conditions have yielded only the monohydrate **9a** · H_2O. A different monohydrate **9b** · H_2O was obtained with a 65 h reaction, either at room temperature or refluxing temperature (MeOH, ~65 °C), but the yield was better in the latter case (79 %). A recrystallization of these products from an H_2O/EtOH (2:1) mixture yielded only monohydrate **9a** · H_2O and from CH_3CN or *p*-xylene the resulting form was anhydrous **9**. From

compound **15** two different and pure forms were also obtained with similar conditions of synthesis. They were also found to be an anhydrous compound and a monohydrate **15** · H_2O. The product **7** was also assumed to contain a hydrate form, but it was not isolated. Compound **8** crystallized slowly as the $CHCl_3$-solvate monohydrate (**8** · $CHCl_3$ · H_2O) form from its $CHCl_3$ solution. The water in the structure must have its origin in impurities or atmospheric moisture. Further details and evidence of these structural forms and their characterization will be discussed below.

4.2.2 Structures

The pathogenic *Nocardia otitidiscaviarum* strains have been reported by Mukai *et al.*[203] to be able to transform CA to compound **14**. Their sample was isolated from a culture broth and their structure elucidation results from NMR, IR and MS investigations were reported. They obtained a $[M+Na]^+$-ion signal by MS corresponding to that of compound **14**. The reported ^1H and ^{13}C NMR chemical shifts in $CDCl_3$, however, are of doubtful quality. At first, due to the very low solubility of **14** in $CDCl_3$ it was not possible to get a reliable ^1H spectrum, not even in an overnight measurement. Second, they report unusual ^{13}C chemical shifts for the steroidal ring carbons, such as for quaternary C10 (44.3 ppm),[170] and finally, their reported chemical shifts do not correspond to shifts observed in this study. The chemical shifts obtained by us and Mukai *et al.*,[203] measured in different solvents, are collected in Table 4. They show that their compound has the same molecular mass and contains 26 carbons, of which four are oxygen bonded, two quaternary and one carbonyl, but according to the present results it appears that their compound was not the compound **14**. Although the NMR spectra of the present study were obtained from a CD_3OD solution, the divergences could not be otherwise explained.

Table 4. ^{13}C and ^1H NMR chemical shifts (ppm) of **14** compared to literature results.

Carbon	^{13}C δ (lit.[203])	Carbon	^{13}C δ (lit.[203])	Proton	^1H δ (lit.[203])
18	13.1 (12.3)	20	37.0 (35.1)	18	0.72 (0.59)
21	17.9 (18.2)	4	40.7 (34.9)	19	0.92 (0.80)
19	23.3 (22.6)	8	41.2 (40.4)	21	1.03 (0.93)
15	24.4 (26.8)	25	43.1 (49.8)	23a	2.13 (1.98)
9	28.1 (30.9)	14	43.2 (46.8)	9	2.24 (1.23)
16	28.8 (27.8)	5	43.4 (41.5)	4a	2.27 (1.80)
11	29.8 (35.3)	13	47.7 (46.1)	23b	2.3 0(2.05)
2	31.4 (30.4)	17	48.2 (46.1)	25	3.28 (3.22)
22	33.4 (31.7)	26	61.8 (60.0)	3	3.37 (3.55)
23	34.3 (32.5)	7	69.2 (71.0)	26	3.58 (3.32)
6	36.0 (33.4)	3	73.1 (66.2)	7	3.80 (3.65)
10	36.1 (44.3)	12	74.2 (71.4)	12	3.95 (3.80)
1	36.7 (34.9)	24	177.4 (172.7)		

All other *N*-hydroxyalkyl cholanamides **6-13** and **15-20** were also characterized in this work in the liquid state with NMR and spectra with a high resolution were obtained. These preliminary structural characterizations of the synthetic products were accompanied with ESI-TOF MS studies. The spectroscopic properties proved to be mostly similar to other cholanoic acid derivatives with the same acid backbone. The first evidence of the gelation of organic solvents of compound **6** was observed during the NMR analysis, while the acquisition temperature had to be elevated in order to increase the solubility of **6** in $CDCl_3$; when the sample was cooled after the measurement, a gel formed in the NMR tube. A more detailed discussion about the gelation properties is below.

N-Hydroxyalkylamide derivatives of LCA were characterized in the solid state, in the absence of single crystal structures, by ^{13}C CP-MAS and powder x-ray diffraction. Compound **6** was found to have a large amorphous content, while **7** with a longer side chain was more crystalline with much more intense diffraction peaks and ^{13}C resonances. Compound **20** with an amino group was found to be almost completely amorphous. The diffraction patterns of **6**, **7**, **18**, and **19** were significantly different indicating crystal structure forms deviating from each other. Different CP-MAS spectra obtained for the LCA derivatives support the conclusion about structural differences. Any other specific details about the solid state properties of these LCA derivatives were not obtained.

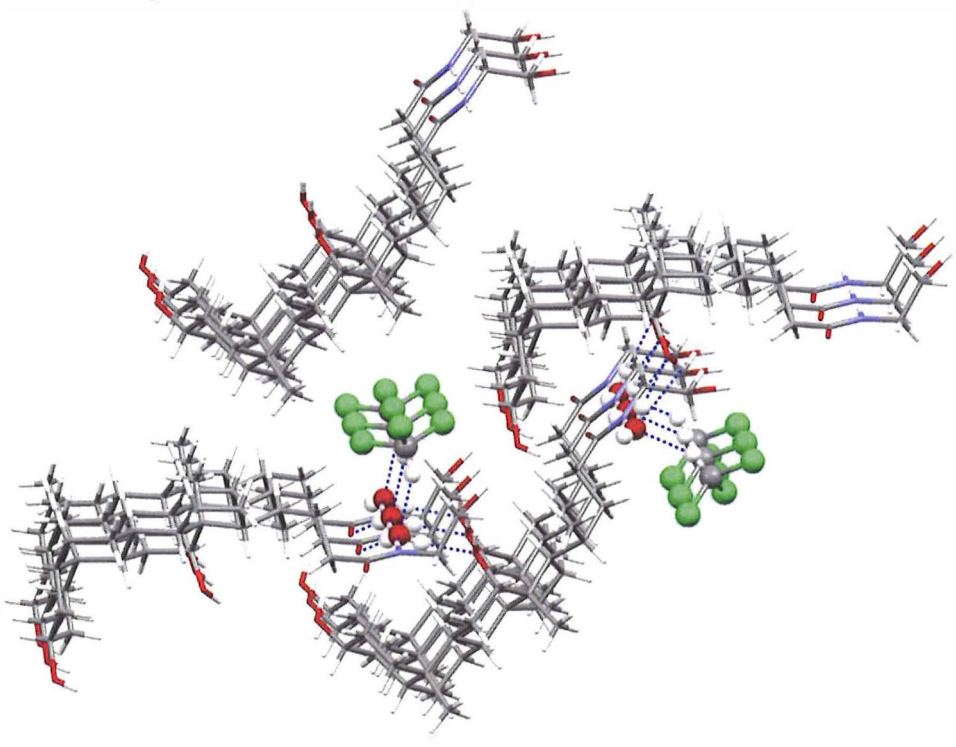

Figure 13. Packing diagram of **8** · $CHCl_3$ · H_2O (all hydrogen bonds not shown). Water and chloroform molecules are emphasized.

For DCA derivative **8**, the standard melting point determination of the product failed, most probably due to the amorphousness of the compound, which was evident in the powder diffraction and CP-MAS studies showing only weak diffraction peaks and broadened resonances. A few single crystals obtained from a chloroform solution contained also $CHCl_3$ and H_2O molecules (Appendix 5). Figure 13 shows that the water molecules are located approximately between the side chains of adjacent steroid units, accepting N-H···O hydrogen bonds, and chloroform is found between the hydrophobic β-faces. The weak C-H···O contact of chloroform to water and O-H···O hydrogen bonds of water to O12 and O24 are also observed in Figure 13. Only five chloroform solvates of steroids with cholanoic acid backbone were found in CSD database,[183] and only one DCA-based cyclic bisimidazolium anion receptor structure[46] was found to contain both $CHCl_3$ and H_2O.

Compound **9** showed an intramolecular hydrogen bond O27-H···O24 (Appendix 6) and a sharp signal at 3620 cm^{-1} in the IR spectrum, indicating the presence of a hydrogen bond-free O-H group similar to cholanoates **2** and **3**. The monohydrate products **9a** · H_2O and **9b** · H_2O showed only a broad O-H stretching absorption (around 3400 cm^{-1}). The free hydroxyl group at 12α in **9** was found also in the single crystal structure. Figure 14 shows the packing diagram of **9**, from which the shortest O12···O12 distance was found to be ~4.4 Å. This free hydroxyl group could be a factor in the easy hydrate formation. In the hydrate **9a** · H_2O (Appendix 7) the hydrogen bond donated by the water molecule was accepted by O12 (Figure 14), as also in **8** · $CHCl_3$ · H_2O. The hydrogen bond donated by the hydroxyl group was accepted by O27 of a neighboring molecule, the same molecule that donates N-H···O contact accepted by the water oxygen. The powder diffraction patterns of **9**, **9a** · H_2O and **9b** · H_2O were different from each other, as were also the ^{13}C CP-MAS spectra, and **9b** · H_2O was found to be less crystalline than the other two forms. The solid obtained from the first synthesis of **9** was also found to be a mixture of **9** and **9a** · H_2O. Similarities between the forms of **8** and **9** were not observed. Unfortunately, a single crystal structure of form **9b** · H_2O was not obtained. The theoretical (B3LYP/6-311G*) ^{13}C NMR parameter calculation was tested for **9** and **9a** · H_2O, starting from their single crystal structures, and was found to be only suggestive, when compared to experimental values. The differences between calculated and experimental shifts could probably be explained by the fact that the shifts were calculated for single molecules in vacuo. The method thus excludes intermolecular interactions between the bile acid molecules. The inclusion of more than one steroidal unit in the calculation would, however, have substantially increased the CPU time needed for the calculations. Reports about more sophisticated methods to calculate NMR chemical shifts starting from single crystal structures with much better correlation were found in the literature,[208,209] including polymorphs of testosterone.[210]

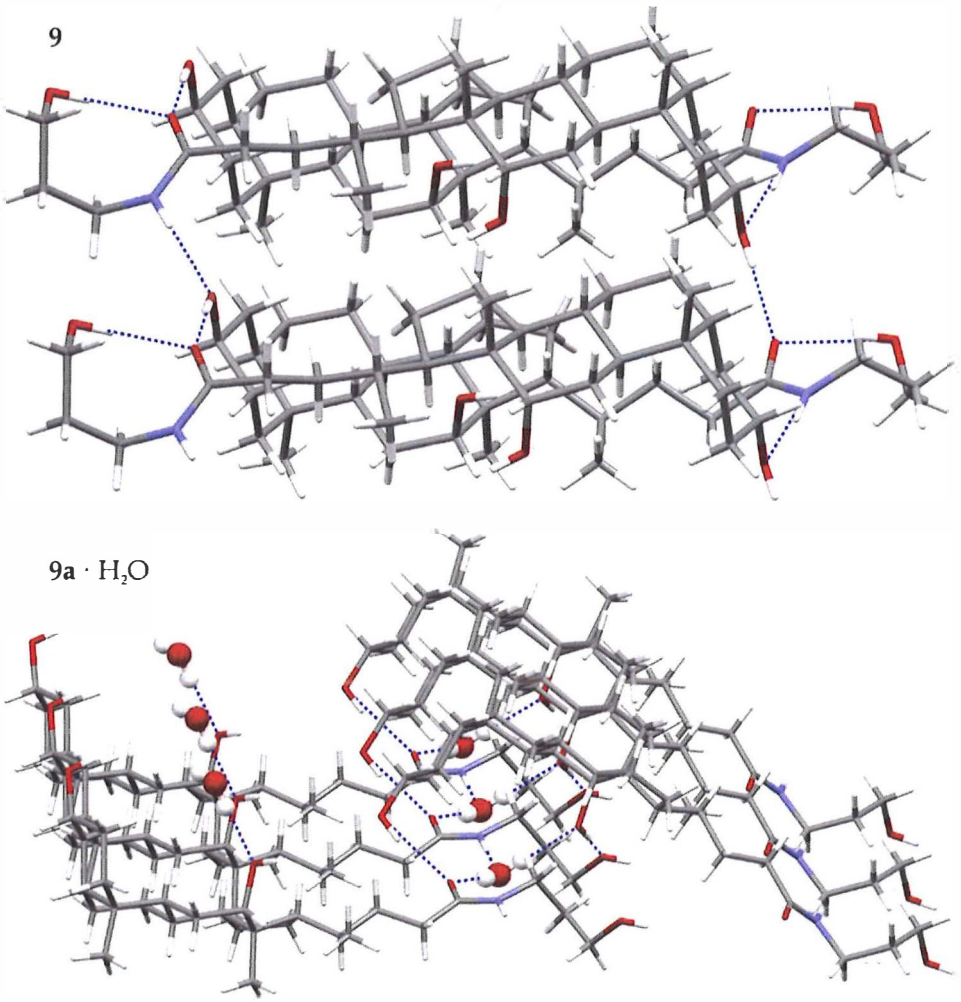

Figure 14. Packing diagrams of **9** and **9a** · H_2O (all hydrogen bonds not shown). Water molecules are emphasized.

The products of CDCA derivatives **10** and **11** from syntheses were completely amorphous, showing no diffraction peaks at all. The resolution of CP-MAS spectra was very poor showing broad ^{13}C signals, but the spectra were almost identical indicating that they were isostructural solid forms. However, compound **11** crystallized out from acetonitrile, showing a similar intramolecular O27-H···O24 hydrogen bond as DCA derivative **9**. This crystalline structure of **11** (Appendix 8) was found isostructural with **9** having also similar unit cell parameters. Most interestingly the hydroxyl group at position 7α in **11** does act neither as a donor nor as an acceptor, similarly to cholanoate **3**, while in **9** the free O-H was observed in position 12α. Figure 15 shows the packing diagram of **11**, from which the shortest O7···O7 distance found was ~6.9 Å. A comparison of Figures 14 and 15 also shows the structural similarity of **9** and **11**.

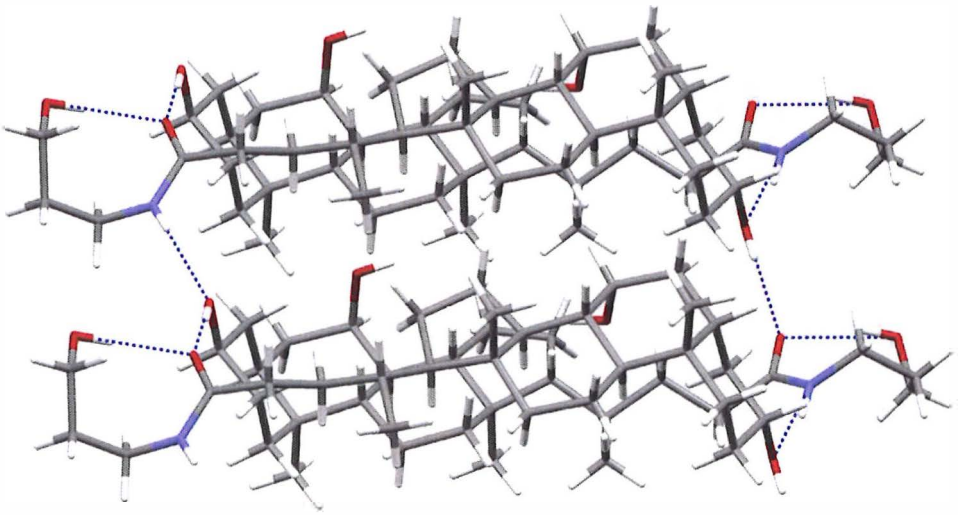

Figure 15. Packing diagrams of **11** (all hydrogen bonds not shown).

Derivatives **12** and **13** carrying the UDCA backbone showed rather similar diffraction patterns. According to single crystal diffraction data, the unit cell dimensions were rather similar but the space group was different, being orthorhombic $P2_12_12_1$ for **12** (Appendix 9) and $P2_1$ of a lower monoclinic symmetry for **13** (Appendix 10), with two crystallographically independent molecules (**13a**, **13b**) in the asymmetric unit. A more precise investigation of the structures, by comparing the geometric parameters and superposition graphics of molecules **12**, **13a** and **13b**, revealed that **12** and **13b** have almost the same conformation, although the hydrogen bond frameworks are different (Figure 16). The structure **13a** was slightly different, practically in the side-chain conformation, but its hydrogen bond framework was very close to that of **12**. The simulated powder pattern of the single crystal structure of **13** had also some similarities with the experimental powder pattern measured from its powdery product, but a different polymorphic form was apparently formed; this in fact was reasonably consistent with an experimental pattern obtained for **12**. This observed inconsistency with the simulated pattern and on the other hand similarity of powder patterns of **12** and **13**, indicated that some pseudoorthorhombic behavior might exist in **13**. It means that in certain conditions compound **13** may also crystallize in orthorhombic space group $P2_12_12_1$ being isostructural with **12**. The structural difference was not extensive and CP-MAS spectra of **13**, taken before and after crystallization from $EtOH/H_2O$ showed significant similarity. The simulated pattern of **12** was also consistent with the experimental one.

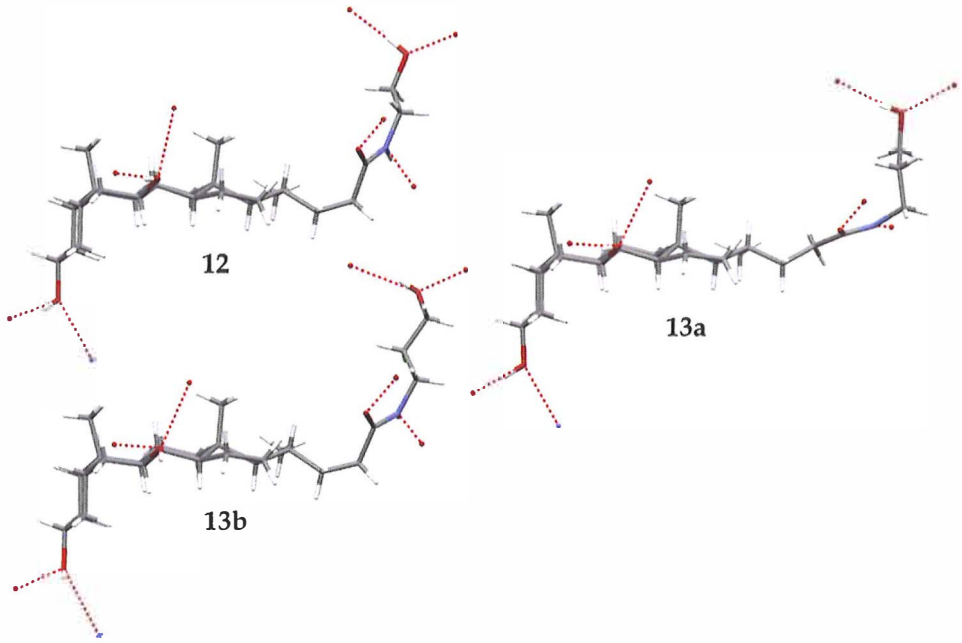

Figure 16. Structures of molecules of **12**, **13a** and **13b**, showing the hydrogen bond directions. Steroidal ring systems superposed before separation.

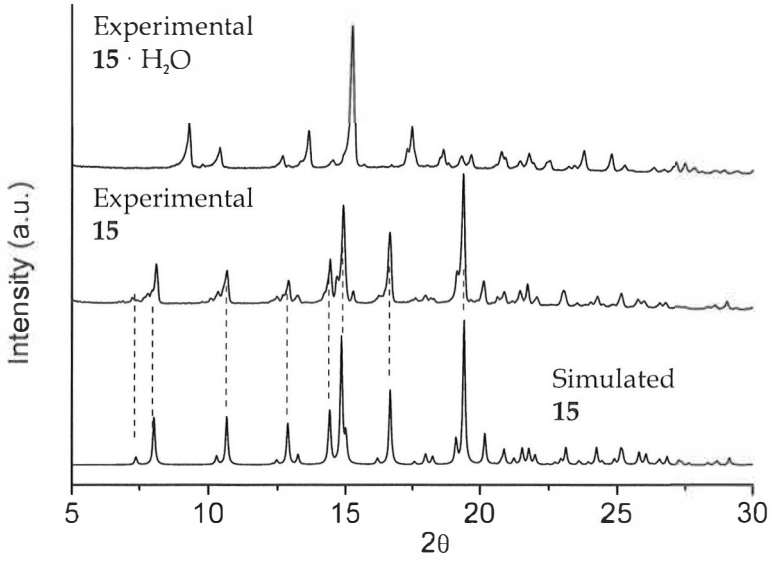

Figure 17. Experimental XRD patterns of **15** and **15** · H_2O with simulated pattern from anhydrous single crystal structure.

Isostructuralism was found between the obtained single crystal forms of CA derivatives **14** (Appendix 11) and **15** (Appendix 12), with the same crystal system and slightly longer cell axes in the latter. The two products of **15**

obtained were found to be different by comparing their diffraction patterns (Figure 17) and ^{13}C CP-MAS spectra. These data were similar for **14** and the first product of **15**, corresponding to the found anhydrous single crystal forms. The second product was found to be of one crystal form, a monohydrate **15** · H_2O, based on the TG analysis discussed below. The recrystallization of the powdery product of **15** led always to the formation of an anhydrous form, even though various organic solvents as well as their aqueous mixtures were tested.

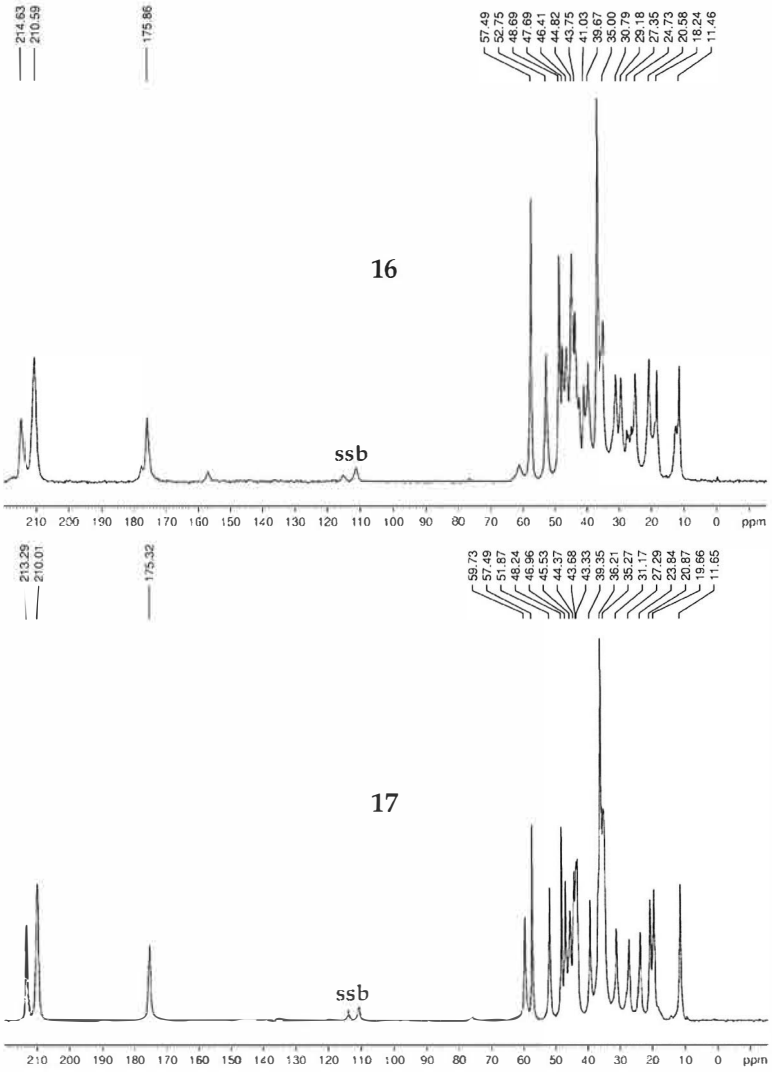

Figure 18. ^{13}C CP-MAS spectra of **16** and **17** (ssb = spinning side band).

Only partial crystallinity was found in DHCA products **16** and **17** according to powder diffraction studies. However, they showed very sharp resonance signals in ^{13}C CP-MAS experiments (Figure 18) indicating a somewhat more ordered content.[211] The spectra appeared to be similar for both

products indicating isostructuralism, but this could not be confirmed due to the lack of adequate crystallographic data.

In the crystallographic studies it was observed that the steroidal ring systems had similar conformations in all structures **8**, **9**, **9a**, and **11-15**. The largest conformational discrepancies occurred in the five-membered ring D, corresponding to the observations by Giglio and Quagliata;[168] this can be easily deduced to arise from differences in the side chain conformation. Discrepancies in the ring D conformations have also some influence on the neighboring C ring, while rings A and B show almost identical conformations. Figure 19 illustrates these observations, and it is easily seen that the deviations increase from left to right. The small substituent in the position 7 or 12 seems to have very small influence on the conformation of the ring system. The side-chain conformations are much less similar. The dihedral angle C17-C20-C22-C23 in **9**, **9a** · H_2O and **11-15** is rather close to 180° as seen from Table 5, establishing a *trans* conformation for the side chain.[168,182] The conformations of the side chains are illustrated in the superposition drawings a) (C26) and b) (C27) in Figure 19, where the different *gauche* conformation of **8** · $CHCl_3$ · H_2O is easily observed. The *trans* conformation was also obtained in the calculations for the HF/6-31G*-optimized structures of **9** and **9a**, where the angle values were -173 ° and -172 °, respectively.

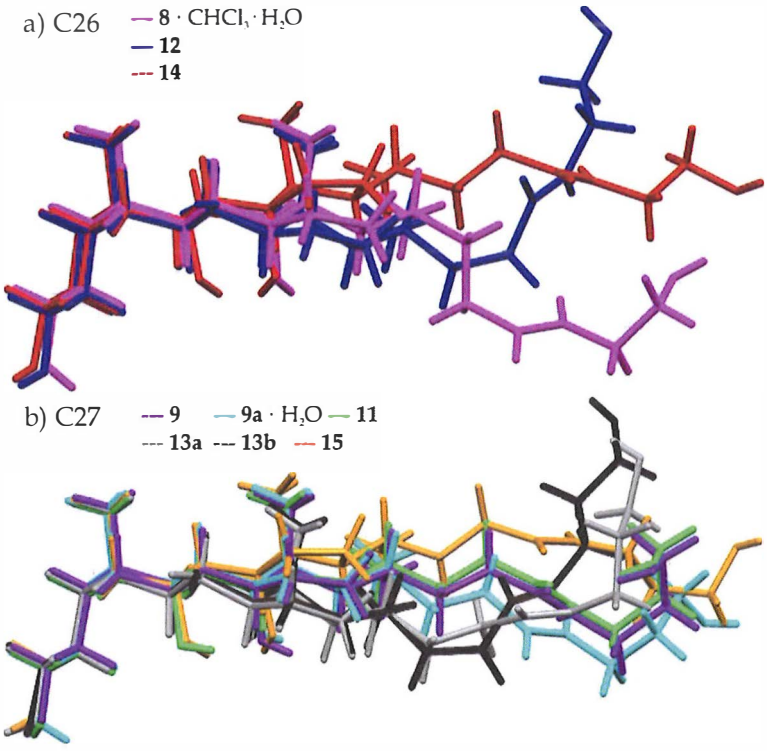

Figure 19. Superposition drawing of the conformations of cholanamides: a) **8** · $CHCl_3$ · H_2O, **12** and **14**; b) **9**, **9a** · H_2O, **13a**, **13b**, and **15**.

In general, all corresponding dihedral angles in structures **12** and **13b** are similar, as well as also in the isostructural pairs **14** & **15** and **9** & **11**. These similarities correlate well with the hydrogen bonding networks found from the structures, which also resemble each other. As seen from Table 5, the side chains of five compounds have a *ttt*i overall conformation, which seems to be rather common in cholanamides. For example, 3α-hydroxy-5β-cholan-24-amide 3-pentanol clathrate,[212] *N*-(*p*-bromo)phenyl 3α,12α-dihydroxy-5β-cholan-24-amide[213] and *N*-isopropyl 3α,7α,12α-trihydroxy-5β-cholan-24-amide[214] have this conformation, while *N*-methyl 3α,12α-dihydroxy-5β-cholan-24-amide hemihydrate[215] is an example of a *tgtg* conformation found also in **8** · $CHCl_3$ · H_2O. The latest structure determination in our laboratory for *N*-[2-([2,2′]-bithiophen-5-ylmethyl)aminoethyl]-3α-hydroxy-5β-cholan-24-amide[216] shows a *ttg*i conformation resembling structure **12**.

Table 5. Dihedral angles of the side chain (°) of *N*-(2-hydroxy)ethyl- and *N*-(3-hydroxy)propyl-cholanamides.

Dihedral angle	**8**[b]	**9**	**9a**[c]	**11**	**12**	**13a**	**13b**	**14**	**15**
C13-C17-C20-C22	176	175	-172	179	176	173	-179	-177	180
C17-C20-C22-C23	65	-172	-178	-170	-177	-173	-179	-165	-164
C20-C22-C23-C24	-178	177	178	180	65	129	67	180	179
C22-C23-C24-N24	-77	123	152	117	-152	167	-158	127	135
C23-C24-N24-C25	-179	-175	175	-177	-179	169	-179	180	174
C24-N24-C25-C26	-118	-98	-96	-97	-129	-84	-111	-133	138
N24-C25-C26-C27	-	60	-72	58	-	-67	-171	-	173
C25-C26-C27-O27	-	55	-66	56	-	-169	175	-	-71
N24-C25-C26-O26	-69	-	-	-	179	-	-	-163	-
Conformation[a]	*tgtg*	*ttt*i	*ttt*i	*ttt*i	*ttg*i	*ttit*	*ttit*	*ttt*i	*ttt*i

[a] *t* = *trans*, *g* = *gauche*, i = intermediate; [b] **8** · $CHCl_3$ · H_2O; [c] **9a** · H_2O

As was mentioned about the structure of **9**, the O-H groups may play a significant role in the hydrate formation. In this study, three pure monohydrate forms of *N*-hydroxyalkyl cholanamides were separated and also one monohydrate with an additional $CHCl_3$ molecule in the crystal lattice was analyzed. The α-face of the cholanoic acid-based molecule, where the most hydroxyl groups are oriented in the same direction, attracts water molecules, but the formation of hydrate is not always favored. The other driving forces, such as a direct hydrogen bond formation between donors and acceptors in the α-faces of two or more steroidal units, are often stronger and the water molecules are left out during the crystallization. According to search results about cholanoic acid, cholanoate and cholanamide hydrates in the CSD database[183] (a total of 36 hydrates) every neutral crystal structure of hydrate has a hydroxyl at position 6α or 12α, or at least a hydrophilic substituent such as D-glucopyranosyl group,[217] attached to that position. This suggests that the position and orientation of the O-H is also significant. Also the hydrates of **8** and **9a** contain an O-H group in the position 12α, as also in **9b** and **15**, but the

crystal structures of the latter pair have not been solved. Although all molecules studied with a hydroxyl at the position 12α were not found to form hydrates, it seems that a 12α hydroxyl is advantageous for hydrate formation in cholanoic acid-based structures. On the other hand, a closer view of cholanamide hydrates found in the literature showed that the water molecule is not necessarily hydrogen bonded to O12, but to the two amide carbonyl oxygens O24 or the four O3.[218] Very definite conclusions should not be made on the basis of these results.

4.2.3 Thermal properties

The thermal properties of the characterized *N*-hydroxyalkyl cholanamide derivatives clearly varied from group to group, and also in each group, according to the side chain length, as seen from Figure 20 and Table 6. The melting temperature of **14** corresponds very well with the melting point reported in the literature (250-253 °C),[202] while those of **10** and **16** do not. The observed low crystallinity of **10** (no mp. observed in this study) and **16** was thought to be the reason for this discrepancy. The increase in the side chain length seems to raise the melting temperature slightly in case of the 3α-hydroxy- (**6**, **7** and **19**), 3α,12α-dihydroxy- (**8**, **9**) and 3,7,12-trioxo-5β-cholanamides (**16**, **17**), but quite the opposite is the case in **12-15,** where the hydroxyl groups are positioned at 3α and 7β (**12**, **13**) or at 3α, 7α and 12α (**14**, **15**). In addition, the presence of a third hydroxyl group in the steroidal ring system **14** and **15** raises the melting temperatures slightly above that found for **12** and **13**. The 3α,7α-dihydroxy derivatives **10** and **11** showed only glass transitions on both heating scans, whereas in 3α,7β-dihydroxy derivatives (**12**, **13**) remarkably higher melting transitions were observed, although both have only a differently oriented hydroxyl group in C7.

The thermal decomposition temperatures of **6-20** increased within each cholanoic acid derivate group (Table 6, Figure 20) so that the compound having a longer side chain length exhibited a higher decomposition temperature. This would be expected due to the slight increase in the molecular weight. The decomposition of most derivatives occurred between 280 and 340°C. As an exception, dehydrocholamides **16** and **17**, and particularly lithocholamide **20**, showed lower decomposition temperatures than were observed for the others. In the case of **20**, an amino group at C27 and, for **16** and **17,** the lack of hydrogen bonding donors on bile acid scaffolds were presumed to be one of the reasons for a lower thermal stability. This hypothesis is supported by the fact that within the lithocholamide group the thermal stability clearly increased from that observed for **20** to compound **19**, where the amino group in C27 is replaced by a hydroxyl group, and by **19** having a similar decomposition temperature as compounds **6** and **7**. Within this group the highest decomposition temperature is observed for **18**, which has the longest side chain with an ether bond functionalization. All other cholanamides, except dehydrocholamides, decompose at a similar or slightly higher temperature than the lithocholamides. Chenodeoxycholamides **10** and **11** decompose at a significantly lower temperature than the isomeric deoxycholamides (**8**, **9**) and ursodeoxycholamides (**12**, **13**). The decomposition temperatures of chenodeoxycholamides and ursodeoxycholamides are also affected by the

different orientation of the hydroxyl group in C7; a similar trend was observed in their melting behavior.

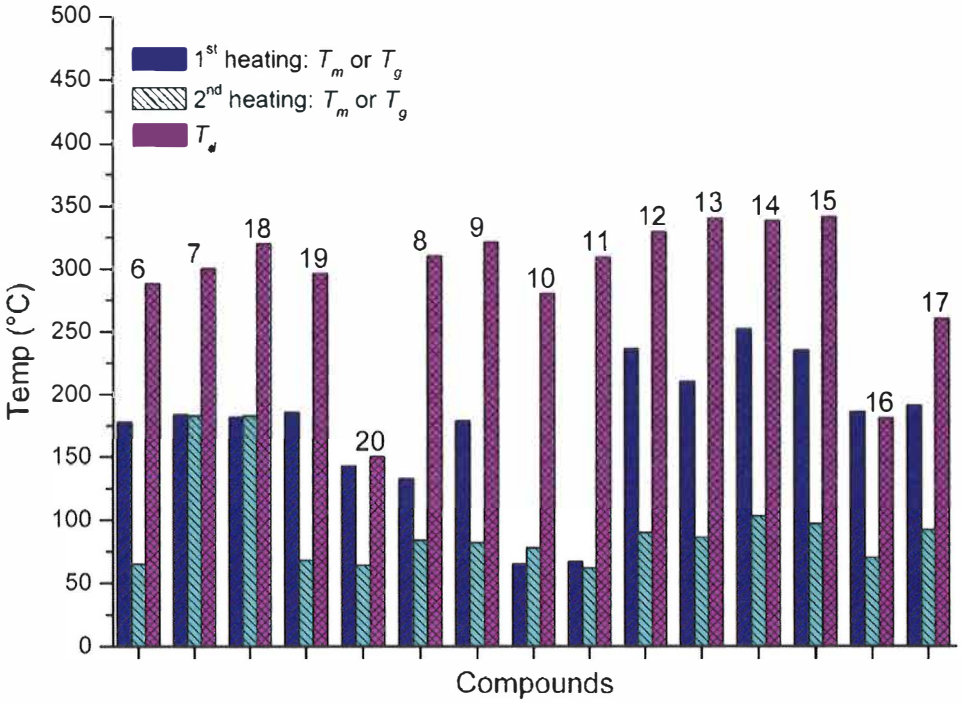

Figure 20. Bar graph representation of melting, glass-transition and decomposition temperatures of compounds **6-20**. The heights of the bars of 1st and 2nd scans represent the highest observed thermal transition (T_m or T_g).

As mentioned in the discussion about the thermal properties of cholanoates, the literature data of cholanoic acids and their derivatives are scarce. No references about cholanamides were found for a comparison with the results of their thermal properties (DSC, TG). Compared to cholanoates **1-5** only compounds **16** and **20** have notably lower decomposition temperatures. The melting transition temperatures of cholanamides are similar, as is the case with **1-3**, except in the case of semicrystalline **8**. Otherwise the observed thermal properties of cholanamides and cholanoates show similar features.

Table 6. Thermal transitions, ΔHs, ΔC_ps and decomposition temperatures of *N*-hydroxyalkyl cholanamides **6-20**.

Sample	Mw.	1st heating T_x, (ΔH); T_g, [ΔC_p]	2nd heating T_x, (ΔH); T_g, [ΔC_p]	Dec. (°C)
6	419.65	T_m 178.4 (29.46)	T_g 65.0 [0.18]	288
7	433.68	T_{dh} 168.98 (7.40) T_c 175.92 (-3.42) T_m 184.06 (39.58)	T_g 59.63 [0.16] T_c 140–175 (-4.64) T_m 183.08 (3.14)	300
8	435.65	T_g 67.01 [0.26] T_m 132.88 (4.71)[a]	T_g 84.21 [0.26]	310
9	449.68	T_m 179.2 (96.12)	T_g 81.5 [0.49]	326
9a · H_2O	467.69	T_{dh}+ T_m 115.4 (147.78) T_c 144.0 (-35.97) T_m 178.7 (88.51)	T_g 82.5 [0.58]	313
9b · H_2O	467.69	T_{dh} + T_m 116.3 (88.16)	T_g 80.1 [0.56]	323
10	435.65	T_g 64.8 [0.34]	T_g 77.61 [0.20]	280
11	449.68	T_g 66.8 [0.41]	T_g 82.6 [0.18]	309
12	435.65	T_m 236.3 (59.13)	T_g 89.6 [0.21]	329
13	449.68	T_m 210.4 (53.92)	T_g 85.8 [0.25]	340
14	451.65	T_m 252.3 (71.15)	T_g 103.1 [0.26]	338
15	465.68	T_m 235.3 (61.36)	T_g 96.6 [0.27]	341
15 · H_2O	483.69	T_{dh} 124.5 (44.87) T_m 236.1 (64.06)	T_g 98.1 [0.23]	341
16	445.60	T_m 185.9 (52.24)[d]	T_g 69.9 [0.16] T_c 104.3 (-15.51)[e] T_m 171.8 (13.18)[e]	181
17	459.63	T_m 191.4 (40.05)	T_g 92.3 [0.19]	260
18	463.71	T_m 182.10 (40.05)	T_g 43.29 [0.11] T_c 93.14 (-21.44) T_m 183.62 (41.70)	320
19	449.68	T_m 186.05 (45.46)	T_g 67.81 [0.14]	296
20	448.70	T_{dh} 72-143 (38.87)[b] T_m 143 (18.79)[c]	T_g 64.4 [0.16]	150

T_m = melting; T_c = crystallization; T_{dh} = dehydration transition (°C) and ΔH = enthalpy change (kJ mol^{-1}); T_g = glass-transition (°C) and ΔC_p = heat capacity change [kJ mol^{-1} °C^{-1}]; [a] Only very weak melting transition was observed occasionally; [b] Based on TG analysis, release of solvent or dehydration (Δwt-% = ~6.5%) followed by melting; [c] T_m taken as peak maximum due to broad transition; 131-148°C; [d] Decompose on melting; [e] Taken from a heating-cooling cycle, in which a turning point set in the middle of melting transition to prevent decomposition.

The pseudopolymorphs of **9** (**9a** · H_2O and **9b** · H_2O) were also examined by TG/DTA and DSC (Table 6). The solid first obtained from a synthesis, a mixture of forms **9** and **9a** · H_2O, showed concurrent dehydration and melting of the monohydrate form, and then a subsequent recrystallization to the anhydrous form **9**, the melting transition of which was finally observed at ~179 °C. The melting temperature observed is consistent with the results from the melting point determinations (178.5-179.5 °C).[I] The monohydrates **9a** · H_2O and **9b** · H_2O also showed concurrent melting and dehydration transitions having onsets at ~115-116 °C. Typically, the dehydration of solid **9b** · H_2O was initiated at somewhat lower temperatures (40–50 °C) than that of solid **9a** · H_2O, for which the dehydration was initiated at ~80-90 °C. In the TG curves the weight loss corresponding to the dehydration on **9b** · H_2O was found to be clearly more gradual than that of **9a** · H_2O. Attempts to obtain separate melting transitions for both hydrate forms by using a faster heating rate and hermetically sealed pans to prevent the initiation of dehydration resulted in melting onsets of 143 °C for **9a** · H_2O and 139 °C for **9b** · H_2O. The consequent crystallization transition to the anhydrous form **9** was readily observed after the dehydration of the monohydrate **9a** · H_2O. The same event was observed only occasionally in **9b** · H_2O, typically if slow heating rates were used. Probably in the case of the clearly more crystalline monohydrate **9a** · H_2O, the remaining seeds for further crystallization are more likely available at the dehydration/melting than in the less crystalline hydrate **9b** · H_2O. For comparison, the monohydrate **15** · H_2O was dehydrated and structurally reordered to **15** at ~125°C (Table 6) without a melting-crystallization event. The observed weight losses in the dehydration in these three monohydrates obtained were ~4.0 wt-% for **9a** · H_2O, 3.3–3.7 % for **9b** · H_2O and ~3.5 % for **15** · H_2O, which correlated well with a theoretical wt-% of 3.7 - 3.8 for the dehydration.

4.2.4 Gelation properties

The synthetic powdery products **6-9** were found to form gels in some chlorinated and aromatic solvents, such as chloroform, chlorobenzene and toluene. Products **6** and **8** were the most effective gelators, while **7-9** formed stable gels only in chlorobenzene. For example, low critical solution concentration (LCSC) determinations showed that the gels from compound **6** are stable at concentrations as low as 0.8% (w/v) in aliphatic chlorinated solvents and 0.5% (w/v) in chlorobenzene. The low critical solution temperature (LCST), at which the gel starts to disappear, is close to 45 °C for chloroform, around 55–60 °C for other aliphatic chlorinated solvents, and around 70 °C for chlorobenzene. Some experiments to study the ability of these compounds to thicken water solutions were attempted and such phenomena were weakly observed for neutral and acidic solutions, but unfortunately their solubility in the aqueous media was too poor.

Further experiments on the gelation properties indicated that the gels formed were not single-component gels. The first synthetic solid of **9**, which was utilized in these gelation tests, was found to be a mixture of the anhydrous form **9** and the monohydrate form **9a** · H_2O according to extensive x-ray diffraction, ^{13}C CP-MAS NMR and thermoanalytical studies. The reason for the observed gelation properties was found to be this mixture, most probably a co-

operative action of these two pseudopolymorphs and/or water. Pure forms **9**, **9a** · H_2O or **9b** · H_2O were not able to induce any observable gelation effects. Still, the detailed mechanism of the gel formation of these cholanamide products remained unknown and products **6-8**, which were also found to form gels, were not found to contain significant amounts of second forms. Only product **7** was observed to contain some hydrate form. The presence of traces of water can be the factor that helps the aggregation of supramolecular hydrogen-bond network, which is often crucial for gel formation. Furthermore, no other investigated *N*-hydroxyalkyl cholanamides **10-20** showed any gelation properties, except in some alcohol/water solutions, but these gels were not stable. However, the related literature shows that compounds of this type are able to form stable gels and that the number of hydroxyl groups on the steroidal ring system is important for the gelation. Amide linkages can also cause aggregation processes.[47,113,204] Such linkages are of course not necessary for the gelation ability of cholanoic acid derivatives.

4.3 Cholaphanes and their intermediates

Cholaphanes, bile acid-derived macrocycles, which consist of steroidal units joined together by various spacer groups, have been continuously in the focus of supramolecular chemistry owing to their versatile properties.[119,134,219-224] One way to tailor a bile acid derivative suitable for cation recognition is to attach a crown ether type moiety either directly to a hydroxy group of a bile acid[225] or by bridging together two steroidal hydroxyls by a polyalkoxy chain.[226] Moreover, various crown ethers and bile acid derivatives are used as building blocks for synthetic ion channels and pores.[227] One future objective for synthesizing ionophorous bile acid macrocycles could also be their suitability for the preparation of ion-selective electrodes.[228] Recently, cholaphane host molecules containing pyridine moieties are reported to have an ability to bind Xavin analogues.[45] These cited properties of cholaphanes inspired the present author to investigate the structures, and alkali as well as earth alkaline metal cation binding properties, of two novel lithocholaphanes with aromatic and alkoxy/aminoalkoxy building blocks.

4.3.1 Structures

The structures of lithocholaphanes **25** and **30** (Figure 21) and their intermediates **21-24** and **26-29** were investigated by liquid state NMR and MS spectroscopy and molecular modeling. Of course, the complete ^{1}H NMR spectral assignment of the steroidal skeleton is very difficult due to seriously overlapping signals, especially in the case of cholaphanes, and such assignments were not performed. The ^{13}C NMR chemical shift assignments of lithocholaphanes **25** and **30** and precursor **21** (of the former) were based on the large amount of reference data[170] and also on extensive correlation spectroscopy. In order to ascertain the molecular weights of **25**, **29** and **30** ESI-TOF MS measurements were performed. Lithocholaphanes and their melting transitions were also investigated by DSC. The precursor **21** is a known synthetic intermediate, utilized recently in the preparation of cholane-based polyamine macrocycles[229]

and other 3,24-substituted cholane derivatives.[143,230-232] The NMR spectra obtained corresponded very well with the literature data,[143,230] as did also the melting point.[233] The benzyl lithocholate derivative **26** is also a known synthetic intermediate[88,96,234] and the ^{1}H NMR spectrum obtained was found to be congruent with literature data.[88,96] The structural characterizations of the other precursors have not been previously published.

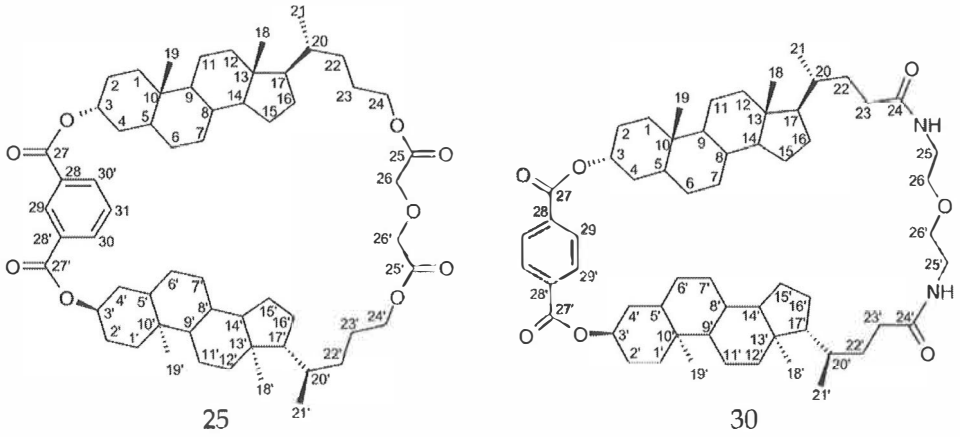

Figure 21. Structures and numbering of cholaphanes **25** and **30**.

In the molecular modeling studies the simulated annealing runs for **30** led to three conformations, which were further optimized semiempirically. For **25** only one conformation was found using molecular dynamics simulations. The diameter of the cavity of **30** is smaller than the cavity of **25**. The width of the cavities is more or less the same, whereas the cavity of **25** is almost 2.5Å longer than that of **30**.

4.3.2 Cation binding

Lithocholaphanes **25** and **30**, with aromatic and alkoxy/aminoalkoxy building blocks, offer proper binding sites, for example, for alkali and earth alkaline metal cations. This ability of lithocholaphane ligands with alkali metal cations was investigated by mixing equimolar amounts of LiCl, NaCl, KCl, and RbCl solutions, respectively, with the ligand solution. The resulting solution was thoroughly mixed and the measurement performed with ESI-TOF MS after 15 minutes. Similarly, as for ionophorous lacalosid-derived antibiotic,[235] as well as for maleonitrile thiacrown ethers,[236] alkali metal adducts with **25** and **30** were also detected in competitive ESI-TOF$^+$ MS binding studies (Appendices 13 and 14). Adducts observed in these studies are listed in the Table 7. According to the results it seems that **25** does not show significant selectivity towards any of the alkali metal cations investigated. On the other hand, ligand **30** seemed to possess some selectivity towards cations with smaller ionic radii, although all the ions were detected. In order to confirm this observation, the adduct formation tendency of the ligand with some earth alkaline metal cations was studied as well (Table 7, Appendix 15). The most intense ion in this series was

the adduct ion $[M-H+Mg]^+$. The ionic radius of Mg^{2+} is ca. 65 pm, close to that of Li^+, which is approximately 60 pm. The intensity of the adduct ion formed with Sr^{2+} was practically negligible, as was that of the one formed with Rb^+ in the alkali metal cation series. These results suggest that the cavity of **30** is smaller than that of **25**, thus preventing the binding of cations with larger ionic radii. On the other hand, this favors the binding of cations with a relatively small ionic radius (60–65 pm). Furthermore, the pyridinium, tetraalkyl-, and dialkyldiarylammonium cations tested did not show significant adduct formation with **25** and **30** in the ESI-TOF$^+$ MS experiments.

Table 7. Observed adduct ions in ESI-TOF$^+$ MS experiments of **25** and **30**.

	Ion	*m/z*	Intensity (%)
25	$[M+Li]^+$,	959.66	18.1
	$[M+Na]^+$,	975.62	61.3
	$[M+K]^+$,	991.61	100
	$[M+Rb]^+$	1037.52	42.5
30	$[M+Li]^+$,	957.66	100
	$[M+Na]^+$,	973.66	46.9
	$[M+K]^+$,	989.64	6.9
	$[M+Rb]^+$	1035.61	0.9
30	$[M+H]^{+a}$	951.65	29.4
	$[M-H+Mg]^+$	973.61	100
	$[M-H+Ca]^+$	989.58	6.3
	$[M-H+Sr]^+$	1037.57	2.5

[a] observed with alkaline earth cations

More accurate information about the relative scale of affinity of the ligands **25** and **30** for the different cations could have been obtained by mixing the ligand with equimolar amounts of two cations X and Y in order to establish the affinity of the ligand for the cation X with respect to Y. In a second experiment the cations should have been X and Z, etc. This method was successfully utilized for CA- and LCA-derived dimers in an investigation of their alkaline metal cation binding ability by Joachimiak and Paryzek.[237] Another method would have been the preparation of $[ligand(X,Y)]^{2+}$ complexes, their isolation and following MS/MS experiments. This more accurate method to investigate the relative affinity of the ligand to X or Y is much more difficult to perform. These relative competition studies were not performed in our preliminary study, which was concentrated on the synthesis and structures of **25** and **30**.

The geometries obtained in molecular modeling studies for the alkali metal ion adducts lowest in energy for both cholaphanes **25** and **30** are shown in Figure 22. In the case of **25** the alkali metal cations with a smaller ionic radius (Li^+ and Na^+) resettled outside the cholaphane cavity. The carbonyl oxygens of the carboxymethoxyacetyl spacer seem to form a "tweezer-like" arrangement, which pinches the cations between the partially negatively charged oxygen atoms. On the other hand, K^+ and Rb^+ thrive inside the cholaphane cavity. The

carbonyl oxygens of the carboxymethoxyacetyl spacer seem to be responsible for the electrostatic attraction of the positively charged ions in these cases as well, except that they are oriented towards the cavity instead of pointing outwards from it. In the case of **30**, Li^+ and Na^+ ions exhibiting smaller ionic radii fit nicely in a partially negatively charged "pocket" formed by the carbonyl and ether oxygens of the (2-amidoethoxy)ethylamido spacer. The alkali metal cations with a larger ionic radius (K^+ and Rb^+), move outside the cholaphane cavity resettling to the close vicinity of the carbonyl oxygen of the (2-amidoethoxy) ethylamido spacer.

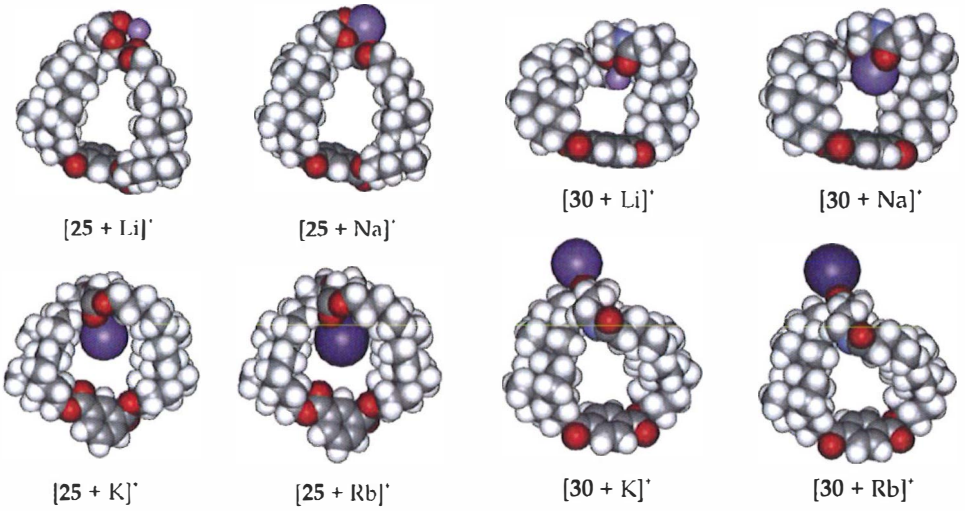

Figure 22. The optimized geometries of the adducts formed by **25** and **30** with the alkali metal ions Li^+, Na^+, K^+, and Rb^+, respectively.

The molecular modeling results support the mass spectrometric ones, according to which cholaphane **25** willingly formed adducts with all of the four alkali metal cations, whereas cholaphane **30** excluded the ions with larger ionic radii. Based on molecular modeling results, K^+ and Rb^+ are located inside the cavity in the case of **25**, whereas Li^+ and Na^+ are sited outside the cavity. Cholaphane **30** behaves oppositely; the cations with smaller ionic radii are inside the cavity, whereas K^+ and Rb^+ are outside. Most probably the arrangement with the cation inside the cavity corresponds to an adduct detected by mass spectrometric measurements. According to the present molecular modeling calculations the tendency of **25** to form adducts with cations located outside the cavity could be explained by the favorable coordination environment of two carbonyls and one ether oxygen of cholaphane **25**. Cholaphane **30** provides only one carbonyl oxygen for the electrostatic interaction for cations sited outside the cavity resulting in a remarkably less stable adduct.

5 CONCLUSIONS

Bile acids are metabolic products of cholesterol. In humans all bile acids are cholanoic acids containing 24 carbons, a *cis* A/B ring juncture, and the carboxyl group at the end of the side chain at position 24. They are conjugated *via* an amide bond to sodium salts of glycine or taurine and play a significant role in the digestion of lipophilic substances in the human intestines. The exact structures of cholanoic acid derivatives are often difficult to obtain because they frequently solidify out from solutions in forms unsuitable for single crystal x-ray structural studies. However, NMR spectroscopy in liquid and solid state together with powder x-ray diffraction opens a direct and pharmaceutically very important way for studies of bile acid derivatives. These studies enable the characterization of the structures, including possible polymorphs and pseudopolymorphs, of many bile acid derivatives, particularly when utilized together with TG and DSC.

In this study five 3-substituted methyl cholanoate ester, fifteen *N*-hydroxyalkyl cholanamide, and two cholaphane derivatives of cholanoic acids were prepared for structural characterization. Twelve new crystal structures of cholanoic acid derivatives were determined. These crystal structures included four cholanoate and six cholanamide derivatives, as well as one cholanamide hydrate and one hydrated chloroform solvate of cholanamide. These structures have similar steroidal ring conformations, but their side chain orientations vary widely. Solid state NMR and powder x-ray data were recorded for all cholanoate and cholanamide derivatives. All these solid state studies together revealed the formation of three different hydrates and one hydrated choloform solvate of cholanamides in addition to anhydrous products. The formation of hydrates was confirmed by thermal studies of all products. The thermal studies showed also that the number and orientation of hydroxyl groups have a significant effect on the melting and decomposition temperatures. For example,

chenodeoxycholamides **10** and **11** decompose at a significantly lower temperature than the isomeric deoxycholamides (**8**, **9**) and ursodeoxycholamides (**12**, **13**).

All synthetic products and intermediates **1-30** were characterized by liquid state NMR and most of them also with ESI-TOF MS. The results of previously analyzed products **1-3**[145] were not included in this thesis. The NMR characterizations found in the literature for products **4**[83] and **14**[203] were found inaccurate and they were corrected. The molecular weights were confirmed by MS; in addition dissimilar cation binding was observed in cholaphanes **25** and **30**. Compound **25** did not show significant selectivity towards any of the alkali metal cations, while ligand **30** seemed to possess some selectivity towards cations with smaller ionic radii. Similar results were obtained with alkaline earth metal cations for **30**, but the relative affinities of ligands towards different cations could not be established in the experiments performed. Molecular modeling studies showed results congruent with MS for both cholaphanes. Lower energy adducts located inside the cavity were found with cations with higher ionic radii for **25**, while for **30** the smaller cations were favored.

In addition to the structure determinations, the gelation properties of *N*-hydroxyalkyl cholanamide derivatives **6-20** were briefly investigated. The powdery products **6-9** were found to gel some aromatic and chlorinated solvents. The crystallized forms **9**, **9a** · H_2O or **9b** · H_2O were not able to cause any observable gelation effects. The powdery product **9** inducing gelation was found to be a mixture of anhydrous form **9** and **9a** · H_2O and, therefore, the gelation was probably caused by co-operative action of these two pseudopolymorphs and/or water. Products **10-20** did not show any gelation effects.

REFERENCES

1. W.H. Elliott, P. Eneroth, S.L. Hsia, D. Kritchevsky, A. Kuksis, J.T. Matschiner, P.P. Nair, R. Ryhage, J. Sjövall, D. Small. In: D. Kritchevsky, P.P. Nair (Eds.), *The Bile Acids: chemistry, physiology, and metabolism*, vol. 1, Plenum Press, New York, 1971.
2. E. Virtanen, E. Kolehmainen, *Eur. J. Org. Chem.* **2004**, 3385-3399.
3. A. Ehnsen, W. Kramer, G. Wess, *Drug Discovery Today* **1998**, *3*, 409-418.
4. S. Mukhopadhyay, U. Maitra, *Curr. Sci.* **2004**, *87*, 1666-1683.
5. A. Moschetta, F. Xu, L.R. Hagey, G.P. van Berge-Henegouwen, K.J. van Erpecum, J.F. Brouwers, J.C. Cohen, M. Bierman, H.H. Hobbs, J.H. Steinbach, A.F. Hofmann, *J. Lipid Res.* **2005**, *46*, 2221-2232.
6. H. Bernstein, C. Bernstein, C.M. Payne, K. Dvorakova, H. Garewal, *Mutat. Res.* **2005**, *589*, 47-65.
7. J. Tamminen, E. Kolehmainen, *Molecules* **2001**, *6*, 21-46.
8. D. Albert, M. Feigel, *Tetrahedron Lett.* **1994**, *35*, 565-568.
9. D. Albert, M. Feigel, *Helv. Chim. Acta* **1997**, *80*, 2168-2181.
10. D. Albert, M. Feigel, J. Benet-Buchholz, R. Boese, *Angew. Chem. Int. Ed. Engl.* **1998**, *37*, 2727-2729.
11. G. Kakiyama, H. Tamegai, T. Iida, K. Mitamura, S. Ikegawa, T. Goto, N. Mano, J. Goto, P. Holz, L.R. Hagey, A.F. Hofmann, *J. Lipid Res.* **2007**, *48*, 2682-2692.
12. D.W. Russell, *Annu. Rev. Biochem.* **2003**, *72*, 137-174.
13. L.F. Fieser, S. Rajagopalan, *J. Am. Chem. Soc.* **1950**, *72*, 5530-5536.
14. M.N. Mitra, W.H. Elliott, *J. Org. Chem.* **1968**, *33*, 175-181.
15. E. Virtanen, A. Valkonen, J. Tamminen, E. Kolehmainen, *J. Mol. Struct.* **2003**, *650*, 201–212.
16. D. Verzele, A. Madder, *Eur. J. Org. Chem.* **2007**, 1793-1797.
17. T.S. Rodriguez, D.G. Giménez, R. de la Puerta Vázquez, *Phytomedicine* **2002**, *9*, 687-693.
18. Nonappa, U. Maitra, *Org. Biomol. Chem.* **2008**, *6*, 657-669.
19. K. Miki, N. Kasai, M. Shibakami, S. Chirachanchai, K. Takemoto, M. Miyata, *Acta Crystallogr.* **1990**, *C46*, 2442-2445.
20. S. Scalia, J.R. Williams, J.-H. Shim, B. Law, E.D. Morgan, *Chromatographia* **1998**, *48*, 785-789.
21. P.W. Swaan, K.M. Hillgren, F.C. Szoka Jr., S. Øie, *Bioconjugate Chem.* **1997**, *8*, 520-525.
22. L.A.J.M. Sliedregt, P.C.N. Rensen, E.T. Rump, P.J. van Santbrink, M.K. Bijsterbosch, A.R.P.M. Valentijn, G.A. van der Marel, J.H. van Boom, T.J.C. van Berkel, E.A.L. Biessen, *J. Med. Chem.* **1999**, *42*, 609-618.
23. J.J.G. Marin, M.R. Romero, M. Vallejo, M.J. Monte, *Cancer Ther.* **2005**, *3*, 57-64.
24. R. Paschke, J. Kalbitz, C. Paetz, M. Luckner, T. Mueller, H.-J. Schmoll, H. Mueller, E. Sorkau, E. Sinn, *J. Inorg. Biochem.* **2003**, *94*, 335-342.
25. M.R. Ruff, J.M. Hill, L.D. Kwart, C.B. Pert, *US Pat. Appl.* **1995**, US5446026.

26. F. Berlati, G. Ceschel, C. Clerici, R. Pellicciari, A. Roda, C. Ronchi, *World Pat. Appl.* **1994**, WO9400126.
27. M.R. Romero, M.C. Martinez-Diez, M.G. Larena, R.I.R. Macias, M. Dominguez, C. Garcia-Monzon, M.A. Serrano, J.J.G. Marin, *Antiviral Chem. Chemother.* **2002**, *13*, 371-380.
28. A.M. Bellini, M.P. Quaglio, G. Cavazzini, R. Ceccherini, *Farmaco Ed. Sci.* **1984**, 39, 305-315.
29. B.A. Marples, R.J. Stretton, *World Pat. Appl.* **1990**, WO9013298.
30. B.G. Hazra, V.S. Pore, S.K. Dey, S. Datta, M.P. Darokar, D. Saikia, S.P.S. Khanuja, A.P. Thakur, *Bioorg. Med. Chem. Lett.* **2004**, *14*, 773-777.
31. D.B. Salunke, B.G. Hazra, V.S. Pore, M.K. Bhat, P.B. Nahar, M.V. Deshpande, *J. Med. Chem.* **2004**, *47*, 1591-1594.
32. D.B. Salunke, B.G. Hazra, V.S. Pore, M.V. Deshpande, B.P. Nahar, *US. Pat. Appl.* **2005**, US05222115.
33. C. Li, A.S. Peters, E.L. Meredith, G.W. Allman, P.B. Savage, *J. Am. Chem. Soc.* **1998**, *120*, 2961-2962.
34. C. Li, L.P. Budge, C.D. Driscoll, B.M. Willardson, G.W. Allman, P.B. Savage, *J. Am. Chem. Soc.* **1999**, *121*, 931-940.
35. A. Rehman, C. Li, L.P. Budge, S.E. Street, P.B. Savage, *Tetrahedron Lett.* **1999**, *40*, 1865-1868.
36. P.B. Savage, C. Li, U. Taotafa, B. Ding, Q. Guan, *FEMS Microbiol. Lett.* **2002**, *217*, 1-7.
37. C. Salmi, J.M. Brunel, *Expert Opin. Invest. Drugs* **2007**, *16*, 1143-1157.
38. P.E. Kish, Y. Tsume, P. Kijek, T.M. Lanigan, J.M. Hilfinger, B.J. Roessler, *Mol. Pharmaceutics* **2007**, *4*, 95-103.
39. I.S. Blagbrough, A.J. Geall, A.P. Neal, *Biochem. Soc. Trans.* **2003**, *31*, 397-406.
40. E. Campazzi, M. Cattabriga, L. Marvelli, A. Marchi, R. Rossi, M.R. Pieragnoli, M. Fogagnolo, *Inorg. Chim. Acta* **1999**, *286*, 46-54.
41. N.M. Sangeetha, U. Maitra, *Chem. Soc. Rev.* **2005**, *34*, 821-836.
42. M. Miyata, N. Tohnai, I. Hisaki, *Acc. Chem. Res.* **2007**, *40*, 694-702.
43. V.K. Khatri, M. Chahar, K. Pavani, P.S. Pandey, *J. Org. Chem.* **2007**, *72*, 10224-10226.
44. P. Chattopadhyay, P.S. Pandey, *Bioorg. Med. Chem. Lett.* **2007**, *17*, 1553-1557.
45. P. Chattopadhyay, P.S. Pandey, *Tetrahedron* **2006**, *62*, 8620-8624.
46. V.K. Khatri, S. Upreti, P.S. Pandey, *Org. Lett.* **2006**, *8*, 1755-1758.
47. P. Terech, N.M. Sangeetha, U. Maitra, *J. Phys. Chem. B.* **2006**, *110*, 15224-15233.
48. S. Mukhopadhyay, U. Maitra, Ira, G. Krishnamoorthy, J. Schmidt, Y. Talmon, *J. Am. Chem. Soc.* **2004**, *126*, 15905-15914.
49. S. Bhat, U. Maitra, *Molecules* **2007**, *12*, 2181-2189.
50. X. Shi, M.G. Bousser, D. Picard, *World Pat. Appl.* **2007**, WO07106049.
51. T. Uekawa, K. Ishigami, T. Kitahara, *Biosci. Biotechnol. Biochem.* **2004**, *68*, 1332-1337.
52. T.Y. Kim, Y.S. Kim, Y.M. Lim, W.Y. Kim, Y.J. Yoon, Y.S. Jin, B.G. Lee, S.J. Choi, S.J. Lee, *World Pat. Appl.* **2007**, WO07078039.

53. A. F. Hofmann, *Ital. J. Gastroenterol.***1995**, *27*, 106-113.
54. S. Solá, J.D. Amaral, M.M. Aranha, C.J. Steer, C.M.P. Rodrigues, *Curr. Med. Chem.* **2006**, *13*, 3039-3051.
55. L.R. Hagey, D.L. Crombie, E. Espinosa, M.C. Carey, H. Igimi, A.F. Hofmann, *J. Lipid Res.* **1993**, *34*, 1911-1917.
56. P.F. Lindley, M.C. Carey, *J. Crystallogr. Spectrosc. Res.* **1987**, *17*, 231-249.
57. A.M. Rotunda, M.S. Kolodney, *Dermatol. Surg.* **2006**, *32*, 465–480.
58. M.N. Jones, *Int. J. Pharm.* **1999**, *177*, 137–159.
59. G.J.S.Jenkins, F.R.D' Souza, S.H. Suzen, Z.S. Eltahir, S.A. James, J.M.Parry, P.A. Griffiths, J.N.Baxter, *Carcinogenesis* **2007**, *28*, 136-142.
60. A.F. Hofmann, *Drug Metab. Rev.* **2004**, *36*, 703-722.
61. J.A. Nehring, C. Zierold, H.F. DeLuca, *Proc. Natl. Acad. Sci. U. S. A.* **2007**, *104*, 10006-10009.
62. G. Cravotto, A. Binello, L. Boffa, O. Rosati, M. Boccalini, S. Chimichi, *Steroids* **2006**, *71*, 469-475.
63. J.R. Dias, R.A. Pascal Jr., J. Morrill, A.J. Holder, H. Gao, C. Barnes, *J. Am. Chem. Soc.* **2002**, *124*, 4647-4652.
64. Z. Łotowski, D. Guzmański, *Monatsh. Chem.* **2005**, *136*, 153-158.
65. H.M. Willemen, T. Vermonden, A.T.M. Marcelis, E.J.R. Sudhölter, *Langmuir* **2002**, *18*, 7102-7106.
66. Nonappa, U. Maitra, *Soft Matter* **2007**, *3*, 1428-1433.
67. H. Wang, W.-H. Chan, *Tetrahedron* **2007**, *63*, 8825-8830.
68. J.A. Summerfield, B.H. Billing, C.H.L. Shackleton, *Biochem. J.* **1976**, *154*, 507-516.
69. P. Zimniak, A. Radominska, M. Zimniak, R. Lester, *J. Lipid Res.* **1988**, *29*, 183-190.
70. J. Trottier, M. Verreault, S. Grepper, D. Monté, J. Bélanger, J. Kaeding, P. Caron, T.T. Inaba, O. Barbier, *Hepatology* **2006**, *44*, 1158-1170.
71. P. Caron, J. Trottier, M. Verreault, J. Bélanger, J. Kaeding, O. Barbier, *Mol. Pharmaceutics* **2006**, *3*, 293-302.
72. S. Ikegawa, H. Okuyama, J. Oohashi, N. Murao, J. Goto, *Anal. Sci.* **1999**, *15*, 625-631.
73. T. Goto, A. Shibata, D. Sasaki, N. Suzuki, T. Hishinuma, G. Kakiyamac, T. Iida, N. Manoa, J. Goto, *Steroids* **2005**, *70*, 185-192.
74. G. Kakiyama, S. Sadakiyo, T. Iida, K. Mushiake, T. Goto, N. Mano, J. Goto, T. Nambara, *Chem. Phys. Lipids* **2005**, *134*, 141-150.
75. T. Iida, R. Nakamori, R. Yabuta, S. Yada, Y. Takagi, N. Mano, S. Ikegawa, J. Goto, T. Nambara, *Lipids* **2002**, *37*, 101-110.
76. T. Goto, Akihiro Shibata, T. Iida, N. Mano, J. Goto, *Rapid Commun. Mass Spectrom.* **2004**, *18*, 2360-2364.
77. G. Kakiyama, A. Hosoda, T. Iida, Y. Fujimoto, T. Goto, N. Manoc, J. Goto, T. Nambara, *J. Chromatogr. A* **2006**, *1125*, 112-116.
78. H.J. Kim, S.-H. Yim, I.-S. Lee, *Arch. Pharmacal Res.* **2004**, *27*, 624-627.
79. T. Yosief, A. Rudi, Y. Kashman, *J. Nat. Prod.* **2000**, 63, 299-304.
80. Nonappa, U. Maitra, *Eur. J. Org. Chem.* **2007**, 3331-3336.
81. D. Czajkowska, J.W. Morzycki, *Tetrahedron Lett.* **2007**, *48*, 2851-2855.

82. G. Pütz, W. Schmider, R. Nitschke, G. Kurz, H.E. Blum, *J. Lipid Res.* **2005**, *46*, 2325-2338.
83. P.C.N. Rensen, S.H. van Leeuwen, L.A.J.M. Sliedregt, T.J.C. van Berkel, E.A.L. Biessen, *J. Med. Chem.* **2004**, *47*, 5798-5808.
84. G.P. Tochtrop, G.T. DeKoster, D.P. Cistola, D.F. Covey, *J. Org. Chem.* **2002**, *67*, 6764-6771.
85. J.E. Gautrot, X.X. Zhu, *Angew. Chem. Int. Ed.* **2006**, *45*, 6872-6874.
86. D.R. Bauman, S.I. Rudnick, L.M. Szewczuk, Y. Jin, S. Gopishetty, T.M. Penning, *Mol. Pharm.* **2005**, *67*, 60-68.
87. T.V. Sokolova, M.A. Maslov, G.A. Serebrennikova, *Russ. J. Biorg. Chem.* **2004**, *30*, 477-481.
88. Y. Li, J.R. Dias, *Synthesis* **1997**, 425–430.
89. L. Nahar, A.B. Turner, *Steroids* **2003**, *68*, 1157-1161.
90. A.J. Ayling, S. Broderick, J.P. Clare, A.P. Davis, M.N. Pérez-Payán, M. Lahtinen, M.J. Nissinen, K. Rissanen, *Chem. Eur. J.* **2002**, *8*, 2197-2203.
91. L. Fang, W.-H. Chan, Y.-B. He, D.W.J. Kwong, A.W.M. Lee, *J. Org. Chem.* **2005**, *70*, 7640-7646.
92. S. Nath, U. Maitra, *Org. Lett.* **2006**, *8*, 3239-3242.
93. Y. Mizushina, N. Kasai, K. Miura, S. Hanashima, M. Takemura, H. Yoshida, F. Sugawara, K. Sakaguchi, *Biochemistry* **2004**, *43*, 10669-10677.
94. L. Liu, W. Zhou, J. Chruma, R. Breslow, *J. Am. Chem. Soc.* **2004**, *126*, 8136-8137.
95. N. Vijayalakshmi, U. Maitra, *J. Org. Chem.* **2006**, *71*, 768-774.
96. N. Vijayalakshmi, U. Maitra, *Macromolecules* **2006**, *39*, 7931-7940.
97. S. Ghosh, U. Maitra, *Org. Lett.* **2006**, *8*, 399-402.
98. N. Vijayalakshmi, U. Maitra, *Org. Lett.* **2005**, *7*, 2727-2730.
99. J. Ropponen, J. Tamminen, E. Kolehmainen, K. Rissanen, *Synthesis* **2003**, 2226-2230.
100. J. Tamminen, E. Kolehmainen, J. Linnanto, H. Salo, P. Mänttäri, *Magn. Reson. Chem.* **2000**, *38*, 877-882.
101. A. Bonaldi, E. Molinari, *Eur. Pat. Appl.* **1994**, EP0582891.
102. A.M. Bellini, M.P. Quaglio, E. Mencini, M. Guarneri, G. Cavazzini, A. Fini, *Arch. Pharm. (Weinheim, Ger.)* **1989**, *322*, 879-883.
103. B. Jing, V. Janout, B.C. Herold, M.E. Klotman, T. Heald, S.L. Regen, *J. Am. Chem. Soc.* **2004**, *126*, 15930-15931.
104. N. Terzić, D. Opsenica, D. Milić, B. Tinant, K.S. Smith, W.K. Milhous, B.A. Šolaja, *J. Med. Chem.* **2007**, *50*, 5118-5127.
105. D.B. Salunke, B.G. Hazra, V.S. Pore, M.K. Bhat, *US Pat. Appl.* **2006**, US060003974.
106. Y. Li, Z. Zhang, Y. Ju, C.-Q. Zhao, *Lett. Org. Chem.* **2007**, *4*, 414-418.
107. M.A. Gallop, K.C. Cundy, *World Pat. Appl.* **2002**, WO0228883.
108. J.E. Polli, E. Coop, D.Y. Maeda, K.A. Lentz, *World Pat. Appl.* **2001**, WO0176531.
109. C.O. Mills, *World Pat. Appl.* **2002**, WO0207771.
110. H.M. Willemen, A.T.M. Marcelis, E.J.R. Sudhölter, W.G. Bouwman, B. Demé, P. Terech, *Langmuir* **2004**, *20*, 2075-2080.

111. H.M. Willemen, T. Vermonden, A.T.M. Marcelis, E.J.R. Sudhölter, *Eur. J. Org. Chem.* **2001**, 2329-2335.
112. U. Maitra, S. Mukhopadhyay, A. Sarkar, P. Rao, S. S. Indi, *Angew. Chem. Int. Ed.* **2001**, *40*, 2281-2283.
113. P. Babu, N.M. Sangeetha, U. Maitra, *Macromol. Symp.* **2006**, *241*, 60-67.
114. E.-H. Ryu, J. Yan, Z. Zhong, Y. Zhao, *J. Org. Chem.* **2006**, *71*, 7205-7213.
115. A.P. Davis, *Molecules* **2007**, *12*, 2106-2122.
116. M. Miyata, N. Tohnai, I. Hisaki, *Molecules* **2007**, *12*, 1973-2000.
117. M. Assfalg, E. Gianolio, S. Zanzoni, S. Tomaselli, V. Lorusso, C. Cabella, L. Ragona, S. Aime, H. Molinari, *J. Med. Chem.* **2007**, *50*, 5257-5268.
118. N. Yoswathananont, K. Sada, K. Nakano, K. Aburaya, M. Shigesato, Y. Hishikawa, K. Tani, N. Tohnai, M. Miyata, *Eur. J. Org. Chem.* **2005**, 5330-5338.
119. J. Tamminen, E. Kolehmainen, M. Haapala, J. Linnanto, *Synthesis* **2000**, 1464-1468.
120. L. King III, S. Barnes, U. Glufke, M.E. Henz, M. Kirk, K.A. Merkler, J.C. Vederas, B.J. Wilcox, D.J. Merkler, *Arch. Biochem. Biophys.* **2000**, 374, 107-117.
121. S.-J. Reilly, E.M. O'Shea, U. Andersson, J. O'Byrne, S.E.H. Alexson, M.C. Hunt, *FASEB J.* **2007**, *21*, 99-107.
122. A. Pellicoro, F.A. J. van den Heuvel, M. Geuken, H. Moshage, P.L.M. Jansen, K.N. Faber, *Hepatology* **2007**, *45*, 340-348.
123. E.M. Shonsey, J. Wheeler, M. Johnson, D. He, C.N. Falany, J. Falany, D. Barnes, Synthesis of bile acid coenzyme A thioesters in the amino acid conjugation of bile acids. In: H. Sies, L. Packer (Eds.), *Methods in enzymology*, vol. 400 (Phase II conjugation enzymes and transport systems), Academic Press, New York, 2005, pp. 360-373.
124. E.M. Shonsey, M. Sfakianos, M. Johnson, D. He, C.N. Falany, J. Falany, D.J. Merkler, D. Barnes, Bile acid coenzyme A: amino acid *N*-acyltransferase in the amino acid conjugation of bile acids. In: H. Sies, L. Packer (Eds.), *Methods in enzymology*, vol. 400 (Phase II conjugation enzymes and transport systems), Academic Press, New York, 2005, pp. 374-394.
125. K. Solaas, A. Ulvestad, O. Söreide, B.F. Kase, *J. Lipid Res.* **2000**, *41*, 1154-1162.
126. M.C. Hunt, S.E.H. Alexson, *Prog. Lipid Res.* **2002**, *41*, 99-130.
127. A.K. Batta, G. Salen, S. Shefer, *J. Lipid Res.* **1989**, *30*, 771-774.
128. P.L. Anelli, L. Lattuada, V. Lorusso, G. Lux, A. Morisetti, P. Morosini, M. Serleti, F. Uggeri, *J. Med. Chem.* **2004**, *47*, 3629-3641.
129. V. Noponen , S. Bhat, E. Sievänen, E. Kolehmainen, *Mat. Sci. Eng., C* **2008**, *28*, 1144-1148.
130. M. Vallejo, M.A. Castro, M. Medarde, R.I.R. Macias, M.R. Romero, M.Y. El-Mir, M.J. Monte, O. Briz, M.A. Serrano, J.J.G. Marin, *Biochem. Pharmacol.* **2007**, *73*, 1394-1404.
131. A. Iuliano, A. Ruffini, *Tetrahedron: Asymmetry* **2005**, *16*, 3820-3828.
132. X. Hu, Z. Zhang, X. Zhang, Z. Li, X.X. Zhu, *Steroids* **2005**, *70*, 531-537.

133. H. Liu, D. Avoce, Z. Song, X. X. Zhu, *Macromol. Rapid Commun.* **2001**, *22*, 675-680.
134. P.S. Pandey, R. Rai, R.B. Singh, *J. Chem. Soc., Perkin Trans. 1* **2002**, 918-923.
135. P.S. Pandey, R.B. Singh, *Tetrahedron Lett.* **1997**, *38*, 5045-5046.
136. W.-H. Chen, X.-B. Shao, R. Moellering, C. Wennersten, S.L. Regen, *Bioconjugate Chem.* **2006**, *17*, 1582-1591.
137. A. Balakrishnan, S.A. Wring, A. Coop, J.E. Polli, *Mol. Pharmaceutics* **2006**, *3*, 282-292.
138. E. Kolehmainen, J. Koivukorpi, E. Sievänen, V. Král, *Supramol. Chem.* **2005**, *17*, 437-441.
139. V. Janout, B. Jing, S.L. Regen, *J. Am. Chem. Soc.* **2005**, *127*, 15862-15870.
140. A. Banerjee, A. Ray, C. Chang, P.W. Swaan, *Biochemistry* **2005**, *44*, 8908-8917.
141. W.-H. Chen, X.-B. Shao, S.L. Regen, *J. Am. Chem. Soc.* **2005**, *127*, 12727-12735.
142. M. Dubber, A. Patel, K. Sadalapure, I. Aumüller, T.K. Lindhorst, *Eur. J. Org. Chem.* **2006**, 5357-5366.
143. K.-H. Chang, L. Lee, J. Chena, W.-S. Li, *Chem. Commun.* **2006**, 629-631.
144. T. Fürst, C. Bott, J. Stein, J.B. Dressman, *J. Pharm. Pharmacol.* **2005**, *57*, 53-60.
145. J.T. Tamminen, E.T. Kolehmainen, M.H. Haapala, H.T. Salo, J.M. Linnanto, *ARKIVOC* **2000**, (i), 80-86.
146. J. Inanaga, K. Hirata, H. Saeki, T. Katsuki, Y. Yamaguchi, *Bull. Chem. Soc. Jpn.* **1979**, *52*, 1989–1993.
147. O. Mitsunobu, Y. Yamada, *Bull. Chem. Soc. Jpn.* **1967**, *40*, 2380–2382.
148. O. Mitsunobu, *Synthesis* **1981**, 1–28.
149. P.L. Anelli, L. Lattuada, F. Uggeri, *Synth. Commun.* **1998**, *28*, 109–117.
150. R.E. Hurd, B.K. John, *J. Magn. Reson.* **1991**, *91*, 648–653.
151. M. Rance, O.W. Sørensen, G. Bodenhausen, G. Wagner, R.R. Ernst, K. Wüthrich, *Biochem. Biophys. Res. Commun.* **1983**, *117*, 479-85.
152. A. Derome, M. Williamson, *J. Magn. Reson.* **1990**, *88*, 177–185.
153. A. Bax, R.H. Griffey, B.L. Hawkins, *J. Magn. Reson.* **1983**, *55*, 301–315.
154. A. Bax, S. Subramanian, *J. Magn. Reson.* **1986**, *67*, 565–569.
155. A. Bax, M.F. Summers, *J. Am. Chem. Soc.* **1986**, *108*, 2093–2094.
156. Z. Otwinowski, W. Minor, Processing of x-ray diffraction data collected in oscillation mode. In: C.W. Carter Jr., R.M. Sweet (Eds.), *Methods in enzymology*, vol. 276 (Macromolecular crystallography, part A), Academic Press, New York, 1997, pp. 307–326.
157. G.M. Sheldrick, *Acta Cryst.* **2008**, *A64*, 112-122.
158. M.C. Burla, M. Camalli, B. Carrozzini, G.L. Cascarano, C. Giacovazzo, G. Polidori, J. Spagna, *J. Appl. Cryst.* **2003**, *36*, 1103.
159. L.J. Farrugia, *J. Appl. Cryst.* **1997**, *30*, 565.
160. C.F. Macrae, P.R. Edgington, P. McCabe, E. Pidcock, G.P. Shields, R. Taylor, M. Towler, J. van de Streek, *J. Appl. Cryst.* **2006**, *39*, 453-457.
161. K. Wolinski, J.F. Hinton, P.J. Pulay, *J. Am. Chem. Soc.* **1990**, *112*, 8251-8260.

162. M.J. Frisch, G.W. Trucks, H.B. Schlegel, G.E. Scuseria, M.A. Robb, R.E. Cheeseman, W.G Zakizewski, J.A. Montgomery Jr., R.E. Stratmann, J.C. Burant, S. Dapprich, J.M. Millam, A.D. Daniels, K.N. Kudin, M.C. Strain, O. Farkas, J. Tomasi, V. Barone, M. Cossi, R. Cammi, B. Mennuci, C. Pomelli, C. Adamo, S. CliVord, J. Ochterski, G.A. Petersson, P.Y. Ayala, Q. Cui, K. Morokuma, D.K. Malick, A.D. Rabuck, K. Raghavachari, J.B. Foresman, J. Cioslowski, J.V. Oritz, B.B. Stefanov, G. Liu, A. Liashenko, P. Piskorz, I. Komaromi, R. Gomperts, R.L. Martin, D.J. Fox, T. Keith, M.A. AlLaham, C.Y. Peng, A. Nanayakkara, C. Gonzalez, M. Challacombe, P.M.W. Gill, B. Johnson, W. Chen, M.W. Wong, J.L. Andres, M. Head-Gordon, E.S. Replogle, J.A. Pople, *Gaussian 98; revision A.9*, Gaussian, Pittsburgh, PA, 1998.
163. N.L. Allinger, *J. Am. Chem. Soc.* **1977**, *99*, 8127-8134.
164. N.L. Allinger, Y.H. Yuh, *Quantum chemistry program exchange*, Bloomington, IN, Program No. 395, 1980.
165. U. Burkert, N.L. Allinger, *Molecular mechanics (ACS Monograph 177)*, American Chemical Society, Washington, 1982.
166. J.J.P. Stewart, *J. Comput. Chem.* **1989**, *10*, 209-220.
167. *HyperChem, release 7.0 for Windows*, Hypercube, Inc., Gainesville, FL, 2002.
168. E. Giglio, C. Quagliata, *Acta Crystallogr.* **1975**, *B31*, 743-746.
169. J.R. Dias, B. Nassim, *J. Org. Chem.* **1980**, *45*, 337-345.
170. J.R. Dias, H. Gao, E. Kolehmainen, *Spectrochim. Acta A* **2000**, *56*, 53-77.
171. J.P. Clare, A.J. Ayling, J.-B. Joos, A.L. Sisson, G. Magro, M.N. Pérez-Payán, T.N. Lambert, R. Shukla, B.D. Smith, A.P. Davis, *J. Am. Chem. Soc.* **2005**, *127*, 10739-10746.
172. E. Virtanen, M. Nissinen, R. Suontamo, J. Tamminen, E. Kolehmainen, *J. Mol. Struct.* **2003**, *649*, 207–218.
173. L.J. D'Souza, U. Maitra, *J. Org. Chem.* **1996**, *61*, 9494-9502.
174. M.C. Wahle, S.R. Byrn, *Acta Crystallogr.* **1996**, *C52*, 2500-2502.
175. G. Aranda, M. Fetizon, N. Tayeb, J. Guilhem, C. Pascard, *Tetrahedron* **1986**, *42*, 329-338.
176. D.R. Boer, H. Kooijman, M. Groen, J. van der Louw, J. Kelder, Jan Kroon, *Acta Crystallogr.* **2001**, *C57*, 1177–1181.
177. H. Liu, F. Bélangér-Gariépy, M. Akram, M. Moskova, X.-X. Zhu, *Acta Crystallogr.* **1998**, *C54*, 801-803.
178. N.I. Garbuz, L.P. Solovei, N.V. Kovganko, Y.G. Chernov, *J. Appl. Spectrosc.* **2002**, *69*, 58-61.
179. Z. Tang, X. Hu, Y. Zhu, *J. Chem. Technol. Biotechnol.* **1997**, *70*, 287-293.
180. Y.N. Levchuk, *Russ. Chem. Rev.* **1968**, *37*, 155-171.
181. Q. Xiao, Y. Ju, X. Yang, Y.-F. Zhao, *Rapid Commun. Mass Spectrom.* **2003**, *17*, 1405–1410.
182. K. Nakano, K. Sada, Y. Kurozumi, M. Miyata, *Chem. Eur. J.* **2001**, *7*, 209–220.
183. F.R. Allen, *Acta Crystallogr.* **2002**, *B58*, 380-388.
184. V. Bertolasi, V. Ferretti, L. Pretto, G. Fantin, M. Fogagnolo, O. Bortolini, *Acta Crystallogr.* **2005**, *B61*, 346–356.

185. S. Limmatvapirat, K. Yamaguchi, E. Yonemochi, T. Oguchi, K. Yamamoto, *Acta Crystallogr.* **1997**, *C53*, 803–805.
186. M. Alvarez, A. Jover, J. Carrazana, F. Meijide, V.H. Soto, J.V. Tato, *Steroids* **2007**, *72*, 535-544.
187. V. Bertolasi, O. Bortolini, G. Fantin, M. Fogagnolo, D. Perrone, *Steroids* **2007**, *72*, 756-764.
188. J.H. Zhang, C.G. Bazuin, S. Freiberg, F. Brisse, X.X. Zhu, *Polymer* **2005**, *46*, 7266-7272.
189. U. Biader Ceipidor, R. Curini, G. D'Ascenzo, M. Tomassetti, *Thermochim. Acta* **1981**, *46*, 279-87.
190. A. Marino, M. Bicchieri, R. Curini, G. D'Ascenzo, V. Carunchio, A. Pierucci, *Thermochim. Acta* **1981**, *46*, 289-94.
191. E. Fukuoka, M. Makita, Y. Nakamura, *Chem. Pharm. Bull.* **1991**, *39*, 2087-2090.
192. Z. Cenuse, D. Fatu, V. Meltzer, *Anal. Univ. Bucuresti, Chim.* **2002**, *11(Vol 1)*, 15-21.
193. T. Kimura, H. Imamura, A. Shimowada, S. Takagi, *J. Mass Spectrom. Soc. Jpn.* **1998**, *46*, 304-307.
194. T. Kimura, H. Imamura, M. Sugahara, T. Arai, S. Takagi, *Mol. Cryst. Liq. Cryst.* **1996**, *276*, 133-139.
195. S.Y. Brichka, L.A. Belyakova, G.P. Prikhod'ko, N.V. Roik, *Russ. Chem. Bull.* **2006**, *55*, 1775-1779.
196. J. Villaverde, J. Cladera, E. Padros, J.L. Rigaud, M. Dunach, *Eur. J. Biochem.* **1997**, *244*, 441-448.
197. E.H. Mosbach, N.K.N. Ayengar, C.K. McSherry, *US Pat. Appl.* **1984**, US4460509.
198. E. H. Mosbach, C.K. McSherry, S. Kuroki, *US Pat. Appl.* **1987**, US4648995.
199. F. della Valle, S. Lorenzi, J.C.J.J. Samson, F. della Valle, *Eur. Pat. Appl.* **1993**, EP0550006.
200. F. della Valle, S. Lorenzi, J.C.J.J. Samson, F. della Valle, *US Pat. Appl.* **1996**, US5506224.
201. F. della Valle, S. Lorenzi, F. della Valle, *US Pat. Appl.* **1997**, US5679667.
202. R. Bundy, J. Mauskopf, J.T. Walker, L. Lack, *J. Lipid Res.* **1977**, *18*, 389-395.
203. A. Mukai, K. Yazawa, Y. Mikami, K. Harada, U. Gräfe, *J. Antibiot.* **2005**, *58*, 356–360.
204. N.M. Sangeetha, R. Balasubramanian, U. Maitra, S. Ghosh, A.R. Raju, *Langmuir* **2002**, *18*, 7154-7157.
205. T. Zou, S.-L. Li, X.-Z. Zhang, X.-J. Wu, S.-X. Cheng, R.-X. Zhuo, *J. Polym. Sci. Polym. Chem.* **2007**, *45*, 5256-5265.
206. J. West, J. Perkins, S. Hok, R. Balhorn, F.C. Lightstone, M. Cosman, S.J. DeNardo, G.L. DeNardo, *Cancer Biother. Radiopharm.* **2006**, *21*, 645-654.
207. A. Fini, A. Roda, R. Fugazza, B. Grigolo, *J. Solution Chem.* **1985**, *14*, 595-603.
208. C. Gervais, C. Coelho, T. Azaïs, J. Maquet, G. Laurent, F. Pourpoint, C. Bonhomme, P. Florian, B. Alonso, G. Guerrero, P.H. Mutin, F. Mauri, *J. Magn. Reson.* **2007**, *187*, 131-140.
209. D. Sebastiani, *Int. J. Quant. Chem.* **2005**, *101*, 849-853.

210. R.K. Harris, S.A. Joyce, C.J. Pickard, S. Cadars, L. Emsley, *Phys. Chem. Chem. Phys.* **2006**, *8*, 137–143.
211. R.K. Harris, *Analyst* **2006**, *131*, 351-373.
212. Y. Hishikawa, Y. Aoki, K. Sada, M. Miyata, *Chem. Lett.* **1998**, 1289-1290.
213. J.P. Schaefer, L.L. Reed, *Acta Crystallogr.* **1972**, *B28*, 1743-1748.
214. Y. Hishikawa, K. Sada, R. Watanabe, M. Miyata, K. Hanabusa, *Chem. Lett.* **1998**, 795-796.
215. K. Sada, Y. Hishikawa, T. Kondo, M. Miyata, *Chem. Lett.* **1994**, 2113-2116.
216. J. Koivukorpi, A. Valkonen, M. Lahtinen, E. Kolehmainen, *J. Mol. Struct.* **2008**, in press.
217. Y. Cheng, D.M. Ho, C.R. Gottlieb, D. Kahne, M.A. Bruck, *J. Am. Chem. Soc.* **1992**, *114*, 7319-7320.
218. M.C. Wahle, S.R. Byrn, *Acta Crystallogr.* **1997**, *C53*, 334-339.
219. A.D. Averin, E.R. Ranyuk, N.V. Lukashev, I.P. Beletskaya, *Chem. Eur. J.* **2005**, *11*, 7030-7039.
220. S. Ghosh, A.R. Choudhury, T.N.G. Row, U. Maitra, *Org. Lett.* **2005**, *7*, 1441-1444.
221. E. Virtanen, J. Tamminen, M. Haapala, P. Mänttäri, R. Kauppinen, E. Kolehmainen, *Magn. Reson. Chem.* **2003**, *41*, 567-576.
222. E. Virtanen, J. Koivukorpi, J. Tamminen, P. Mänttäri, E. Kolehmainen, *J. Organomet. Chem.* **2003**, *668*, 43-50.
223. Z. Łotowski, J. Piechowska, Ł. Jarocki, *Monatsh. Chem.* **2008**, *139*, 213-222.
224. D. Czajkowska, J.W. Morzycki, *Pol. J. Chem.* **2006**, *80*, 663-666.
225. U. Maitra, S. Nath, *ARKIVOC* **2005**, (iii), 133-143.
226. P. Babu, U. Maitra, *Proc. Indian Acad. Sci. Chem. Sci.* **2003**, *115*, 607-612.
227. S. Matile, A. Som, N. Sordé, *Tetrahedron* **2004**, *60*, 6405-6435.
228. P. Bühlmann, E. Pretsch, E. Bakker, *Chem. Rev.* **1998**, *98*, 1593-1687.
229. A.D. Averin, E.R. Ranyuk, N.V. Lukashev, S.L. Golub, A.K. Buryak, I.P. Beletskaya, *Tetrahedron Lett.* **2008**, *49*, 1188-1191.
230. V.A. Khripach, V.N. Zhabinskii, A.V. Antonchick, A.P. Antonchick, *Russ. J. Bioorg. Chem.* **2006**, *32*, 651-659.
231. S.R. Gondi, D.Y. Son, *Synth. Commun.* **2006**, *36*, 1317-1331.
232. J. Koivukorpi, A. Valkonen, E. Kolehmainen, *J. Mol. Struct.* **2004**, *693*, 81-86.
233. S.R. Choon, W.C. Sang, W.C. Jae, *Bull. Korean Chem. Soc.* **2000**, *21*, 342-344.
234. R. Adachi, Y. Honma, H. Masuno, K. Kawana, I. Shimomura, S. Yamada, M. Makishima, *J. Lipid Res.* **2005**, *46*, 46-57.
235. R. Pankiewicz, G. Schroeder, B. Brzezinski, *J. Mol. Struct.* **2007**, *829*, 120–127.
236. I. Starke, S. Fürstenberg, H. Müller, H.-J. Holdt, E. Kleinpeter, *Rapid Commun. Mass Spectrom.* **2006**, *20*, 897-903.
237. R. Joachimiak, Z. Paryzek, *J. Inclusion Phenom. Macrocyclic Chem.* **2004**, *49*, 127-132.

APPENDIX

Single crystal data and structure refinement parameters are presented in the following appendices 1-12 with ORTEP[159] -plots for compounds **2-5**, **9** and **11-15**, as well as for solvates **8** · $CHCl_3$ · H_2O and **9** · H_2O.

Mass spectra for lithocholaphanes **25** and **30** with alkali metal chlorides and for lithocholaphane **30** alkaline earth metal chlorides are presented in the appendices 13-15.

Appendix 1

Crystal data and structure refinement parameters for **2**.

CCDC number	652751	
Empirical formula	$C_{32}H_{44}Cl_2O_5$	
Formula weight	579.57	
Wavelength	0.71073 Å	
Crystal system	Orthorhombic	
Space group	$P2_12_12_1$ (No. 19)	
Unit cell dimensions	a = 11.9892(3) Å	α = 90°.
	b = 13.0931(3) Å	β = 90°.
	c = 19.1539(5) Å	γ = 90°.
Volume	3006.70(13) Å^3	
Z	4	
Density (calculated)	1.280 Mg/m^3	
Absorption coefficient	0.255 mm^{-1}	
F(000)	1240	
Crystal size	0.40 x 0.40 x 0.30 mm^3	
Crystal color, shape	Colorless, block	
Theta range for data collection	3.11 to 25.00°.	
Index ranges	-11<=h<=14, -14<=k<=15, -19<=l<=22	
Reflections collected	10783	
Independent reflections	5201 [R_{int} = 0.0748]	
Completeness to theta = 25.00°	99.7 %	
Absorption correction	None	
Refinement method	Full-matrix least-squares on F^2	
Data / restraints / parameters	5201 / 0 / 354	
Goodness-of-fit on F^2	0.954	
Final R indices [I>2σ(I)]	R_1 = 0.0550, wR_2 = 0.0872	
R indices (all data)	R_1 = 0.1438, wR_2 = 0.1078	
Absolute structure parameter	-0.06(8)	
Largest diff. peak and hole	0.228 and -0.211 e.Å^{-3}	

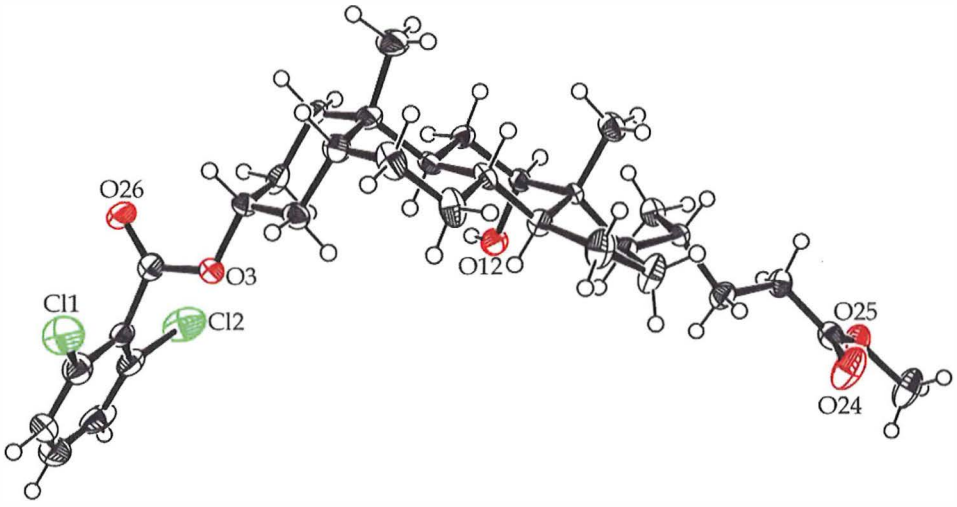

Appendix 2

Crystal data and structure refinement parameters for **3**.

CCDC number	652752	
Empirical formula	$C_{32}H_{44}Cl_2O_6$	
Formula weight	595.57	
Wavelength	0.71073 Å	
Crystal system	Orthorhombic	
Space group	$P2_12_12_1$ (No. 19)	
Unit cell dimensions	a = 11.9296(3) Å	α = 90°.
	b = 13.0375(4) Å	β = 90°.
	c = 19.3694(6) Å	γ = 90°.
Volume	3012.56(15) Å^3	
Z	4	
Density (calculated)	1.313 Mg/m^3	
Absorption coefficient	0.258 mm^{-1}	
F(000)	1272	
Crystal size	0.60 x 0.30 x 0.30 mm^3	
Crystal color, shape	Colorless, block	
Theta range for data collection	3.13 to 25.70°.	
Index ranges	-13<=h<=13, -15<=k<=13, -23<=l<=21	
Reflections collected	14205	
Independent reflections	5547 [R_{int} = 0.0753]	
Completeness to theta = 25.70°	98.2 %	
Absorption correction	None	
Refinement method	Full-matrix least-squares on F^2	
Data / restraints / parameters	5547 / 0 / 367	
Goodness-of-fit on F^2	1.113	
Final R indices [I>2σ(I)]	R_1 = 0.0789, wR_2 = 0.1914	
R indices (all data)	R_1 = 0.1063, wR_2 = 0.2083	
Absolute structure parameter	-0.09(12)	
Largest diff. peak and hole	0.634 and -0.360 e.Å^{-3}	

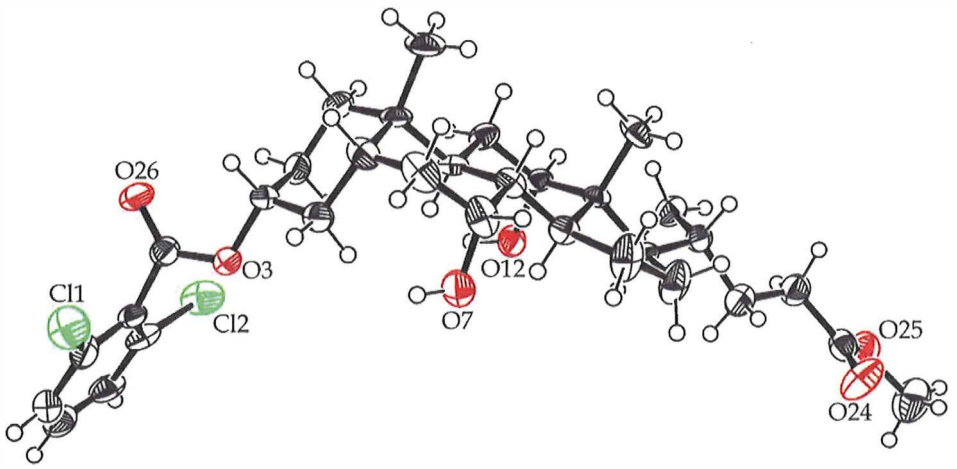

Appendix 3

Crystal data and structure refinement parameters for 4.

CCDC number	652753	
Empirical formula	$C_{25}H_{41}N_3O_2$	
Formula weight	415.61	
Wavelength	0.71073 Å	
Crystal system	Orthorhombic	
Space group	$P2_12_12_1$ (No. 19)	
Unit cell dimensions	a = 7.5810(2) Å	α = 90°.
	b = 17.1651(6) Å	β = 90°.
	c = 17.8372(4) Å	γ = 90°.
Volume	2321.13(11) Å^3	
Z	4	
Density (calculated)	1.189 Mg/m^3	
Absorption coefficient	0.075 mm^{-1}	
F(000)	912	
Crystal size	0.30 x 0.30 x 0.20 mm^3	
Crystal color, shape	Colorless, block	
Theta range for data collection	2.92 to 25.00°.	
Index ranges	-8<=h<=8, -17<=k<=20, -21<=l<=21	
Reflections collected	9935	
Independent reflections	2331 [R_{int} = 0.0703]	
Completeness to theta = 25.00°	99.6 %	
Absorption correction	None	
Refinement method	Full-matrix least-squares on F^2	
Data / restraints / parameters	2331 / 6 / 285	
Goodness-of-fit on F^2	1.047	
Final R indices [I>2σ(I)]	R_1 = 0.0425, wR_2 = 0.0832	
R indices (all data)	R_1 = 0.0738, wR_2 = 0.0937	
Absolute structure parameter	2(2)*	
Largest diff. peak and hole	0.141 and -0.155 e.Å^{-3}	

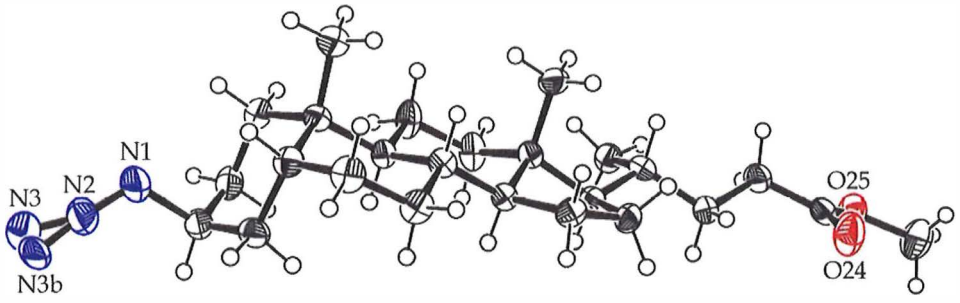

*absolute structure parameter is meaningless

Appendix 4

Crystal data and structure refinement parameters for **5**.

CCDC number	652754	
Empirical formula	$C_{26}H_{42}O_4$	
Formula weight	418.60	
Wavelength	0.71073 Å	
Crystal system	Monoclinic	
Space group	$P2_1$ (No. 4)	
Unit cell dimensions	a = 10.9622(5) Å	α = 90°.
	b = 7.6846(4) Å	β = 93.513(3)°.
	c = 14.0545(6) Å	γ = 90°.
Volume	1181.73(10) Å^3	
Z	2	
Density (calculated)	1.176 Mg/m^3	
Absorption coefficient	0.077 mm^{-1}	
F(000)	460	
Crystal size	0.50 x 0.20 x 0.10 mm^3	
Crystal color, shape	Colorless, plate	
Theta range for data collection	3.02 to 25.00°.	
Index ranges	-12<=h<=13, -9<=k<=8, -16<=l<=16	
Reflections collected	3642	
Independent reflections	2229 [R_{int} = 0.0421]	
Completeness to theta = 25.00°	99.1 %	
Absorption correction	None	
Refinement method	Full-matrix least-squares on F^2	
Data / restraints / parameters	2229 / 17 / 299	
Goodness-of-fit on F^2	1.050	
Final R indices [I>2σ(I)]	R_1 = 0.0660, wR_2 = 0.1559	
R indices (all data)	R_1 = 0.0982, wR_2 = 0.1780	
Absolute structure parameter	2(5)*	
Largest diff. peak and hole	0.467 and -0.295 e.Å^{-3}	

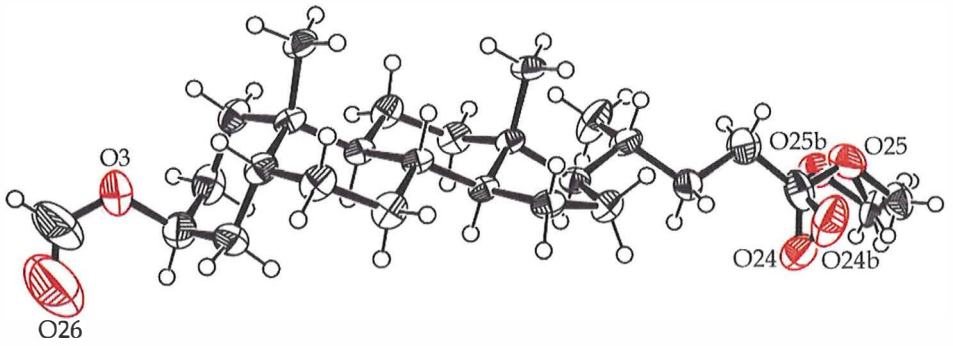

*absolute structure parameter is meaningless

Appendix 5

Crystal data and structure refinement parameters for **8** · $CHCl_3$ · H_2O.

CCDC number	670879	
Empirical formula	$C_{27}H_{48}Cl_3NO_5$	
Formula weight	573.01	
Wavelength	0.71073 Å	
Crystal system	Monoclinic	
Space group	$P2_1$ (No. 4)	
Unit cell dimensions	a = 7.0541(3) Å	α = 90°.
	b = 17.8370(8) Å	β = 105.098(3)°.
	c = 12.3267(6) Å	γ = 90°.
Volume	1497.46(12) Å^3	
Z	2	
Density (calculated)	1.271 Mg/m^3	
Absorption coefficient	0.341 mm^{-1}	
F(000)	616	
Crystal size	0.15 x 0.12 x 0.03 mm^3	
Crystal color, shape	Colorless, plate	
Theta range for data collection	2.28 to 25.00°.	
Index ranges	-8<=h<=7, -21<=k<=21, -14<=l<=14	
Reflections collected	9185	
Independent reflections	5276 [R_{int} = 0.0672]	
Completeness to theta = 25.00°	99.9 %	
Absorption correction	None	
Refinement method	Full-matrix least-squares on F^2	
Data / restraints / parameters	5276 / 7 / 343	
Goodness-of-fit on F^2	1.109	
Final R indices [I>2σ(I)]	R_1 = 0.0699, wR_2 = 0.1098	
R indices (all data)	R_1 = 0.1157, wR_2 = 0.1266	
Absolute structure parameter	0.02(10)	
Largest diff. peak and hole	0.368 and -0.379 e.Å^{-3}	

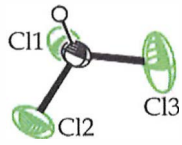

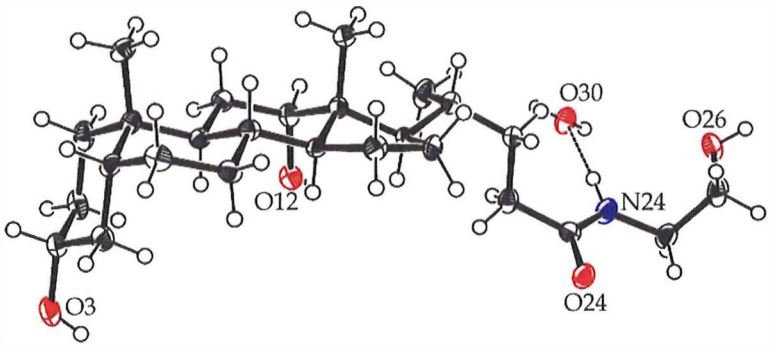

Appendix 6

Crystal data and structure refinement parameters for **9**.

CCDC number (CSD)	219569 (JAQFIR)	
Empirical formula	$C_{27}H_{47}NO_4$	
Formula weight	449.66	
Wavelength	0.71073 Å	
Crystal system	Monoclinic	
Space group	$P2_1$ (No. 4)	
Unit cell dimensions	a = 11.5110(4) Å	α = 90°.
	b = 7.5535(2) Å	β = 100.444(2)°.
	c = 14.5483(6) Å	γ = 90°.
Volume	1243.99(7) Å^3	
Z	2	
Density (calculated)	1.200 Mg/m^3	
Absorption coefficient	0.079 mm^{-1}	
F(000)	496	
Crystal size	0.40 x 0.20 x 0.10 mm^3	
Crystal color, shape	Colorless, rod	
Theta range for data collection	2.49 to 24.70°.	
Index ranges	-12<=h<=13, -8<=k<=8, -17<=l<=16	
Reflections collected	6788	
Independent reflections	3978 [R_{int} = 0.0594]	
Completeness to theta = 24.70°	99.8 %	
Absorption correction	None	
Refinement method	Full-matrix least-squares on F^2	
Data / restraints / parameters	3978 / 5 / 301	
Goodness-of-fit on F^2	1.018	
Final R indices [I>2σ(I)]	R_1 = 0.0467, wR_2 = 0.1090	
R indices (all data)	R_1 = 0.0650, wR_2 = 0.1185	
Absolute structure parameter	-0.2(13)	
Largest diff. peak and hole	0.172 and -0.241 e.Å^{-3}	

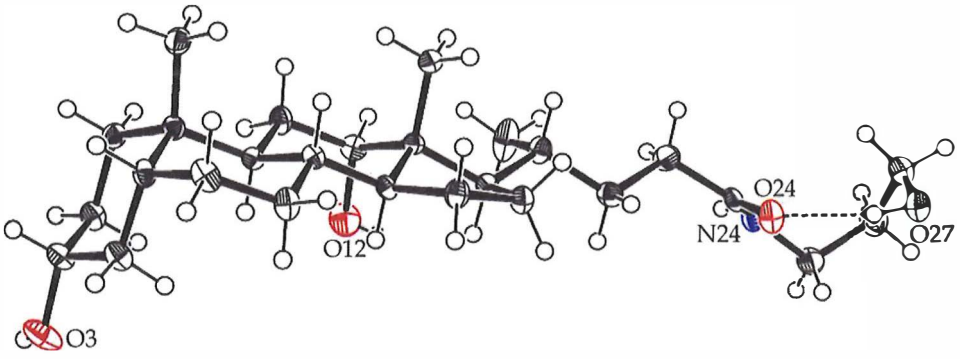

Appendix 7

Crystal data and structure refinement parameters for **9a** · H_2O.

CCDC number (CSD)	635027 (NIMMIG)	
Empirical formula	$C_{27}H_{49}NO_5$	
Formula weight	467.67	
Wavelength	0.71073 Å	
Crystal system	Orthorhombic	
Space group	$P2_12_12_1$ (No. 19)	
Unit cell dimensions	a = 7.1151(2) Å	α = 90°.
	b = 18.1803(4) Å	β = 90°.
	c = 20.1803(5) Å	γ = 90°.
Volume	2610.42(11) Å^3	
Z	4	
Density (calculated)	1.190 Mg/m^3	
Absorption coefficient	0.080 mm^{-1}	
F(000)	1032	
Crystal size	0.30 x 0.10 x 0.10 mm^3	
Crystal color, shape	Colorless, needle	
Theta range for data collection	2.31 to 25.00°.	
Index ranges	-8<=h<=8, -21<=k<=21, -23<=l<=23	
Reflections collected	17693	
Independent reflections	2649 [R_{int} = 0.1650]	
Completeness to theta = 25.00°	99.9 %	
Absorption correction	None	
Refinement method	Full-matrix least-squares on F^2	
Data / restraints / parameters	2649 / 6 / 319	
Goodness-of-fit on F^2	1.070	
Final R indices [I>2σ(I)]	R_1 = 0.0595, wR_2 = 0.0960	
R indices (all data)	R_1 = 0.0870, wR_2 = 0.1062	
Absolute structure parameter	3(4)*	
Largest diff. peak and hole	0.202 and -0.227 e.Å^{-3}	

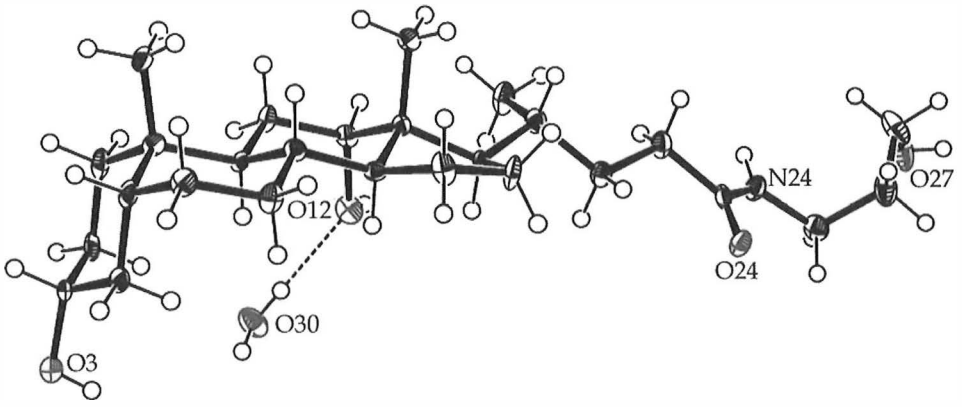

*absolute structure parameter is meaningless

Appendix 8

Crystal data and structure refinement parameters for **11**.

CCDC number	667964	
Empirical formula	$C_{27}H_{47}NO_4$	
Formula weight	449.66	
Wavelength	1.54184 Å	
Crystal system	Monoclinic	
Space group	$P2_1$ (No. 4)	
Unit cell dimensions	a = 11.5552(3) Å	α = 90°.
	b = 7.5760(2) Å	β = 100.084(2)°.
	c = 14.5609(4) Å	γ = 90°.
Volume	1255.00(6) Å^3	
Z	2	
Density (calculated)	1.190 Mg/m^3	
Absorption coefficient	0.613 mm^{-1}	
F(000)	496	
Crystal size	0.60 x 0.15 x 0.08 mm^3	
Crystal color, shape	Colorless, rod	
Theta range for data collection	3.08 to 66.95°.	
Index ranges	-13<=h<=13, -8<=k<=7, -17<=l<=17	
Reflections collected	6254	
Independent reflections	3525 [R_{int} = 0.0265]	
Completeness to theta = 66.95°	95.9 %	
Absorption correction	None	
Refinement method	Full-matrix least-squares on F^2	
Data / restraints / parameters	3525 / 5 / 301	
Goodness-of-fit on F^2	1.025	
Final R indices [I>2σ(I)]	R_1 = 0.0401, wR_2 = 0.0998	
R indices (all data)	R_1 = 0.0434, wR_2 = 0.1031	
Absolute structure parameter	0.2(2)	
Largest diff. peak and hole	0.229 and -0.170 e.Å^{-3}	

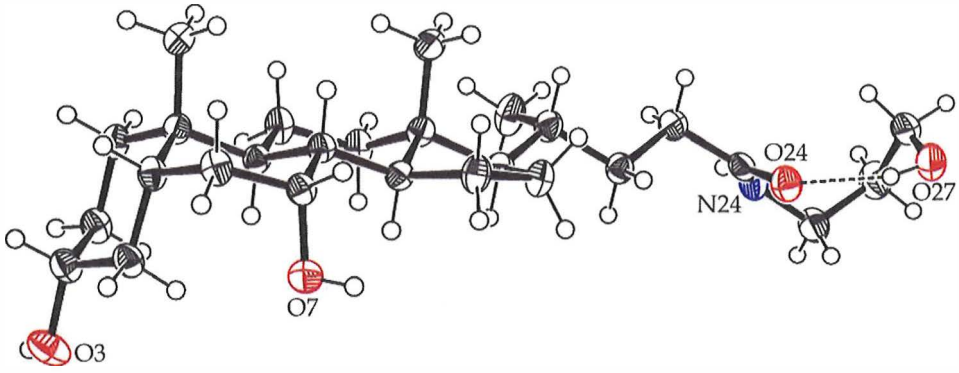

Appendix 9

Crystal data and structure refinement parameters for **12**.

CCDC number	667965	
Empirical formula	$C_{26}H_{45}NO_4$	
Formula weight	435.63	
Wavelength	0.71073 Å	
Crystal system	Orthorhombic	
Space group	$P2_12_12_1$ (No. 19)	
Unit cell dimensions	a = 6.8749(2) Å	α = 90°.
	b = 17.1530(4) Å	β = 90°.
	c = 20.9758(3) Å	γ = 90°.
Volume	2473.57(10) Å^3	
Z	4	
Density (calculated)	1.170 Mg/m^3	
Absorption coefficient	0.077 mm^{-1}	
F(000)	960	
Crystal size	0.45 x 0.20 x 0.15 mm^3	
Crystal color, shape	Colorless, block	
Theta range for data collection	3.07 to 25.00°.	
Index ranges	-8<=h<=8, -20<=k<=20, -24<=l<=24	
Reflections collected	16682	
Independent reflections	2501 [R_{int} = 0.0967]	
Completeness to theta = 25.00°	99.8 %	
Absorption correction	None	
Refinement method	Full-matrix least-squares on F^2	
Data / restraints / parameters	2501 / 4 / 292	
Goodness-of-fit on F^2	1.089	
Final R indices [I>2σ(I)]	R_1 = 0.0498, wR_2 = 0.0994	
R indices (all data)	R_1 = 0.0645, wR_2 = 0.1064	
Absolute structure parameter	-2(2)*	
Largest diff. peak and hole	0.179 and -0.207 e.Å^{-3}	

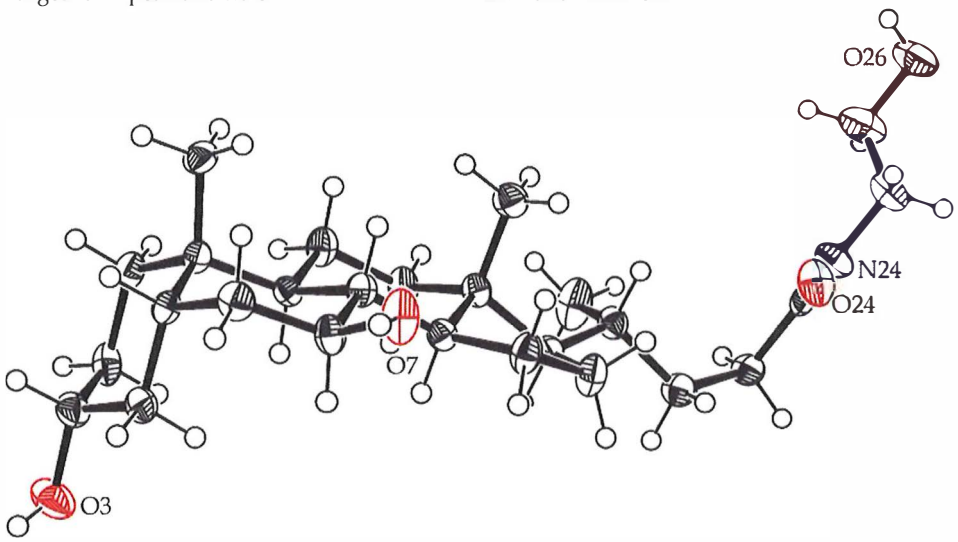

*absolute structure parameter is meaningless

Appendix 10

Crystal data and structure refinement parameters for **13**.

CCDC number	667966	
Empirical formula	$C_{27}H_{47}NO_4$	
Formula weight	449.66	
Wavelength	0.71073 Å	
Crystal system	Monoclinic	
Space group	$P2_1$ (No. 4)	
Unit cell dimensions	a = 6.9052(2) Å	α = 90°.
	b = 18.1407(5) Å	β = 92.149(2)°.
	c = 20.5149(6) Å	γ = 90°.
Volume	2568.00(13) Å^3	
Z	4	
Density (calculated)	1.163 Mg/m^3	
Absorption coefficient	0.076 mm^{-1}	
F(000)	992	
Crystal size	0.30 x 0.15 x 0.10 mm^3	
Crystal color, shape	Colorless, plate	
Theta range for data collection	3.73 to 25.00°.	
Index ranges	-7<=h<=8, -21<=k<=21, -24<=l<=24	
Reflections collected	15462	
Independent reflections	4634 [R_{int} = 0.0568]	
Completeness to theta = 25.00°	99.1 %	
Absorption correction	None	
Refinement method	Full-matrix least-squares on F^2	
Data / restraints / parameters	4634 / 9 / 601	
Goodness-of-fit on F^2	1.128	
Final R indices [I>2σ(I)]	R_1 = 0.0912, wR_2 = 0.2197	
R indices (all data)	R_1 = 0.1022, wR_2 = 0.2268	
Absolute structure parameter	0(3)	
Largest diff. peak and hole	0.424 and -0.348 e.Å^{-3}	

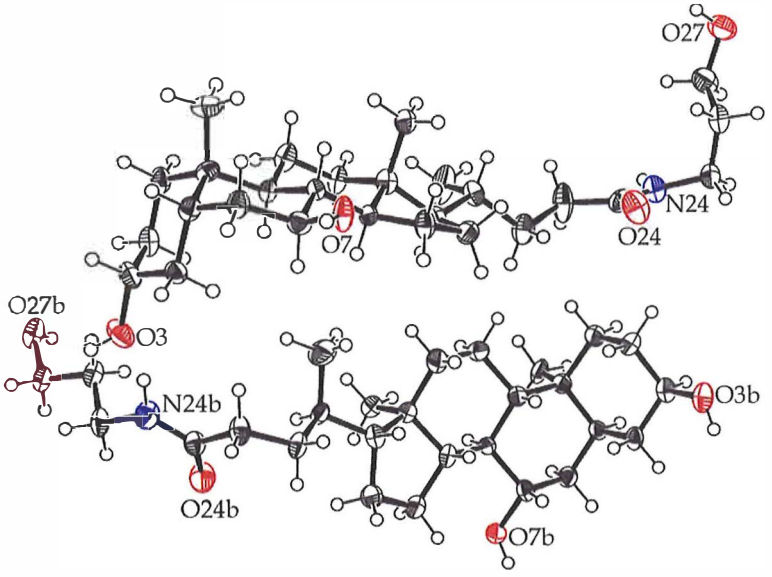

Appendix 11

Crystal data and structure refinement parameters for **14**.

CCDC number	667967	
Empirical formula	$C_{26}H_{45}NO_5$	
Formula weight	451.63	
Wavelength	0.71073 Å	
Crystal system	Orthorhombic	
Space group	$P2_12_12_1$ (No. 19)	
Unit cell dimensions	a = 8.70900(10) Å	α = 90°.
	b = 11.8120(2) Å	β = 90°.
	c = 23.2400(5) Å	γ = 90°.
Volume	2390.72(7) Å^3	
Z	4	
Density (calculated)	1.255 Mg/m^3	
Absorption coefficient	0.085 mm^{-1}	
F(000)	992	
Crystal size	0.33 x 0.20 x 0.05 mm^3	
Crystal color, shape	Colorless, plate	
Theta range for data collection	2.46 to 25.00°.	
Index ranges	-10<=h<=10, -14<=k<=14, -27<=l<=27	
Reflections collected	16156	
Independent reflections	2413 [R_{int} = 0.0915]	
Completeness to theta = 25.00°	99.9 %	
Absorption correction	None	
Refinement method	Full-matrix least-squares on F^2	
Data / restraints / parameters	2413 / 5 / 304	
Goodness-of-fit on F^2	1.083	
Final R indices [I>2σ(I)]	R_1 = 0.0457, wR_2 = 0.0862	
R indices (all data)	R_1 = 0.0572, wR_2 = 0.0907	
Absolute structure parameter	3(2)*	
Largest diff. peak and hole	0.183 and -0.189 e.Å^{-3}	

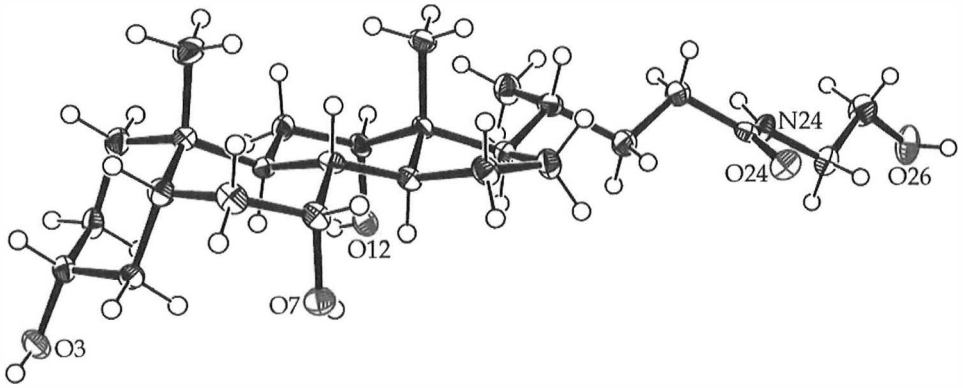

*absolute structure parameter is meaningless

Appendix 12

Crystal data and structure refinement parameters for **15**.

CCDC number	667968	
Empirical formula	$C_{27}H_{47}NO_5$	
Formula weight	465.66	
Wavelength	0.71073 Å	
Crystal system	Orthorhombic	
Space group	$P2_12_12_1$ (No. 19)	
Unit cell dimensions	a = 8.7653(2) Å	α = 90°.
	b = 12.2671(2) Å	β = 90°.
	c = 23.6423(4) Å	γ = 90°.
Volume	2542.13(8) Å^3	
Z	4	
Density (calculated)	1.217 Mg/m^3	
Absorption coefficient	0.082 mm^{-1}	
F(000)	1024	
Crystal size	0.35 x 0.30 x 0.10 mm^3	
Crystal color, shape	Colorless, plate	
Theta range for data collection	1.87 to 25.00°.	
Index ranges	-10<=h<=10, -14<=k<=14, -28<=l<=28	
Reflections collected	17139	
Independent reflections	2553 [R_{int} = 0.0786]	
Completeness to theta = 25.00°	99.9 %	
Absorption correction	None	
Refinement method	Full-matrix least-squares on F^2	
Data / restraints / parameters	2553 / 5 / 313	
Goodness-of-fit on F^2	1.079	
Final R indices [$I>2\sigma(I)$]	R_1 = 0.0417, wR_2 = 0.0837	
R indices (all data)	R_1 = 0.0530, wR_2 = 0.0886	
Absolute structure parameter	4(2)*	
Largest diff. peak and hole	0.204 and -0.186 e.Å^{-3}	

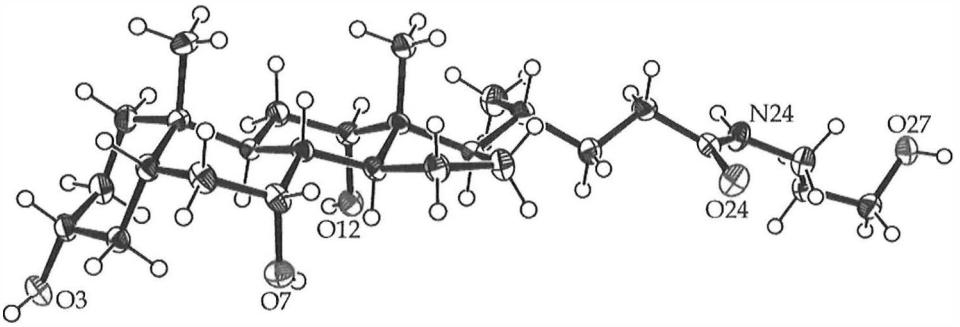

*absolute structure parameter is meaningless

Appendix 13

ESI-TOF$^+$ mass spectrum of **25** with alkali metal (Li, Na, K, and Rb) chlorides.

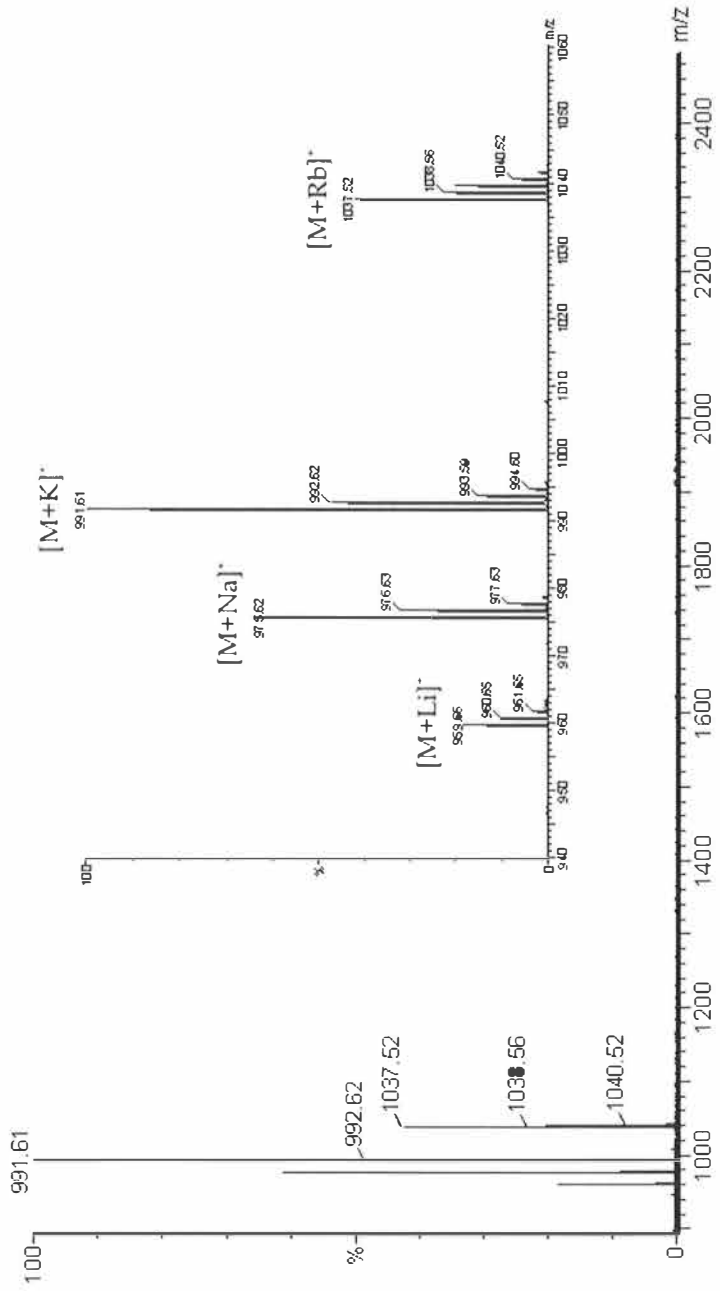

Appendix 14

ESI-TOF$^+$ mass spectrum of **30** with alkali metal (Li, Na, K, and Rb) chlorides.

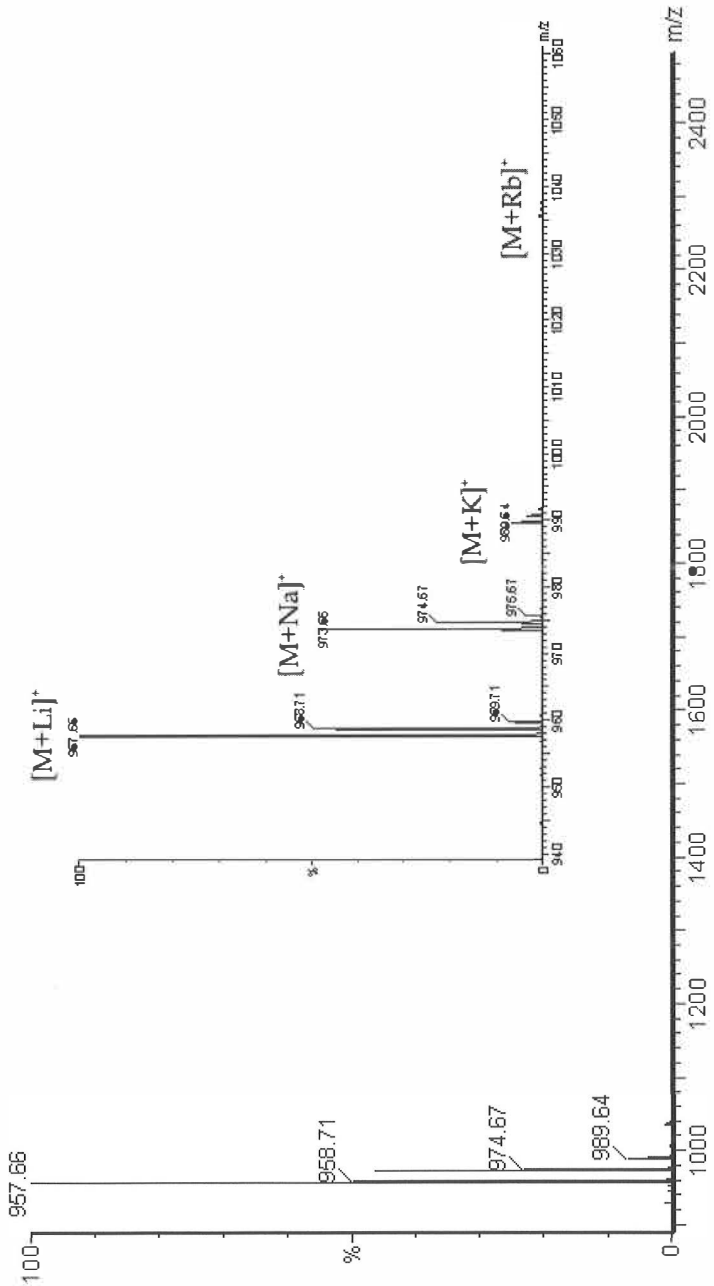

Appendix 15

ESI-TOF$^+$ mass spectrum of **30** with alkaline earth metal (Mg, Ca, and Sr) chlorides.

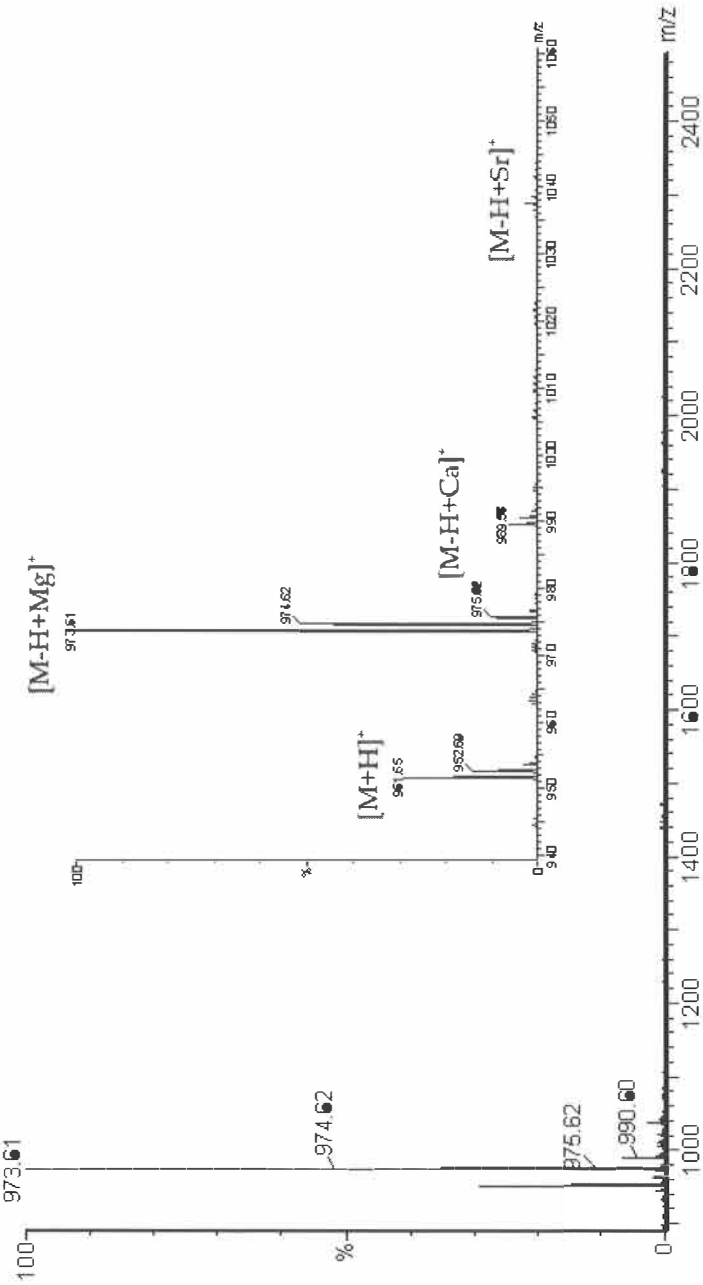

PAPER I

https://doi.org/10.1016/j.bios.2004.06.029

PAPER II

https://doi.org/10.3390/12092161

PAPER III

https://doi.org/10.1016/j.molstruc.2007.01.030

PAPER IV

https://doi.org/10.1016/j.molstruc.2007.11.018

PAPER V

https://doi.org/10.1016/j.steroids.2008.06.006